# The art of calorimetry
# part II

Erika Garutti
DESY

# Result from yesterday starting test

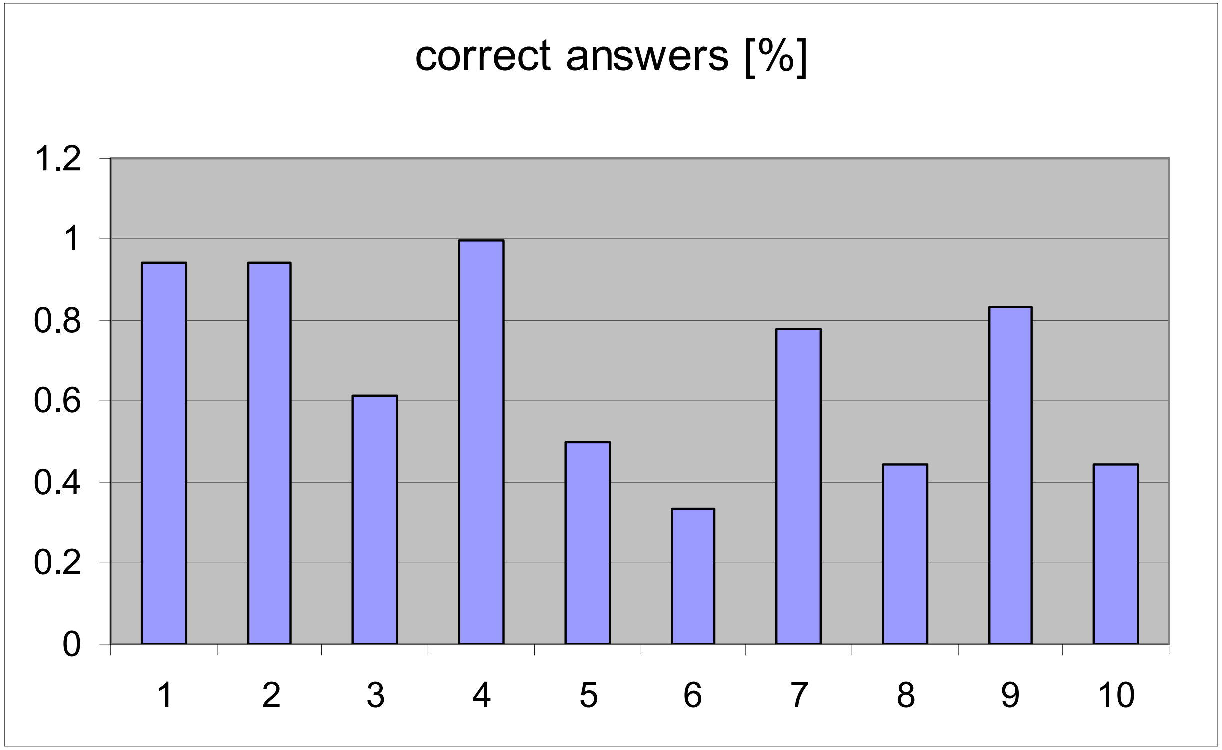

# How to “look” at the signal

1) Convert particle energy to light: scintillator (org. / in-org.)

& measure light: PMT / APD / HPD / SiPM …

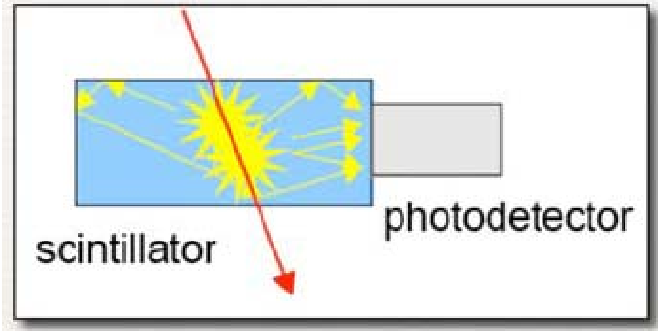


2) Measure ionization E:
gas
noble liquids
semiconductors

& measure charge signal

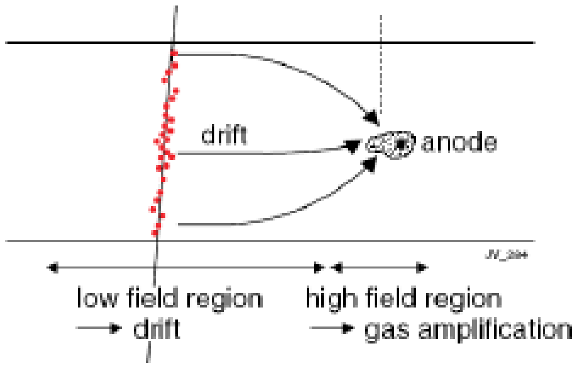


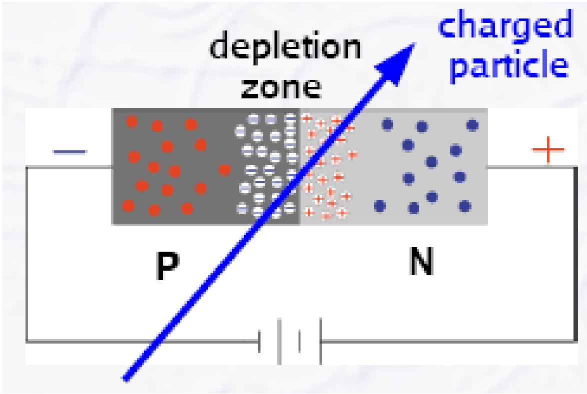


3) Measure temperature:

specialized detectors for: DM, solar $\nu$s, magnetic monopoles, double $\beta$–decay
very precise measurements of small energy deposits
phenomena that play a role in the 1 Kelvin to few milli-Kelvin range

# The measurement of showers

or “from energy to signal”

Step 1: Convert energy to light

Step 2: Convert light to electrical signal

Step 3: Reading an electrical signal

# The measurement of showers

or “from energy to signal”

Step 1: Convert energy to light

Step 2: Convert light to electrical signal

Step 3: Reading an electrical signal

# Introduction to scintillators

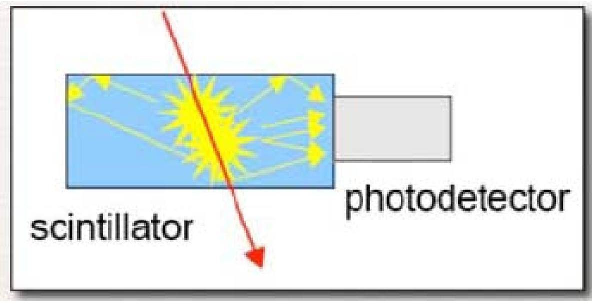


Energy deposition by a ionizing particle

→generation
→transmission } of scintillation light
→detection

Two categories: Inorganic and organic scintillators

Inorganic
(crystalline structure)

Up to 40000 photons per MeV
High Z *>2.5 eV / photon*
Large variety of Z and $\rho$
Undoped and doped
ns to $\mu$s decay times
Expensive

E.m. calorimetry (e, $\gamma$)
Medical imaging
Fairly Rad. Hard (100 kGy/year)

Organic
(plastics or liquid solutions)

Up to 10000 photons per MeV
Low Z *>10 eV / photon*
$\rho$~1gr/cm$^3$
Doped, large choice of emission wavelength
ns decay times
Relatively inexpensive

Tracking, TOF, trigger, veto counters,
sampling calorimeters.
Medium Rad. Hard (10 kGy/year)

# Scintillators in brief

Convert energy deposited by charged particles or high energy photons into light: atoms or molecules of the scintillating medium are excited and decay emitting photons which are detected and converted into electric signals (photo-detector).

Scintillating materials:

organic: aromatic hydrocarbon compounds, solid crystals, plastics or liquids. Typically faster but have lower light yields

inorganic: ionic crystals doped with activator centres or glasses. Typically larger light yields

Two types of light emission:

Fluorescence: prompt ns → μs in visible wavelength range, temperature independent (component useful for particle detection)

Phosphorescence: emission over longer period μs → ms, hrs with longer wavelength and temperature dependent

# Properties of scintillators

Parameters characterizing scintillators:

- Efficiency $R_s$ = average n. of emitted photons/energy of incident radiation
- Scintillation yield = $R_s h\nu$ with $h\nu$ = energy of emitted photons
- Time response: depends on decay time of fast component
- linearity

- the scintillator should be transparent to its own scintillation light (Stokes' shift: the emission wavelength is longer than absorption one)

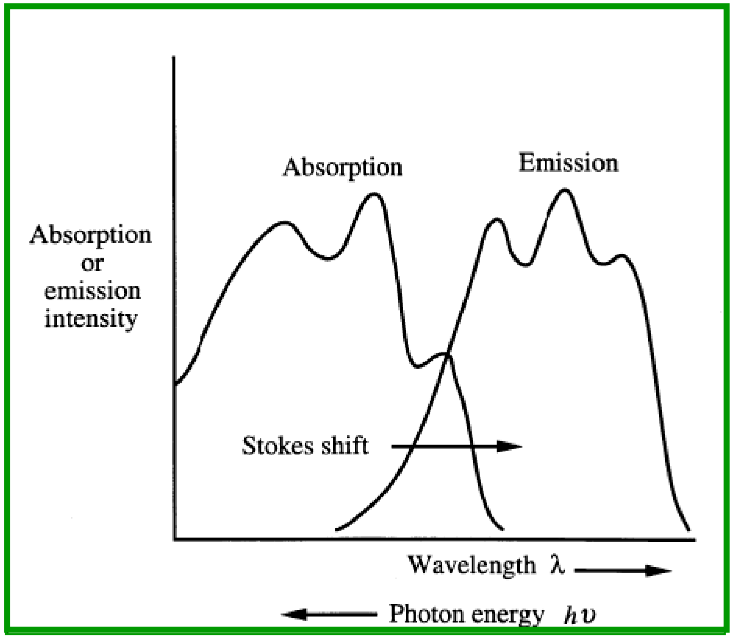

# Organic scintillators

## Organic scintillators

(plastics or liquids) are composed of aromatic hydrocarbon compounds.
Typically consist of solvent + scintillator and a secondary fluor as wavelength shifter.
No crystal structure is needed.

The emission of light is due to excitation of molecular levels in a primary fluorescent material that emits UV light during de-excitation.

This light is absorbed in most organic materials with an absorption length of ~mm.
The extraction of a light signal becomes possible only by introducing a second fluorescent material in which the UV light is converted into visible light (wavelength shifter).

Organic scintillators are typically made of low Z materials and have low density.
Hence the main interaction >20keV process is not photoelectric absorption (such as in the case of inorganic scintillators) but Compton scattering.
Typically, because of the low density more volume is required to obtain a reasonable detection efficiency, but they have low cost.

# Reminder : Photons

**Increasing Z**

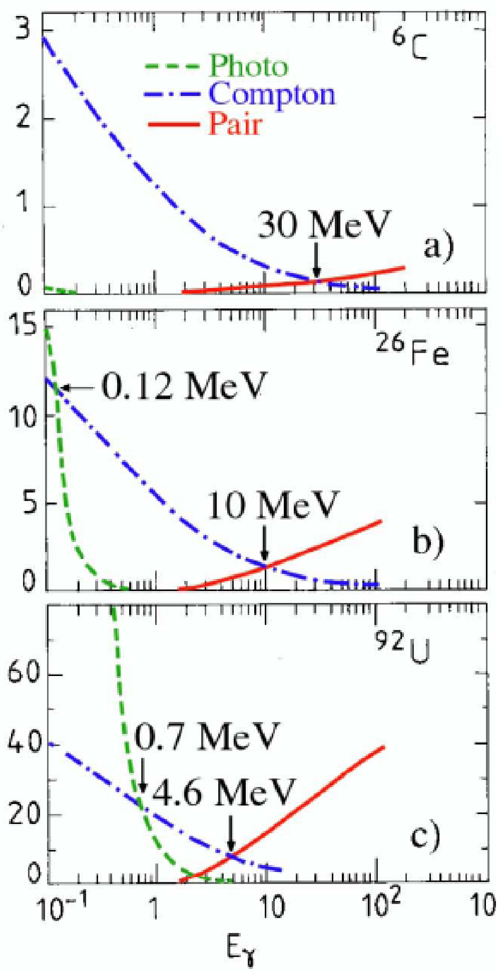


- *Photons* interact by:

1) *Photoelectric effect* $\sigma \propto Z^5,\ E^{-3}$
2) *Compton scattering* $\sigma \propto Z,\ E^{-1}$
3) *Conversion into* $e^+e^-$ $\sigma$ increases with $E$, $Z$, asymptotic at $\sim 1$ GeV

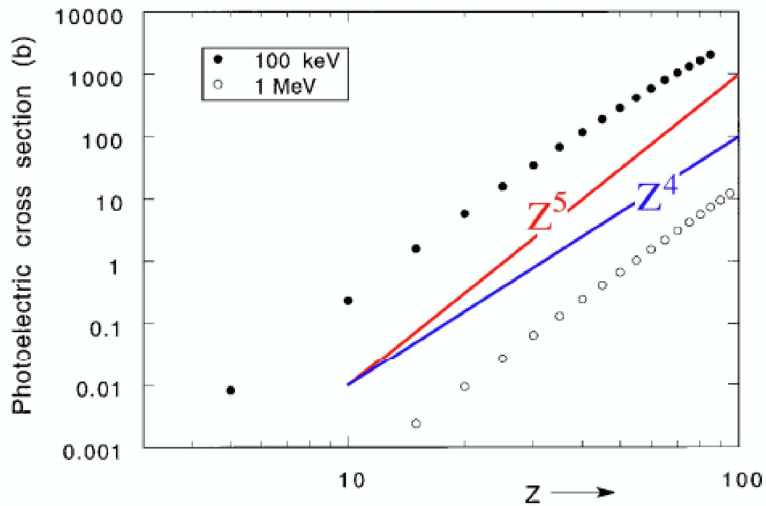


FIG. 2.3. Cross section for the photoelectric effect as a function of the $Z$ value of the absorber. Data for 100 keV and 1 MeV $\gamma$s.

# Organic scintillators

Energy levels of organic scintillators: at room $T_a$ ($KT_a$ = 0.025 eV) electrons on ground state, incident radiation excites electrons to S1 states, radiation-less decays to base S1 state, emission of light to S0.
S1 can decay to a triplet state with lower energy and longer decay time.
The fluorescence UV light (250-370 nm) is absorbed by most organic materials, so the light signal can be extracted using a second fluorescent material (wavelength shifter) that converts UV in visible light (320-500 nm)

Non-radiative transfer

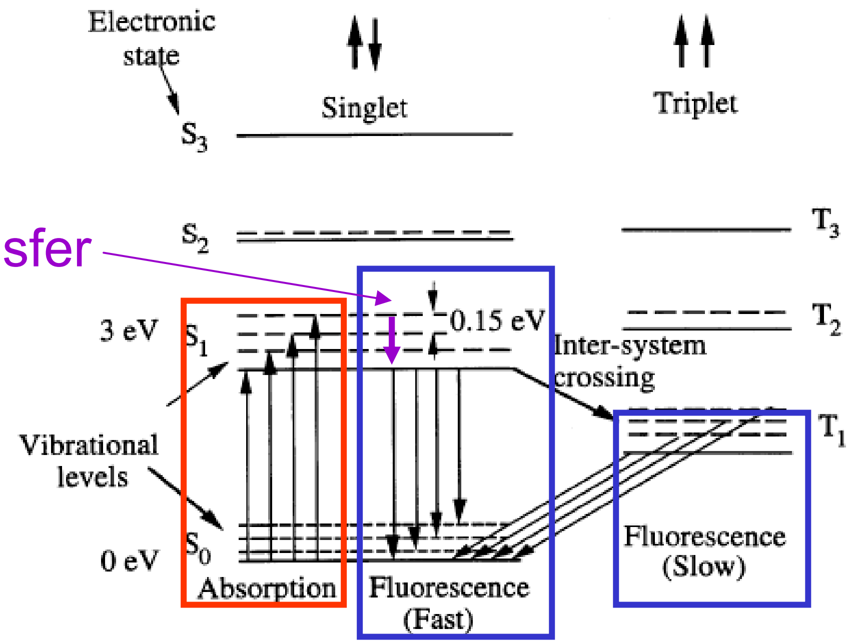


# photons produced
~ 2 $10^4$ $cm^{-1}$ [for a MIP]
~ 10 eV / photon

# Time dependence of emitted light

Non-radiative transfer of energy from vibrational states to fluorescence state S1: 0.2-0.4 ns

Decay of fluorescent state: 1-3 ns $I(t) \propto 1 - e^{-t/\tau_r}$ $\tau_r$ = rise time constant

Fall with time constant $\tau_f$ $I(t) \propto e^{-t/\tau_f}$

total pulse shape

$$I(t) = I_0 \left(e^{-t/\tau_f} - e^{-t/\tau_r}\right)$$

Decay time in stilbene for various particles

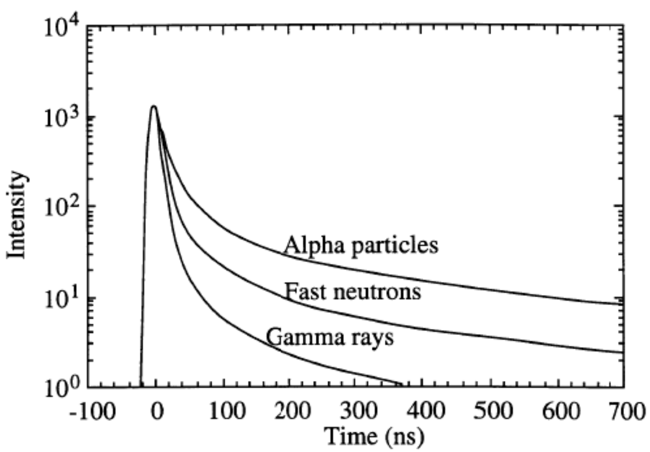


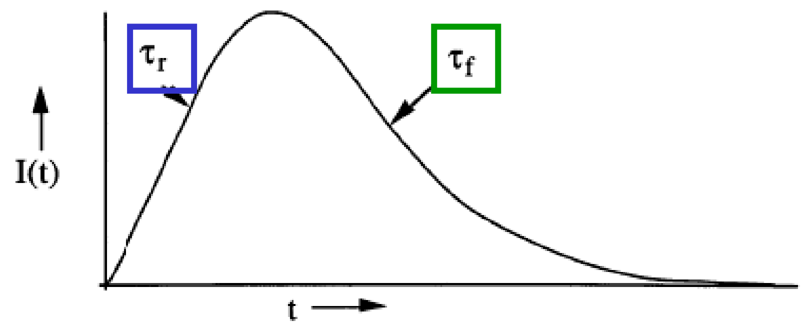


The decay time depends on the ionization density

| Material | State | $\lambda_{max}$ [nm] | $\tau_f$ [ns] | $\rho$ [g/cm$^3$] | photons/MeV |
|---|---|---|---|---|---|
| Anthracene | crystal | 447 | 30 | 1.25 | $1.6 \cdot 10^4$ |
| Pilot U | plastic | 391 | 1.4 | 1.03 | $1.0 \cdot 10^4$ |
| NE104 | plastic | 406 | 1.8 | 1.03 | $1.0 \cdot 10^4$ |
| NE102 | liquid | 425 | 2.6 | 1.51 | $1.2 \cdot 10^4$ |

# Birk's law

For organic scintillators the relation between emitted light and energy loss is not linear. Deviations from linearity are due to quenching interactions between excited molecules created along the ionizing particle path absorbing energy

For an ideal scintillator and low ionization density
Luminescence $\propto$ Energy dissipated in scintillator

$$L = SE \quad \text{or} \quad \frac{dL}{dr} = S\frac{dE}{dr}$$

The light output depends on the ionization density

$$\frac{dL}{dr} = \frac{S\frac{dE}{dr}}{1 + kB\frac{dE}{dr}}$$

Density of ionized and excited molecules along track
Quenching parameter

For small $dE/dr$ this yields the luminescence yield postulated above.

For large $dE/dr$ the specific luminescence saturates, as indicated by the data.

$$\frac{dL}{dr} = \frac{S}{kB} = const$$

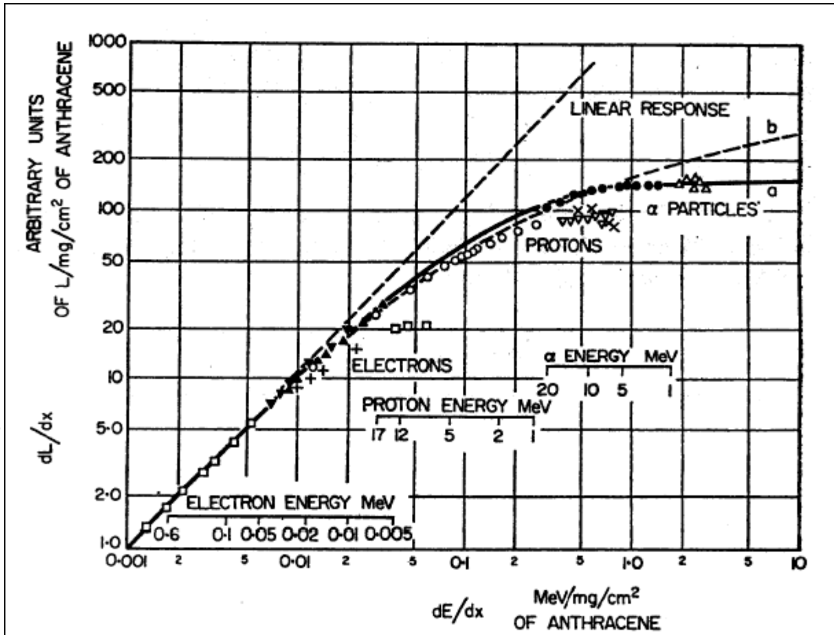

# Radiation hardness in plastic

500 kGy irradiation of SCSN81T and SCSN38 from Kuraray

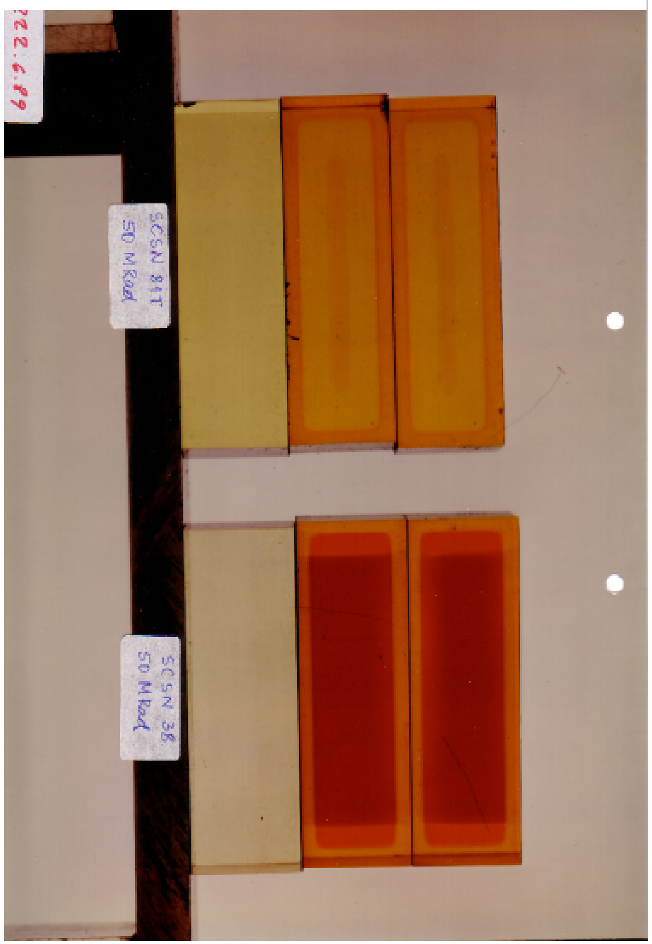


and after 3 weeks recovery in an oxygen-rich atmosphere

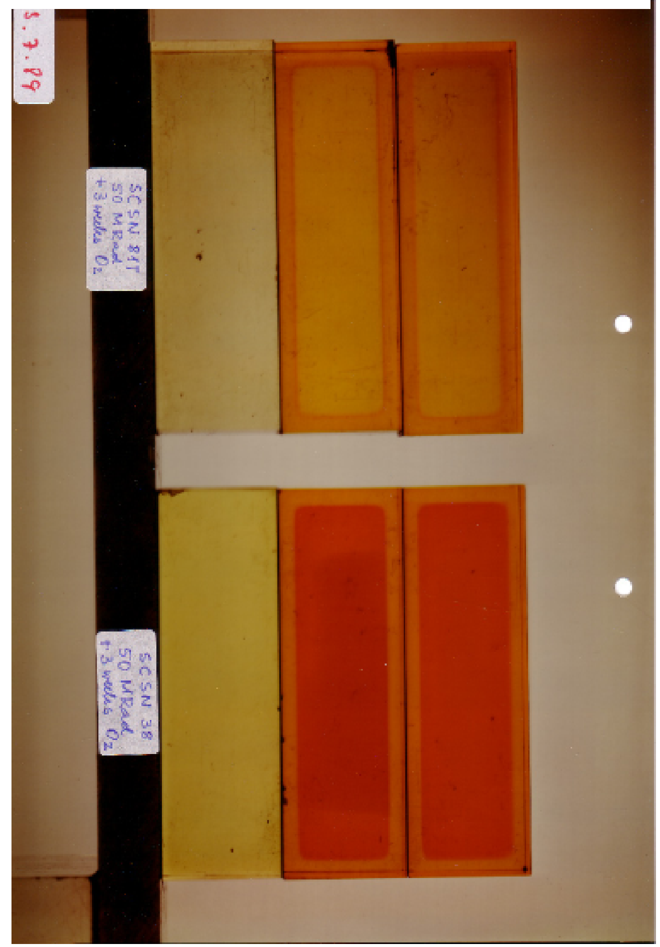

# Most common applications of organic scintillators

Large volume liquid or solid detectors (in form of tiles): underground experiments, sampling calorimeters (HCAL in CMS or ATLAS, etc.), counters, light guides.

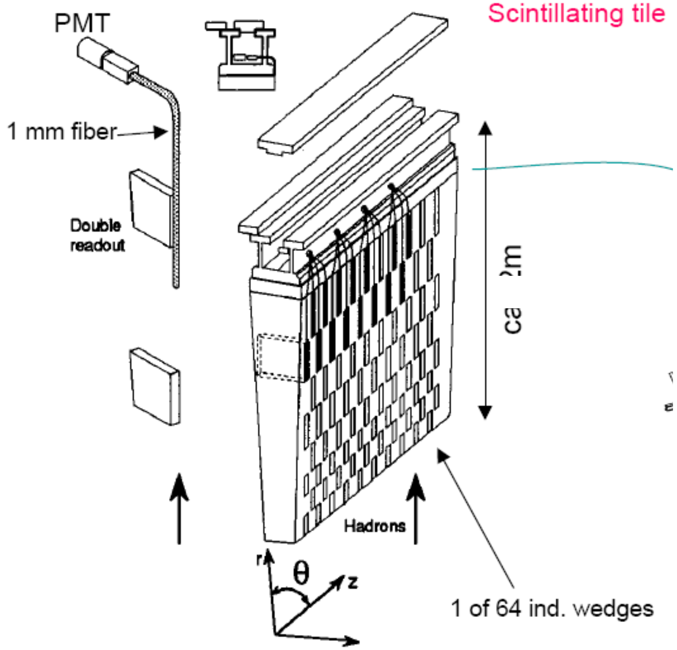


ATLAS hadron calorimeter

High precision, small volume active targets and fibre tracking (UA2, D0, CHORUS)

RD7 development: bundles of hexagonal fibres (typ. 60 µm dia.,2.5 mm bundle size) for tracking

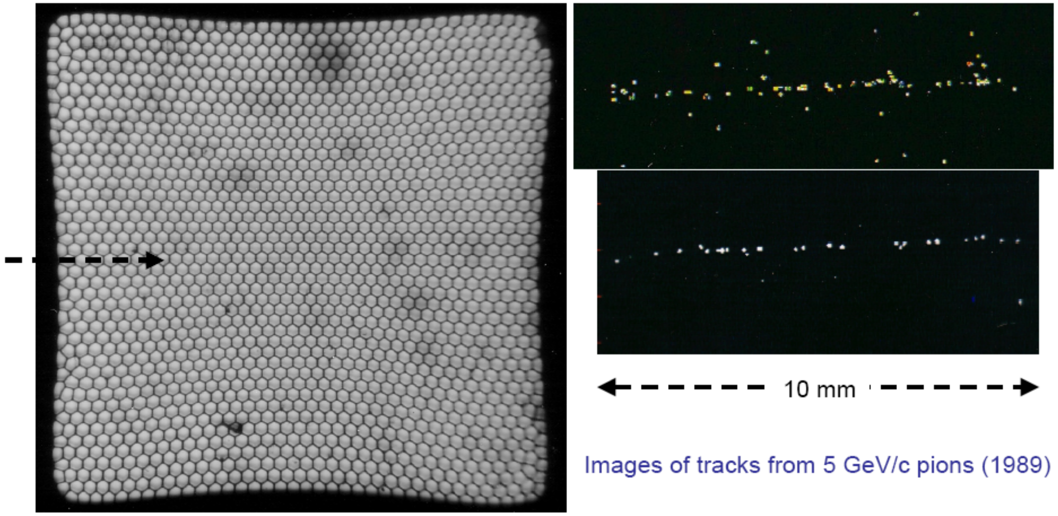


Images of tracks from 5 GeV/c pions (1989)

# Scintillator fibers

scintillating plastic fibre working principle:

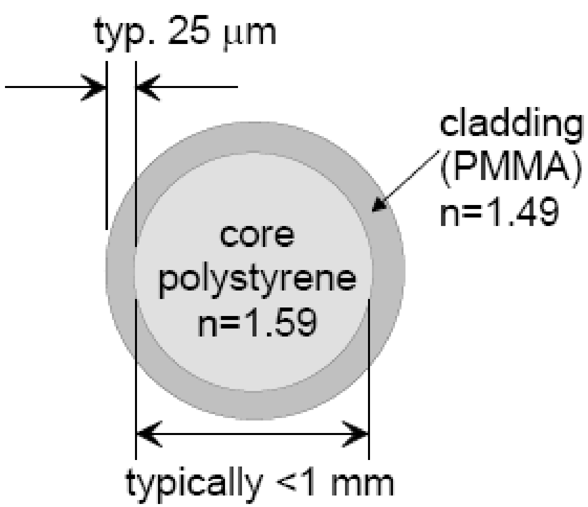


light transport by total internal reflection

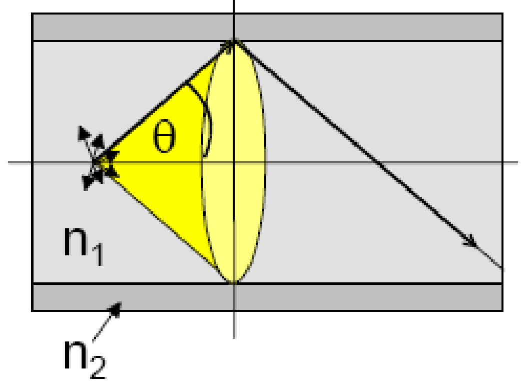


Double cladding system
(developed by RD7)

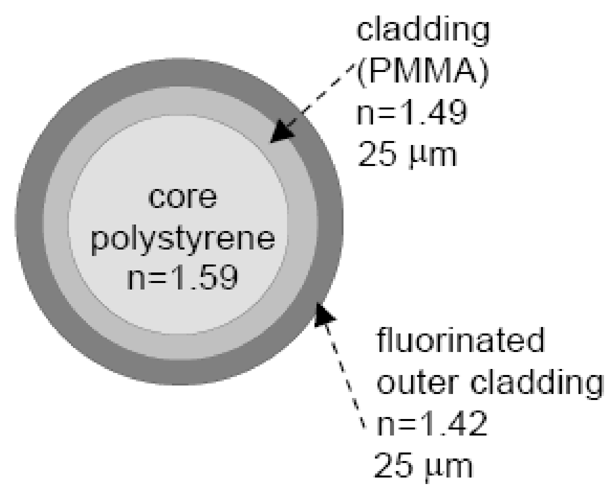


$$\frac{d\Omega}{4\pi} = 0.5\,(1 - \cos^2\theta) = 3\%$$

$$\theta \le \arccos\frac{n_2}{n_1} \approx 69.6^\circ$$

$$\frac{d\Omega}{4\pi} = 0.5\,(1 - \cos^2\theta) \approx 5.3\%$$

# Main R&D on organic scintillators

- New dopants with better light yield and larger Stokes shift
- High granularity readout of fibres
- Larger attenuation lengths in plastic fibres
- New radiation hard plastics to stand 100 kGy/year dose

# Inorganic scintillators

- Usually made of high Z materials ➔ high density
- High Z enhances the photoelectric interaction contribution and high density increases the interaction efficiency.
- Crystals are grown in high temperature furnaces and are made of Alkali Halides (ie. NaI, CsI) or Oxides (eg. BGO).
- The crystalline structure creates energy bands between which electrons can jump ➔ scintillation light
- Some crystals need activators to enable emission in the visible (Thallium in NaI(Tl))

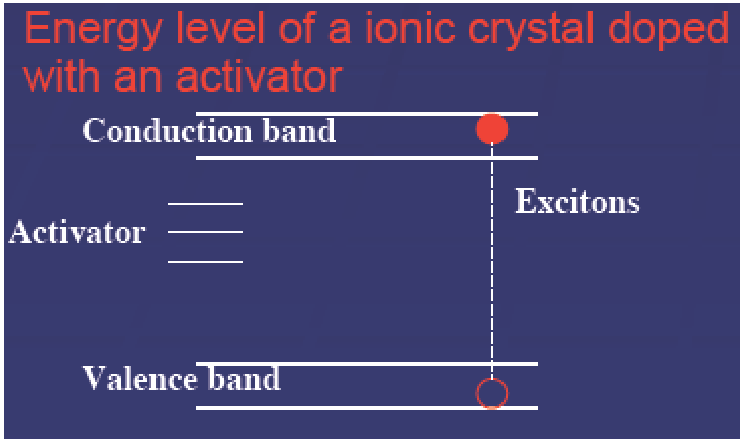

# Inorganic scintillators II

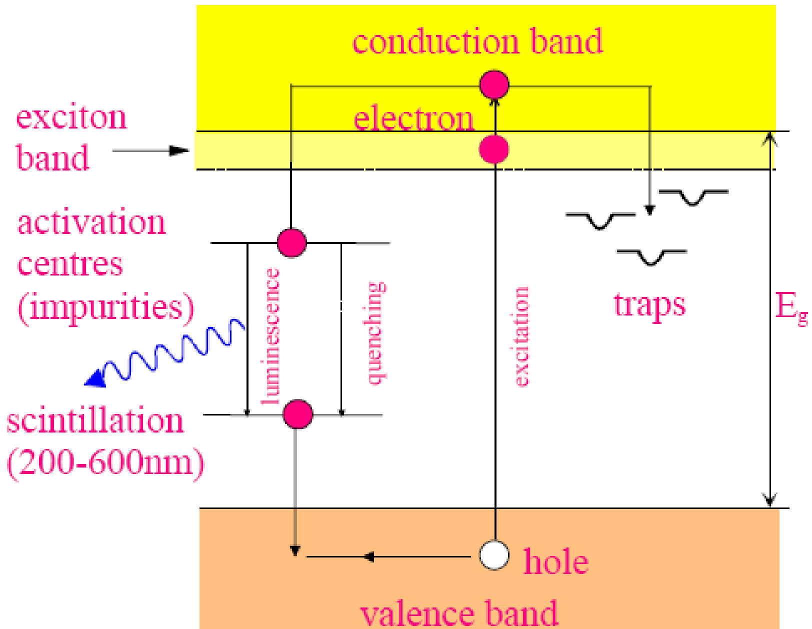


Ionizing particles produce free electrons, holes and couples of electron-holes (excitons). These move around the crystal lattice until they meet an activation centre that they transform into an excited state A* of energy E1 that can decay emitting light. The decay time depends on the temperature as exp[-E1/(KT)]

Warning, sometimes ≥ 2 time constants

- fast recombination (ns-μs) from activation centers
- delayed recombination due to trapping (μs-ms)

➔ full control of growth, doping and impurities is imperative to optimize light yield, transmission and decay time

| Material | Form | $\lambda_{max}$ (nm) | $\tau_f$ (ns) | ρ (g/cm$^3$) | Photons per MeV |
|---|---|---|---|---|---|
| NaI(Tl) (20°C) | crystal | 415 | 230 | 3.67 | 38,000 |
| pure NaI (-196°C) | crystal | 303 | 60 | 3.67 | 76,000 |
| $Bi_4Ge_3O_{12}$ (20°C) | crystal | 480 | 300 | 7.13 | 8,200 |
| $Bi_4Ge_3O_{12}$ (-100°C) | crystal | 480 | 2000 | 7.13 | 24,000 |
| CsI(Na) | crystal | 420 | 630 | 4.51 | 39,000 |
| CsI(Tl) | crystal | 540 | 800 | 4.51 | 60,000 |

# Temperature dependence of crystals

Light output of crystals depends on temperature

(From Bicron catalogue)

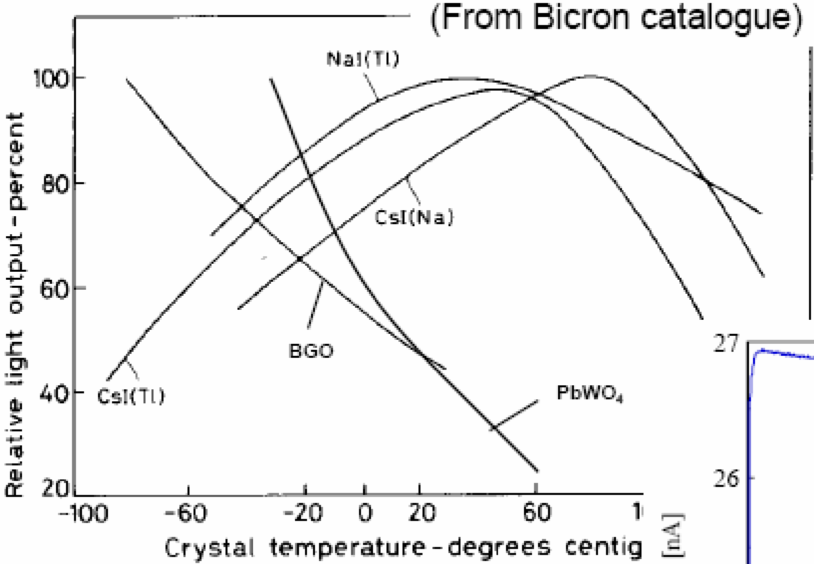


Low dose irradiation of an old $PbWO_4$ crystal and check of the temperature dependence of its light yield (1996). The blue curve is the photocurrent generated by the irradiation and the red curve is the temperature of the sample.

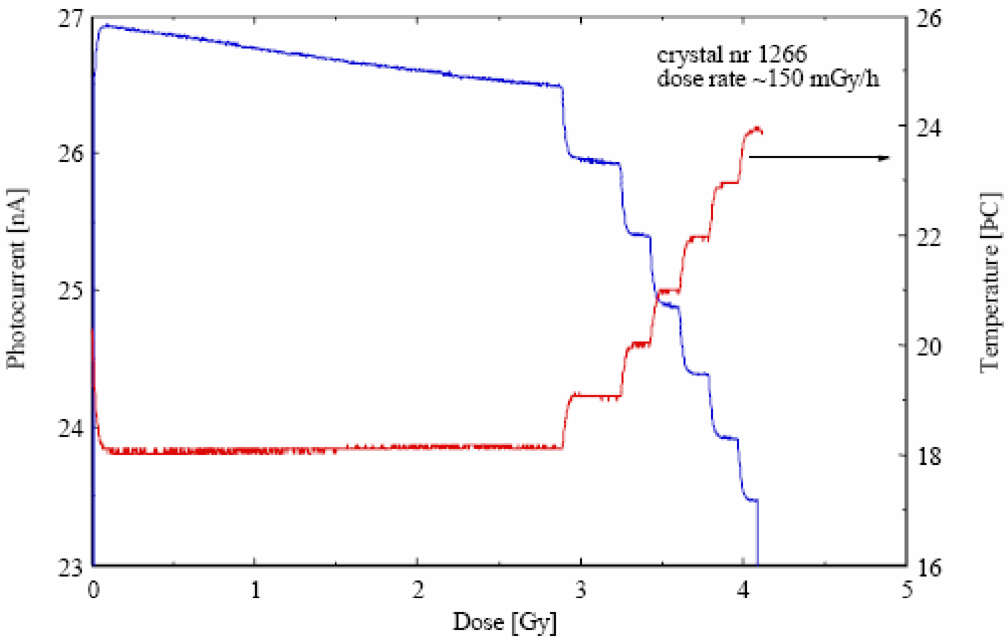


The $PbWO_4$ crystal is used in CMS ECAL and its ~2% light yield decrease per $^oC$ asks for temp. control and monitoring

# For your reference …

| Scintillator composition | Density ($g/cm^3$) | Index of refraction | Wavelength of max.Em. (nm) | Decay time Constant (μs) | Scinti Pulse height[1)] | Notes |
|---|---|---|---|---|---|---|
| NaI(Tl) | 3.67 | 1.9 | 410 | 0.25 | 100 | 2) |
| CsI | 4.51 | 1.8 | 310 | 0.01 | 6 | 3) |
| CsI(Tl) | 4.51 | 1.8 | 565 | 1.0 | 45 | 3) |
| $CaF_2$(Eu) | 3.19 | 1.4 | 435 | 0.9 | 50 | |
| $BaF_2$ | 4.88 | 1.5 | 190/220<br>310 | 0,0006<br>0.63 | 5<br>15 | |
| BGO | 7.13 | 2.2 | 480 | 0.30 | 10 | |
| $CdW0_4$ | 7.90 | 2.3 | 540 | 5.0 | 40 | |
| $PbWO_4$ | 8.28 | 2.1 | 440 | 0.020 | 0.1 | |
| $CeF_3$ | 6.16 | 1.7 | 300<br>340 | 0.005<br>0.020 | 5 | |
| GSO | 6.71 | 1.9 | 430 | 0.060 | 40 | |
| LSO | 7 | 1.8 | 420 | 0.040 | 75 | |
| YAP | 5.50 | 1.9 | 370 | 0.030 | 70 | |

1) Relative to NaI(Tl) in %; 2) Hygroscopic; 3) Water soluble

# Most common applications of inorganic scintillators

- Calorimetry
- X-ray and gamma spectroscopy
- Imaging
  - Positron Emission Tomography (PET) in medical imaging
  - Gamma Imaging (Anger camera)
- Monitoring in nuclear plants
- Oil wells, Mining, etc.

# Positron Emission Tomography

How can a calorimeter save your life? ➔ PET

a commercial PET system
for hospital treatment

the same system without cover
doesn't it look like something familiar?

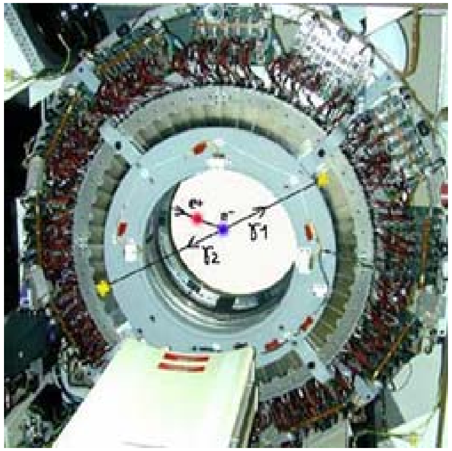


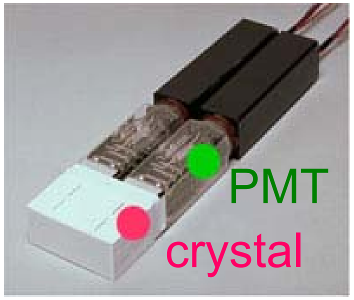


basic unit of a PET:
crystal (LSO, BGO) + PMT

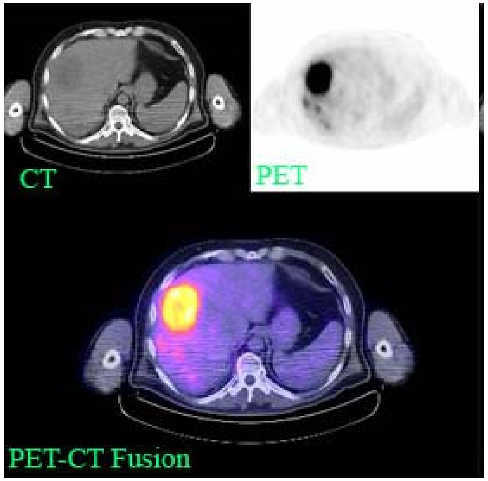


**PET scan** is a powerful tool for detecting several types of cancer. PET works by having the ability to detect sites of high metabolic activity. Since many cancers have significantly higher metabolism than normal tissues or noncancerous masses, PET allows sensitive detection of even small cancers.
**PET-CT Fusion** is a refinement of the technique that allows the most accurate correlation of anatomic information (from the CT) and metabolic information (from the PET scan) and helps to ensure the highest degree of accuracy for the exam.

# PET performance

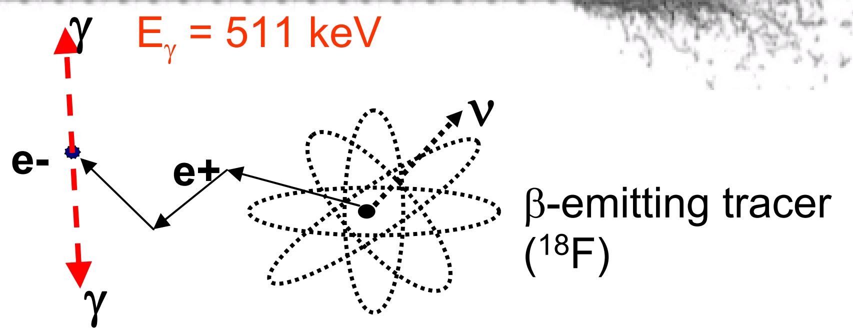


The physics process to detect:
$e^+e^- \rightarrow \gamma\gamma$ ($E_\gamma$ = 511 keV)

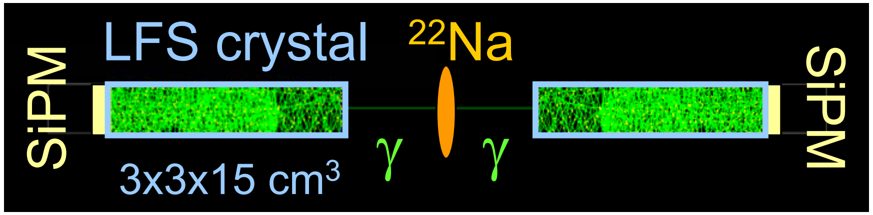


Simple system for prove of principle studies: Two crystals in coincidence to detect back to back 511keV photons

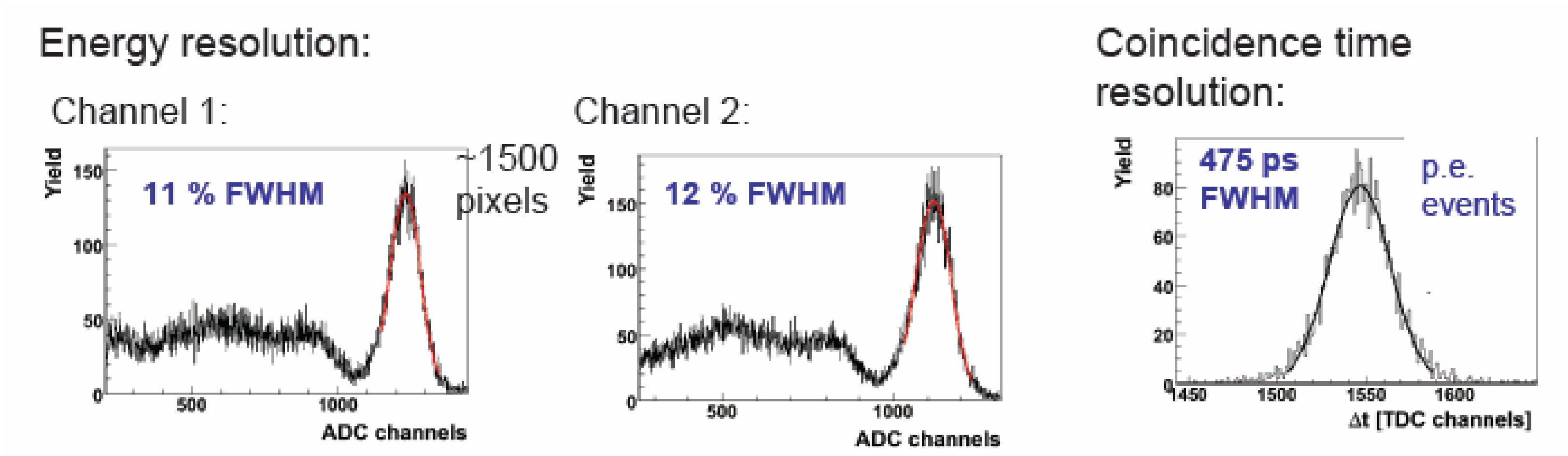

# Main R&D on inorganic scintillators

- Higher densities for higher Z (improve photoabsorption)
- High light yield (NaI(Tl) light yield still unchallenged)
- Short decay time (improve time resolution)
- Improve light coupling with photon detector
- More radiation hard
- Inexpensive, “easy” to manufacture, reproducible
- Large size, easy handling and “machinable”
- Smaller size ➔ fiber crystals

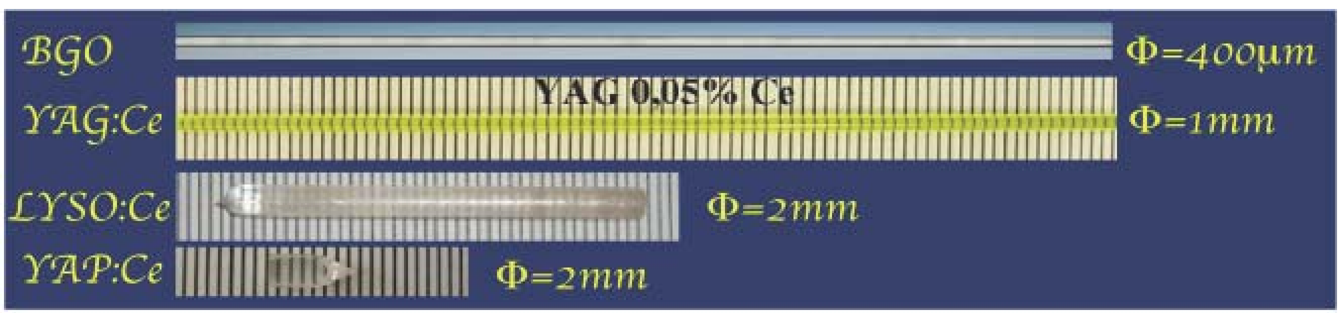


The micro-pulling down crystal growth technology (Courtesy Fibercryst)

# Liquefied noble gases

Liquefied noble gases: LAr, LXe, LKr

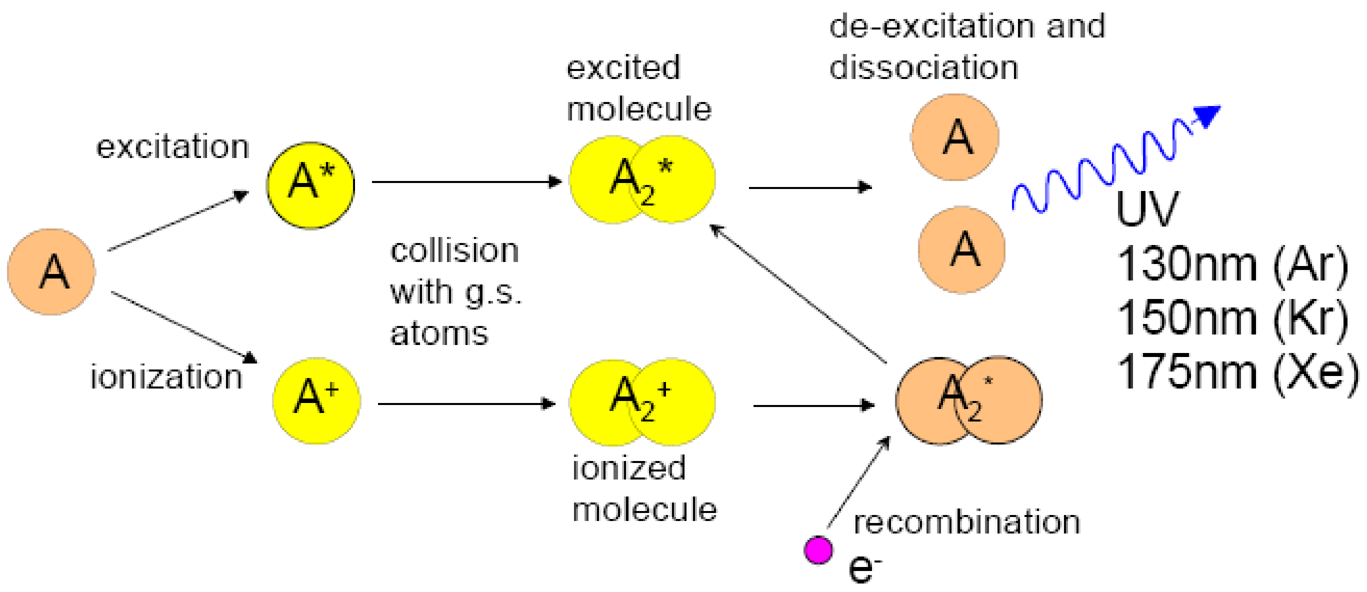


Also here one finds 2 time constants: from a few ns to 1 μs.

# Cherenkov effect

A charged particle traveling in a dielectric medium with n>1 radiates **Cherenkov light** if its velocity is larger than the phase velocity of light **v>c/n or β > 1/n (threshold)**

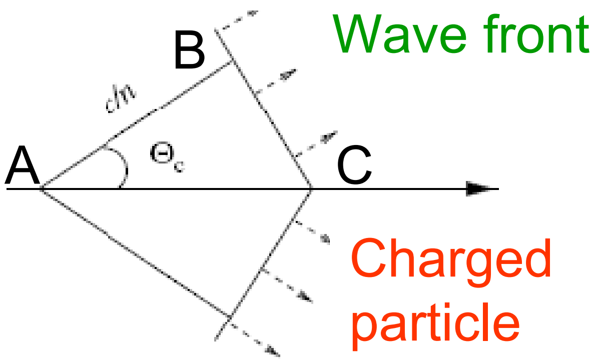


The emission is due to an asymmetric polarization of the medium in front and at the rear of the particle, giving rise to a varying electric dipole momentum.

Some of the particle energy is converted into light. A coherent wave front is generated moving at velocity v at an angle $\Theta_c$.

If the media is transparent the Cherenkov light can be detected.

If the particle is ultra-relativistic (β~1) $\Theta_c$ = const and has max value

$$\cos\Theta_c = \frac{AB}{AC} = \frac{c}{n} t \cdot \frac{1}{\beta ct} = \frac{1}{\beta n}$$

In water $\Theta_c$ = 43°, in ice 41°

# Cherenkov effect

The intensity of the Cherenkov radiation (number of photons per unit length of particle path and per unit of wave length) depends on charge and velocity of particle

$$\frac{d^2N}{dx\,d\lambda} = \frac{4\pi^2 z^2 e^2}{hc\lambda^2}\left(1 - \frac{1}{n^2\beta^2}\right) = \frac{2\pi z^2}{\lambda^2}\alpha \sin^2\Theta_C$$

$$\alpha = \frac{2\pi e^2}{hc}$$

In the range 400-700 nm:

$$\frac{dN_\gamma}{dx} = \int_{\lambda_1}^{\lambda_2} d\lambda \frac{d^2N_\gamma}{dx\,d\lambda} = 2\pi z^2 \alpha \sin^2\Theta_C \int_{\lambda_1}^{\lambda_2} \frac{d\lambda}{\lambda^2} = 2\pi z^2 \alpha \sin^2\Theta_C \left(\frac{1}{\lambda_1} - \frac{1}{\lambda_2}\right) = 490\, z^2 \sin^2\Theta_c \quad photons/cm$$

for electrons in quartz z=1, at $\Theta_c = 45^o$ $\sin^2\Theta_c = 0.5$

$$E_{thr} = m_{particle}\gamma_{thr} = m_{particle}\frac{1}{\sqrt{1-\beta_{thr}^2}}$$

for quartz $E_{th}(e) > 0.5$ MeV

in water energy loss by Ch. is about $10^4$ less than by ionization (ion: 2 MeV/cm )
➔ but directional effect!!!
$E_{th}(e) > 0.26$ MeV and $E_{th}(\mu) > 54$ MeV (neutrino exper.)

# PID with a threshold cherenkov detector

The Cherenkov threshold can be used to separate particles of momentum p and masses m1 and m2 > m1.
The radiator medium can be chosen such that the heavier particle is just below threshold: $\beta_2 \approx 1/n$

Calculate the number of produced photo-electrons / cm of a given Cherenkov radiator material by a 1 GeV pion when discriminating $K/\pi$ (assume photo-detector efficiency = 20%)

# Solution

Choose a radiator medium such that K=$m_2$ is below threshold:
$\beta_2 \approx 1/n$ while $\beta_1 > 1/n$

$$\sin^2\Theta_C = 1 - \frac{1}{\beta_1^2 n^2} \approx 1 - \frac{\beta_2^2}{\beta_1^2} \approx 1 - \frac{\beta_2^2}{\beta_1^2} = 1 - \frac{E_1^2}{E_2^2} \approx \frac{c^2(m_2^2 - m_1^2)}{p^2}$$

$$p >> m_2$$

For 20% PDE one gets:

$$N / L = 100 \sin^2\Theta_C = 100 \frac{c^2(m_2^2 - m_1^2)}{p^2}$$ [# photoelectrons / cm]

$m_2$=$m_K$=493.7 MeV
$m_\pi$=139.6 MeV

for K/π separation at 1 GeV $N_{pe}/L \approx 22$ pe/cm for $m_1$=$m_\pi$
and by design 0 for $m_1$=$m_K$

# The measurement of showers

or “from energy to signal”

Step 1: Convert energy to light

Step 2: Convert light to electrical signal

Step 3: Reading an electrical signal

# Reading out light from a scintillator

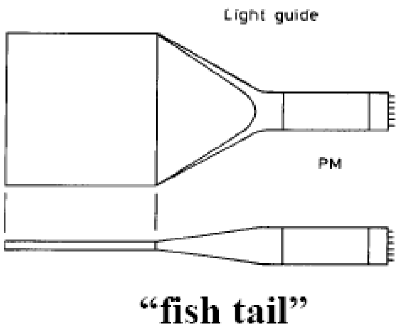


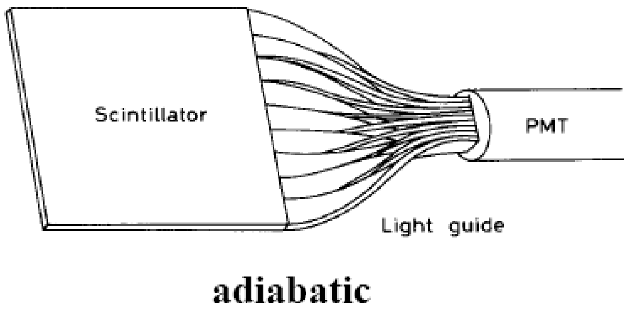


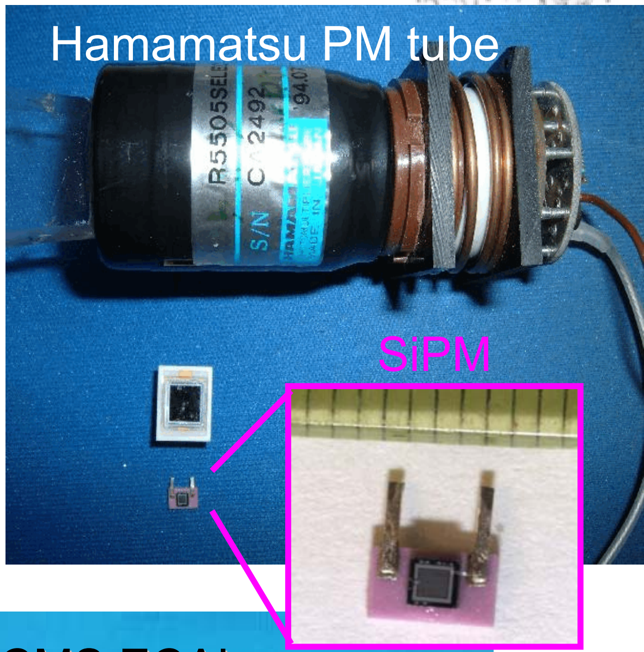


Photo-multiplier tubes are the past!

Be modern: go silicon!

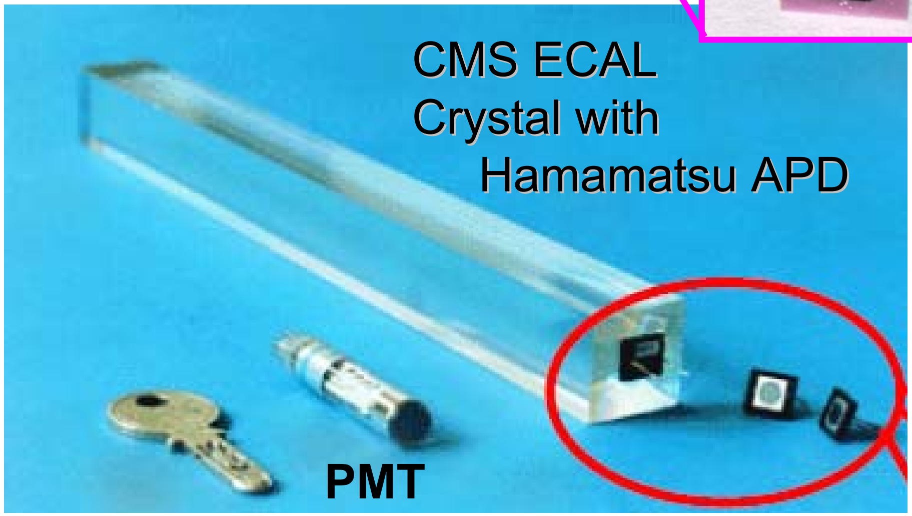

# New photo-detecotrs

Main drawbacks of PMTs: bulky shape, the high price and the sensitivity to magnetic fields.

Photodiodes are semiconductors light sensors that generate a current or voltage when light illuminates the p-n junction.

➔ Allow detection of light in 200-1150 nm

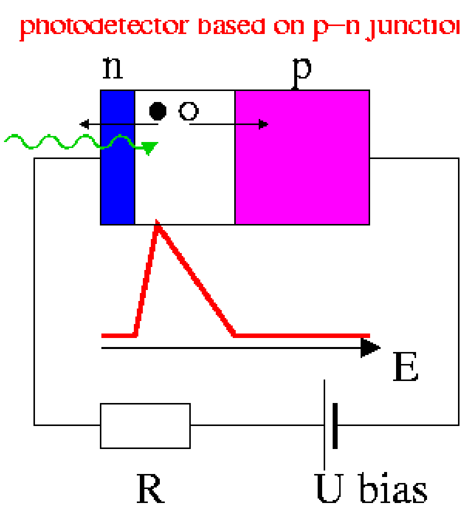


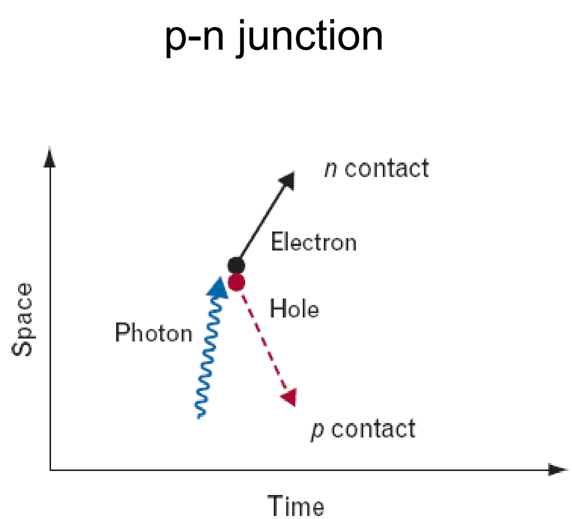


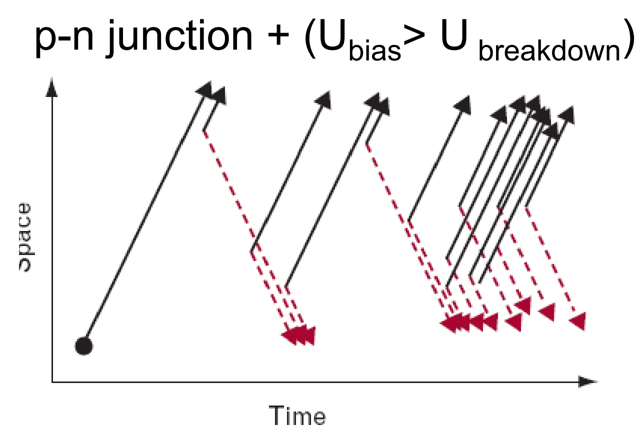

# Photon detection in Semiconductors

• PIN photodiodes are Near IR detectors (InGaAs or Si) have excellent linearity with light, high speed, low noise and dark current but major drawback: low gain ~ 1

• Avalanche Si photodiodes (APDs) have internal gain so are more sensitive and have much higher QE > 70%.

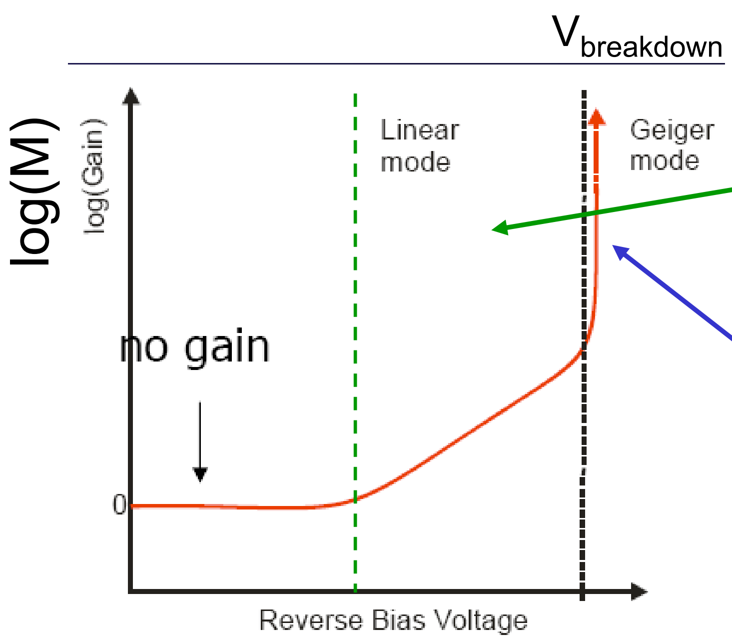


**Avalanche Photo-Diode (APD)**
operated in linear mode ~ AMPLIFIER (Gain M~ 50-500)
!! signal proportional to energy deposited
➔ used in CMS ECAL

**Geiger mode Avalanche Photo-Diode**
operate above breakdown voltage (Gain M ~$1*10^6$)
!! It's a BINARY device
➔for practical application use ARRAY of single Geiger mode Avalanche Photo-Diodes:
the Silicon Photo-Multiplier

# APD for various applications

Pick the right one for your application:

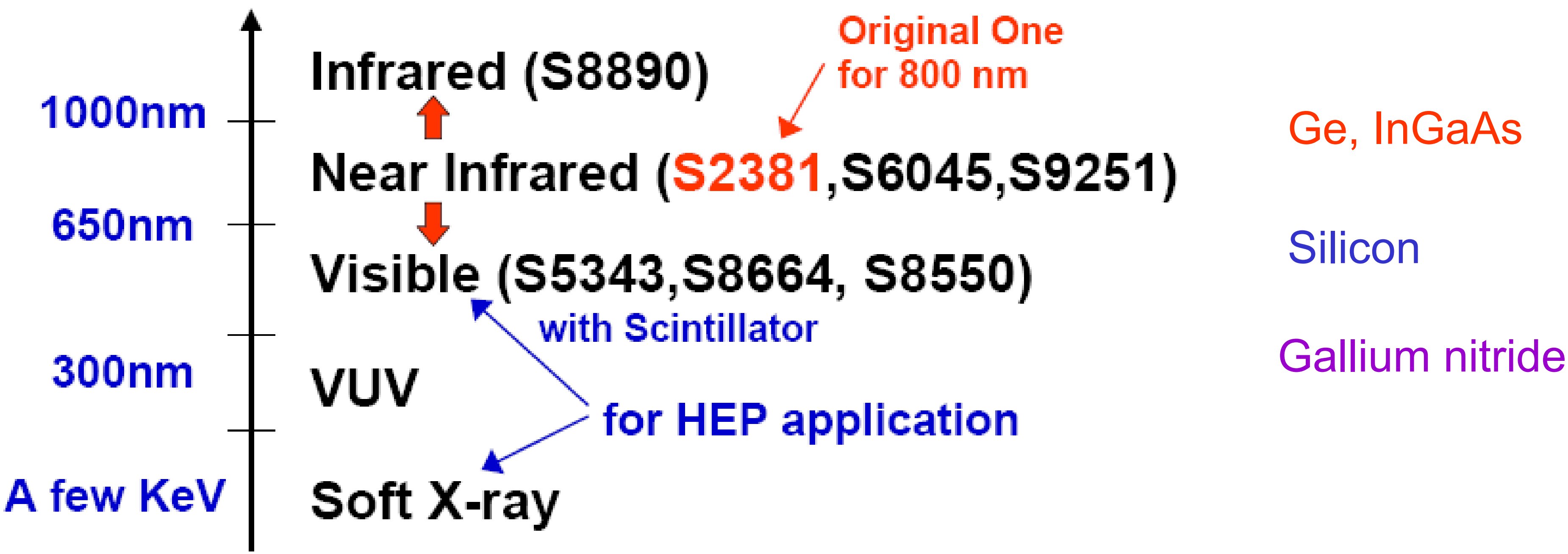

# Excess noise

Noise due to the multiplication process at a gain, *M*, denoted by *F*(*M*) often expressed as:

$$F(M) = \kappa M + \left(2 - \frac{1}{M}\right)(1 - \kappa)$$

For an electron multiplication device $\kappa$ is given by the hole impact ionization rate divided by the electron impact ionization rate.

It is desirable to have a large asymmetry between these rates, in order to minimize *F*(*M*) since *F*(*M*) is one of the main factors which limit the energy resolution obtainable.

Typical values of $\kappa$ are: 0.02-0.06 for Si, 0.9 for Ge, 0.45 for InGaAs

Typical values of *F(M)* are: 5-8 for Si, 9 for Ge, 5 for InGaAs

# Geiger-mode APD

In principle an APD could be operated in a supercritical state above breakdown and could detect single photons but it would not stay long in this state and the recovery time would be much longer than the time between consecutive generation of free carriers (dark counts).

Way out:

Subdivide the APD into many cells and connect them all in parallel via an individual limiting (quenching) resistor.

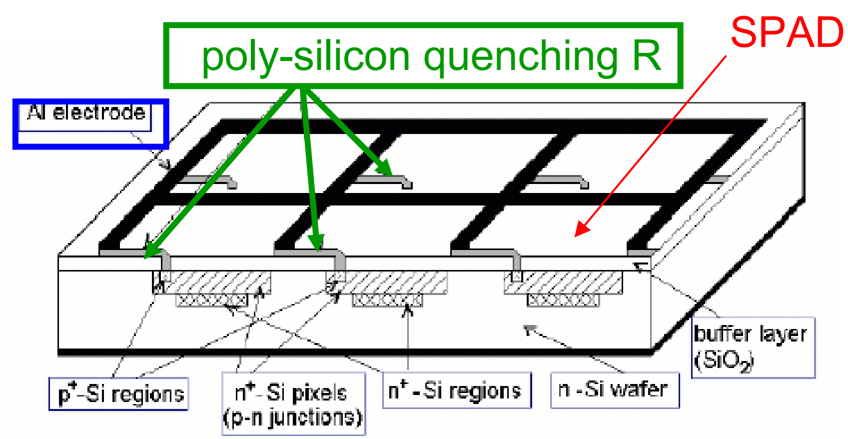


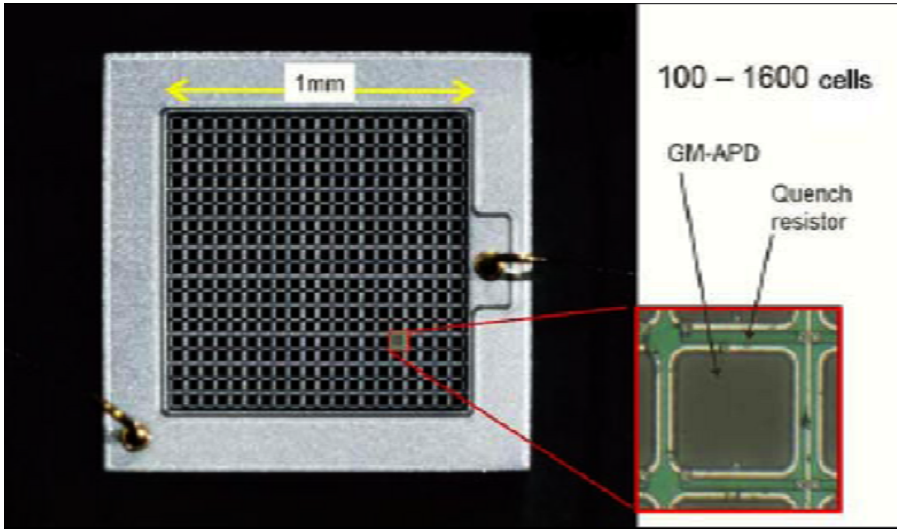


➔ typically 100-1000 pixels / mm²

Some typical pixel parameter:

-pixel size ~20-30μm

-pixel capacitance $C_{pixel}$ ~ 50fmF

-quenching resistor $R_{pixel}$ ~ 1-10 MΩ

# Working principle

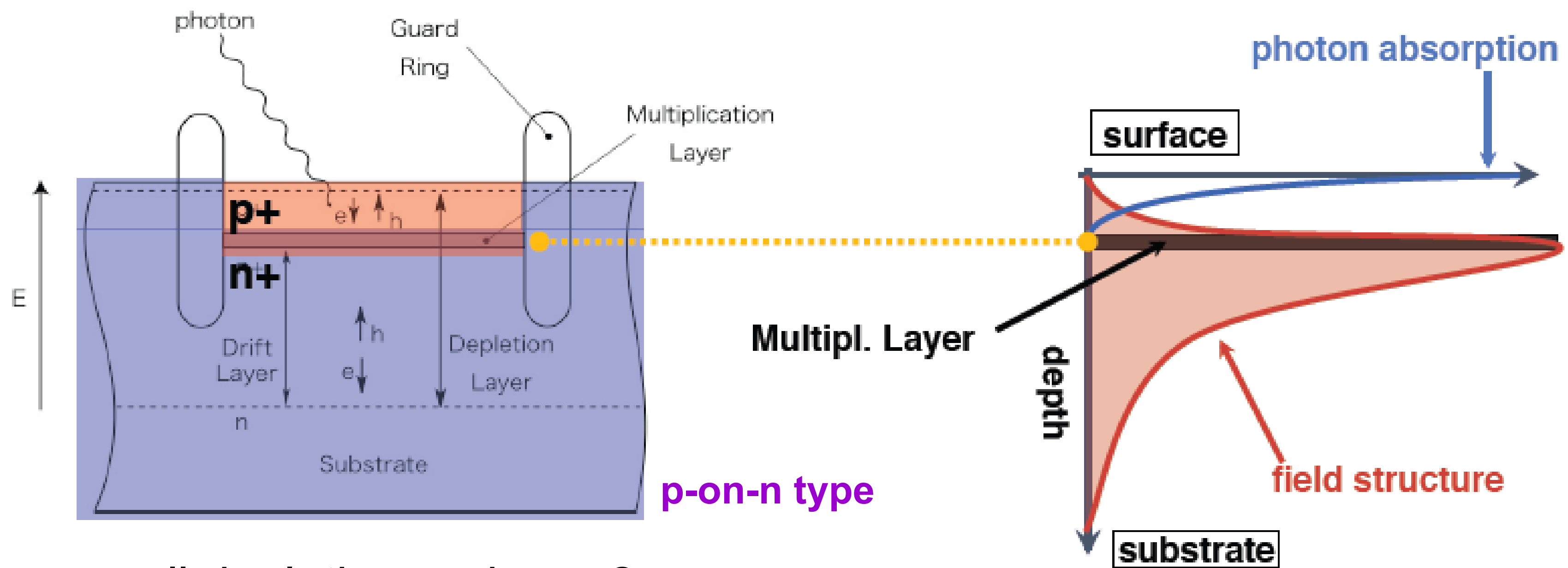


-small depletion region ~ 2$\mu$m

-strong electric field (2-3)x$10^5$ V/cm

-carrier drift velocity ~ $10^7$ cm/s

-very short Geiger discharge development < 500 ps

Photoelectric conversions occur above the multiplication layer

➔ electrons drift to the multiplication layer

Random excitations occur mainly below the multiplication layer

➔ holes drift to the multiplication layer

# High gain

G-APDs produce a standard signal when any of the cells goes to breakdown. The amplitude $A_i$ is proportional to the capacitance of the cell divided by the electron charge times the overvoltage:

$A_i \sim C/q \cdot (V - V_b)$ $(V - V_b)$ we call “overvoltage”

$V$ is the operating bias voltage and $V_b$ is the breakdown voltage

When many cells are fired at the same time, the output is the sum of the standard pulses.

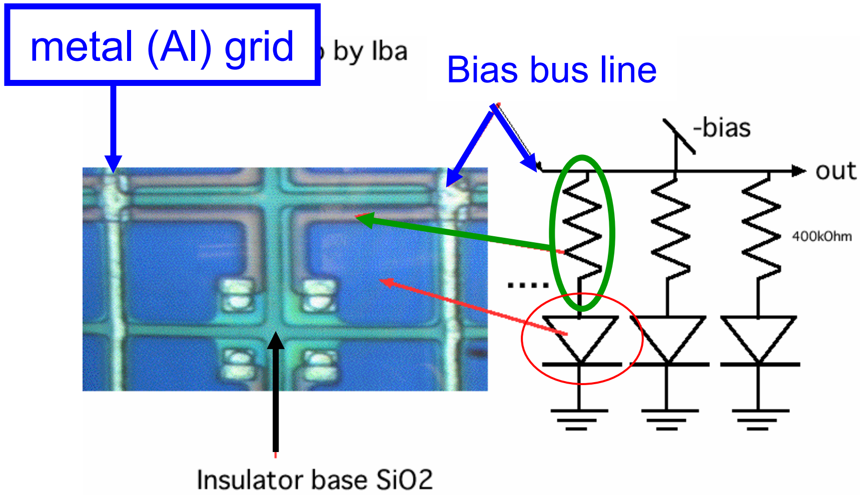


all pixels connected in parallel
only one signal line

➔ output $A = \Sigma A_i$ (individual pixel signals)
sometimes non-linear because of crosstalk

typical Bias voltage ~ 2 V above breakdown

# SiPM properties

G-APDs behave like PMTs, thereby the name: Silicon Photomultiplier (SiPM)

The gain is in the range of $10^5$ to $10^7$. Single photons produce a signal of several mV on a 50 Ohm load. No or at most a simple amplifier is needed!

Pickup noise is no more a concern (no shielding).

There is no nuclear counter effect – even a heavily ionizing particle produces a signal which is not bigger than that of a photon.

Since there are no avalanche fluctuations (as we have in normal APDs) the excess noise factor is very small, could eventually be one.

Grooms theorem (the resolution of an assembly of a scintillator and a semiconductor photodetector is independent of the area of the detector Nucl. Instr. and Meth. 219 (1984) 141) is no more valid.

# SiPM properties: single pixel resolution

SiPM output is the analog sum of all pixel signals

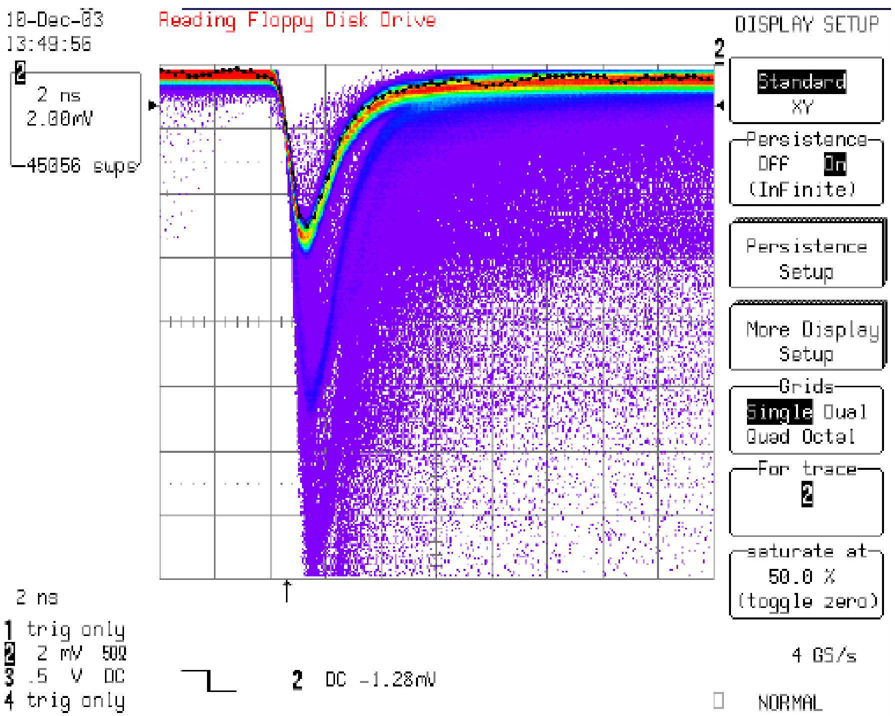


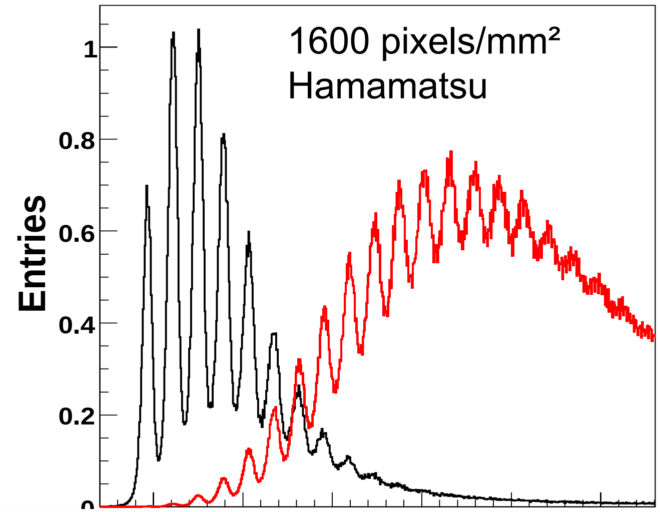


T=22 C, λ = 550 nm, AMPD type: PC1-mikr.

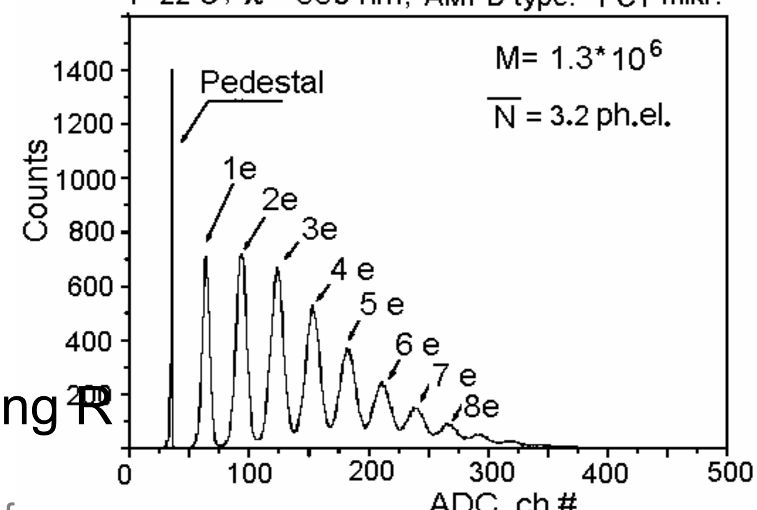


AMPD tested in LNP JINR and PSI

high gain ➔ pixel signal visible on scope

- signal rise time < 1 ns
- fast fall ~ 5-10 ns

recovery time tunable by choice of quenching R

$\tau \sim R_{pixel} C_{pixel} \sim 20 – 500$ ns

# Dynamic range

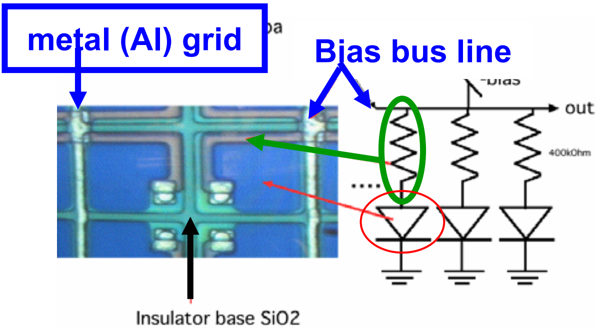


➔ output = Σ pixel signals

output ≤ total N pixel

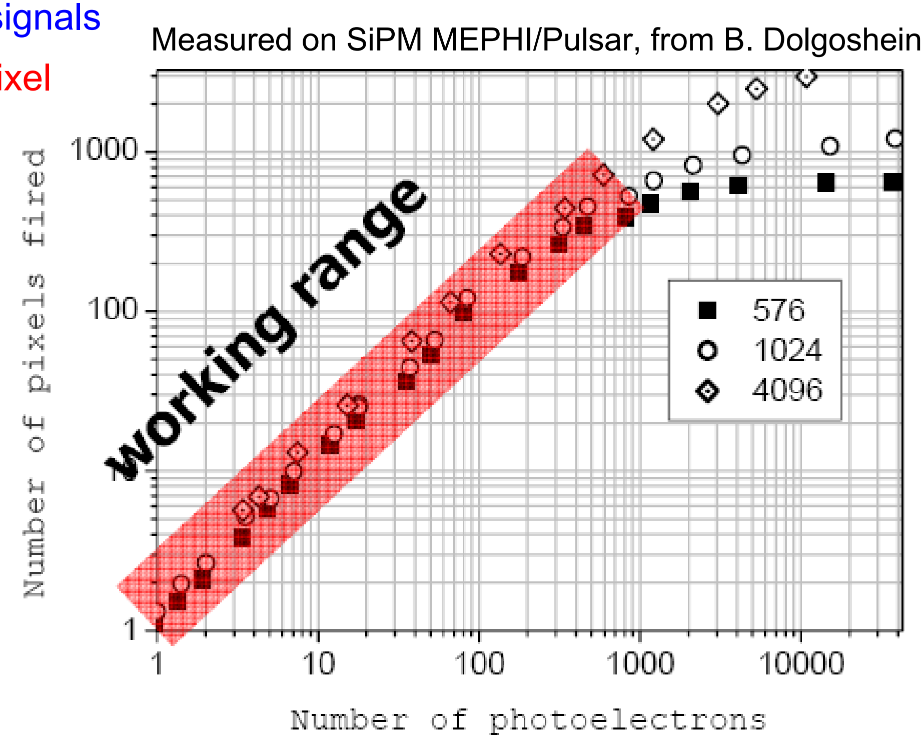


Dynamic range naturally limited by number of pixels

Optimal working condition:
number of photo-electrons < N pixels

from probability considerations:

$$A \approx N_{pixels} = N_{total} \cdot \left[ 1 - e^{\frac{N_{photon} \cdot PDE}{N_{total}}} \right]$$

~20% deviation from linearity if 50% of pixels are fired

2 or more photons in one cell look exactly like 1 single photon

# Dark count rate

Only the very basics:

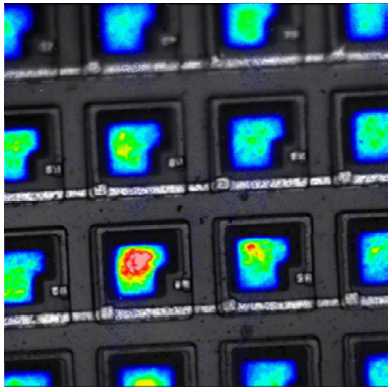

a SiPM pixel can be fired by an incoming photon but free carries can be generated also by thermal effects or tunneling (field-assisted generation)

these lead to a dark count rate of 100 kHz – 10 MHz / mm$^2$ (@25°C) with threshold at half of one photo-electron amplitude (~0.5x10$^6$)

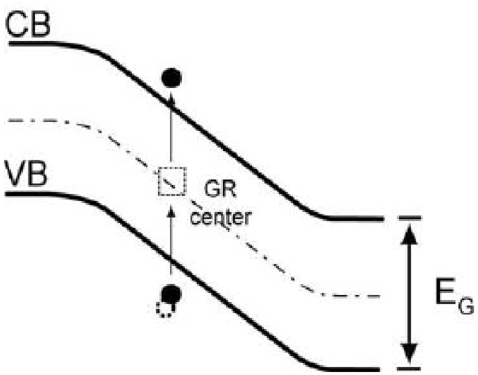


Free carrier generation
by thermal effects

Depends on temperature
(can be cooled away)

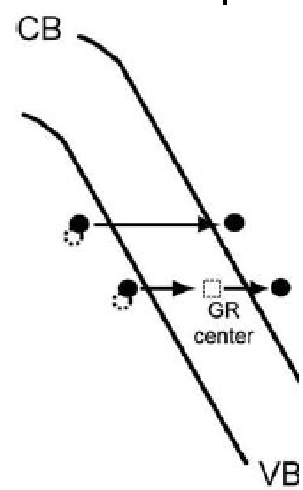


Tunneling

Depends on operation voltage (E field)
Influenced by technological design

# Dark count rate

In first order the thermal generation of carriers is proportional to the depleted volume which is for every cell the area times the thickness of all the layers on top of the low ohmic substrate.

In the n-on-p type layers the electrons (in the p-on-n type layers the holes) drift towards the high field region of the junction.
The electrons will trigger there a breakdown with higher probability than the holes.
In a G-APD with a p-on-n type substrate the volume of the p-layer is much smaller than in the G-APD on a n-on-p type substrate.

Devices with a p-on-n-type substrate show smaller dark count rates.

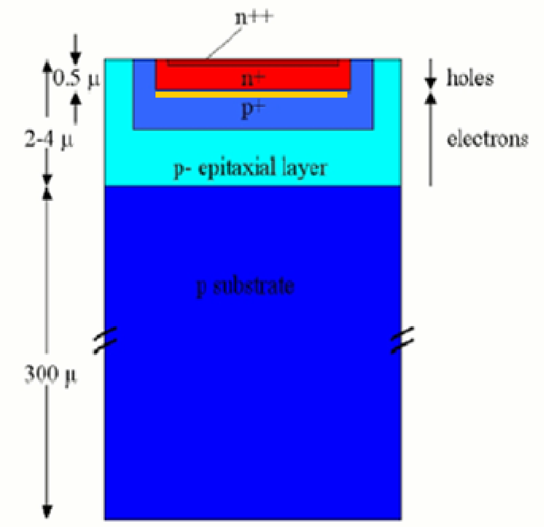


n-on-p type

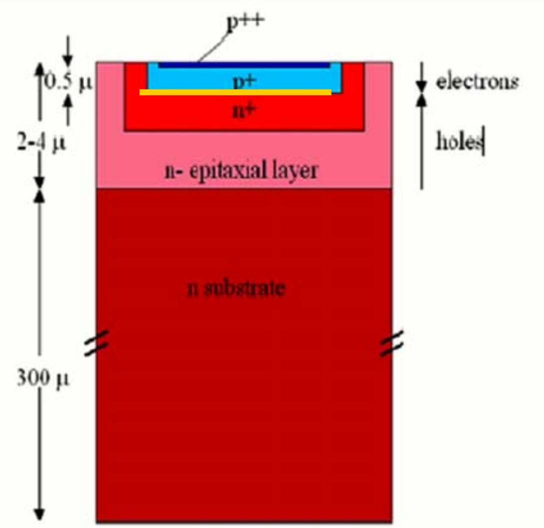


p-on-n type

# Dark count rate

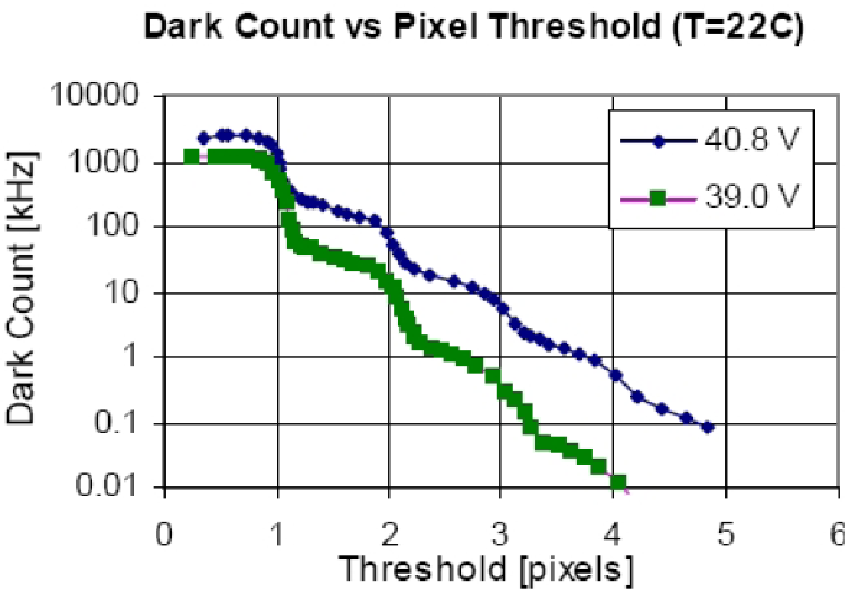


dark count rate > 0.5 pixel ~ MHz
decrease rapidly with threshold

➔ what is the relevant threshold for physics?

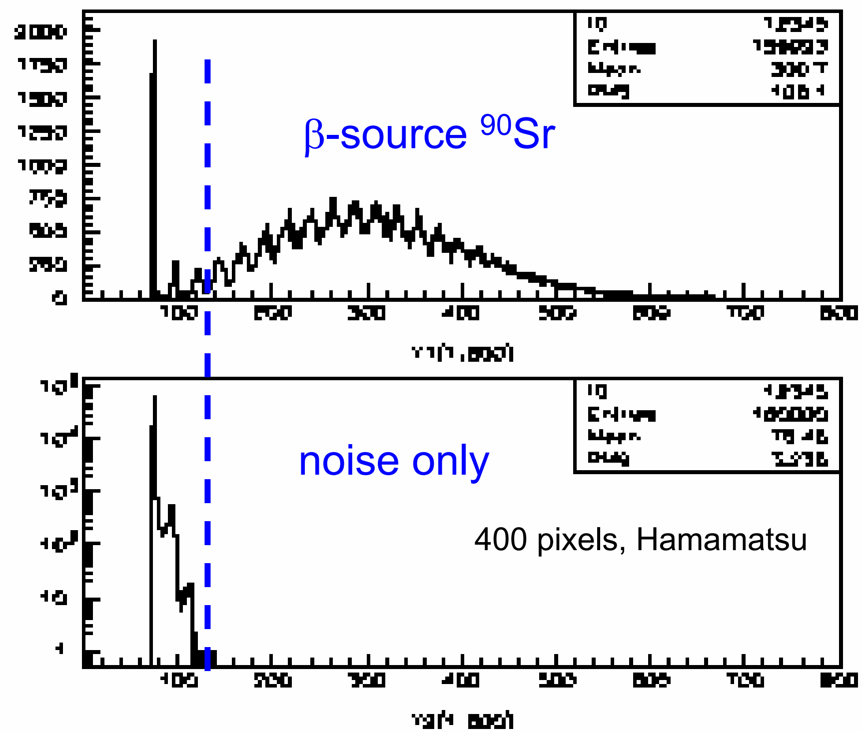


Blue sensitive SiPM directly coupled on $3x3x0.5\ cm^3$ scintillator tile

# Pixel: a closer look

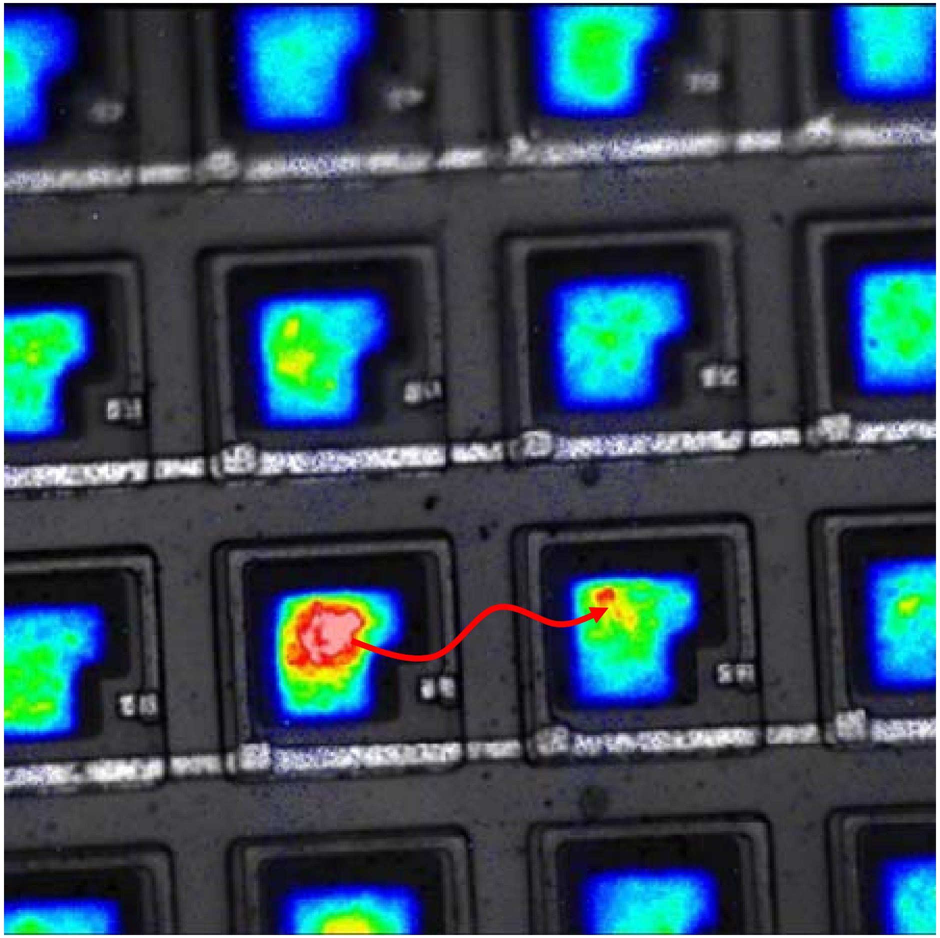

Emission microscopy picture, MPI

## Optical inter-pixel cross talk:

during Geiger avalanche
~3 emitted $\gamma$ / $10^5$ carriers
with $E\gamma > 1.14$ eV

*A. Lacaita et al, IEEE TED (1993)*

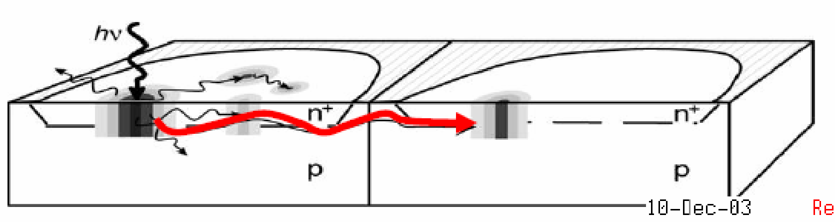


➔Leads to artificial increase of signal

# Suppress optical cross talk

Possible counter measures:

- lower $V_{Bias}$ → lower breakdown probability (lower PDE)
- optical insulation between pixels ➔
- technological modifications: i.e. smaller $C_{pixel}$

Inter-pixel trench to block $\gamma$

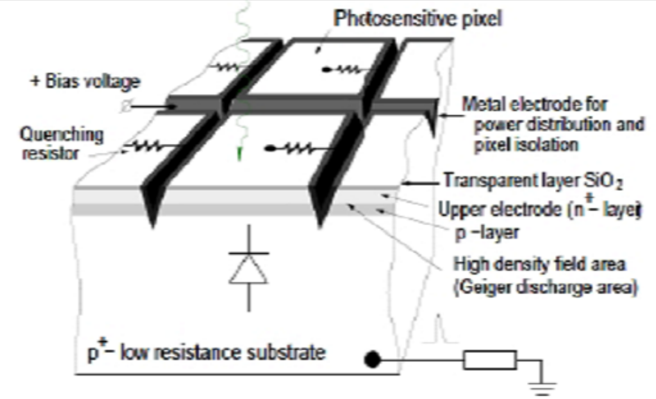


Before

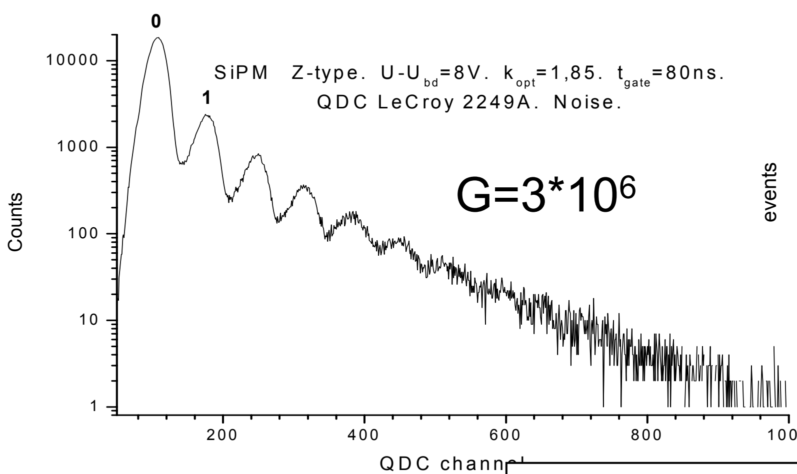


After

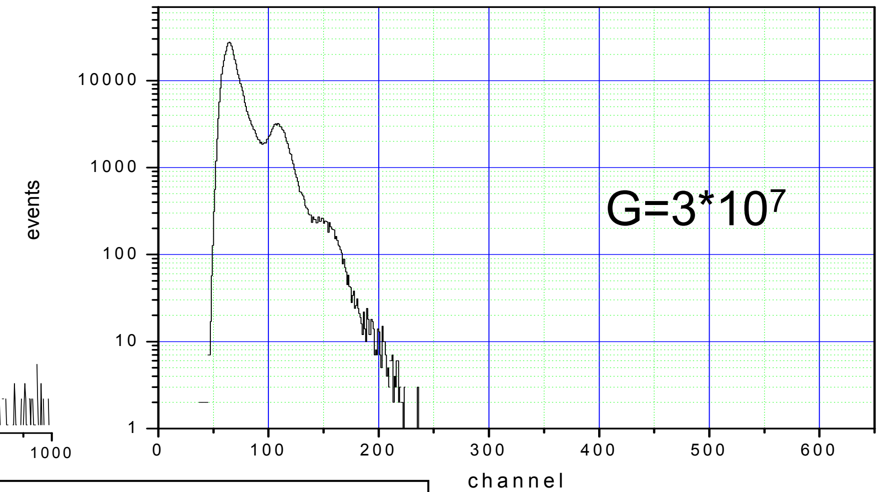


SiPM, MEPHI/Pulsar, PRELIMINARY

# After pulse

In the silicon volume, where a breakdown happened, a plasma with high temperatures (few thousand degree C) is formed and deep lying traps in the silicon are filled. Carrier trapping and delayed release causes afterpulses during a period of several 100 ns after a breakdown.

The probability for afterpuses increases with higher overvoltage (higher gain).

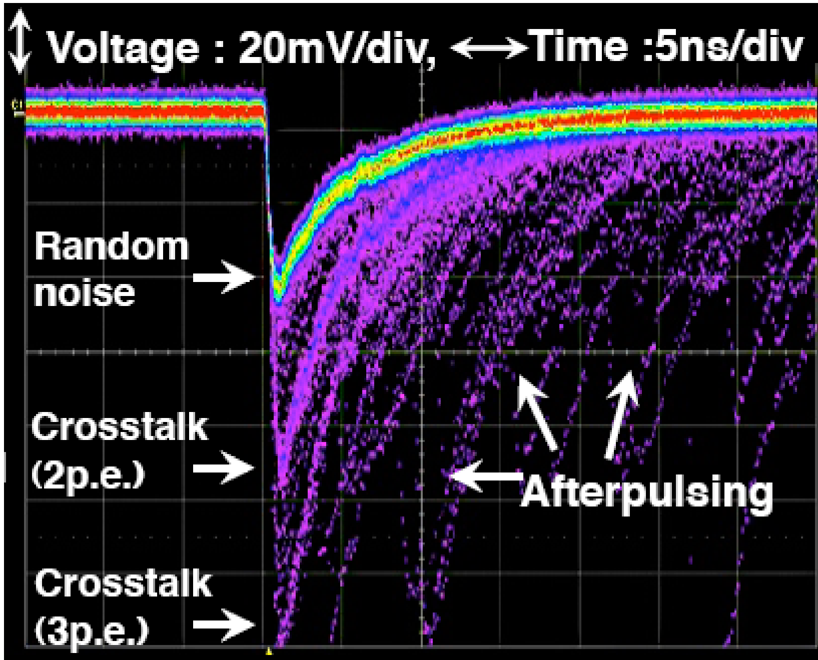

Fig.1 Persistence of Dark Noise

# Photon Detection Efficiency (PDE)

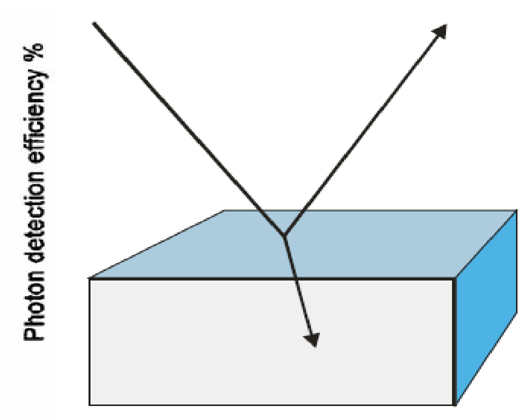


PDE is the product of mainly three components:

$PDE = QE \cdot \varepsilon \cdot P_{Geiger}$

- intrinsic Quantum Efficiency (~80% for Si) ➔ λ dependent
- fraction of sensitive area (20-80%) ➔ technology
- probability of Geiger breakdown (~100%) ➔ $V_{Bias}$ (or E) dep.

- surface reflection losses
- pixel recovery time ($R_{pixel}$)

influence of quantum efficiency

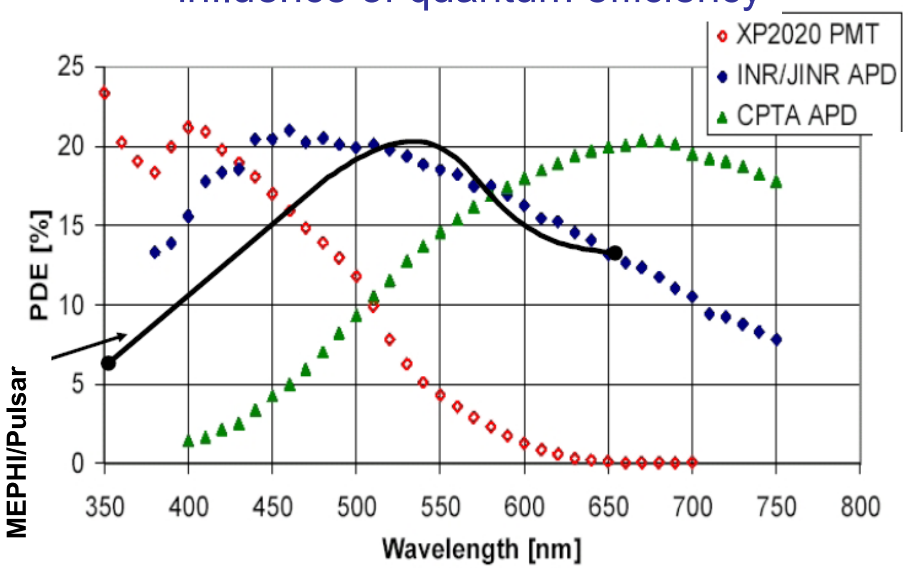


influence of sensitive area

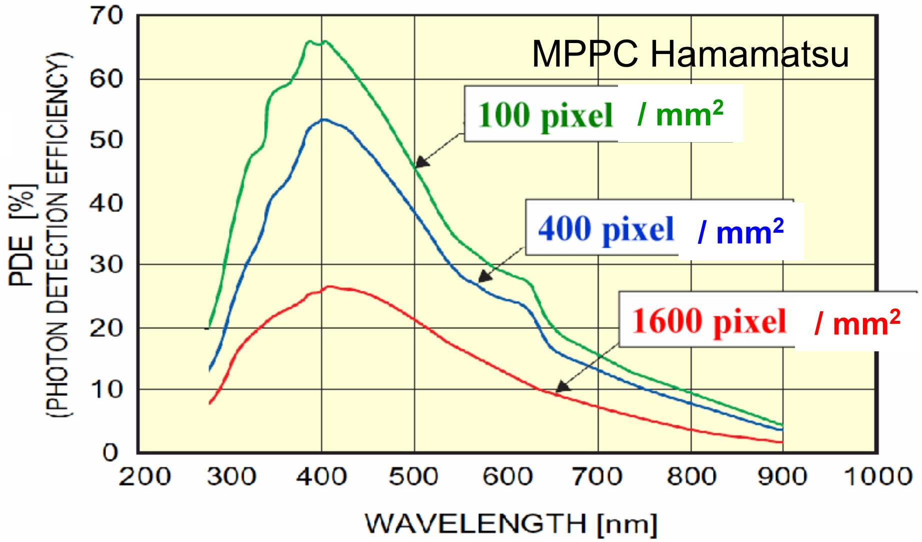


=400nm, including the cross-talk and after pulse

# Photon Detection Efficiency (PDE)

The triggering probability depends on the position where the primary electron-hole pair is generated and it depends on the overvoltage.

Electrons have in silicon a better chance to trigger a breakdown than holes. Therefore a conversion in the p+ layer has the highest probability to start a breakdown.

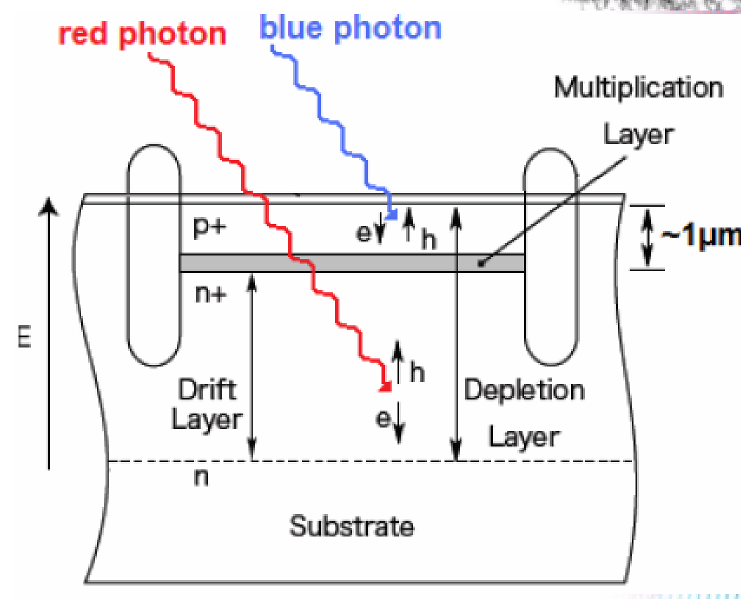


Wavelength dependence of PDE linked to depth of penetration of photon

| | |
|---|---|
| Blue (470nm) | 0.6 µm |
| Green (525nm) | 1.2 µm |
| Yellow (590nm) | 2.2 µm |
| Red (625nm) | 2.9 µm |

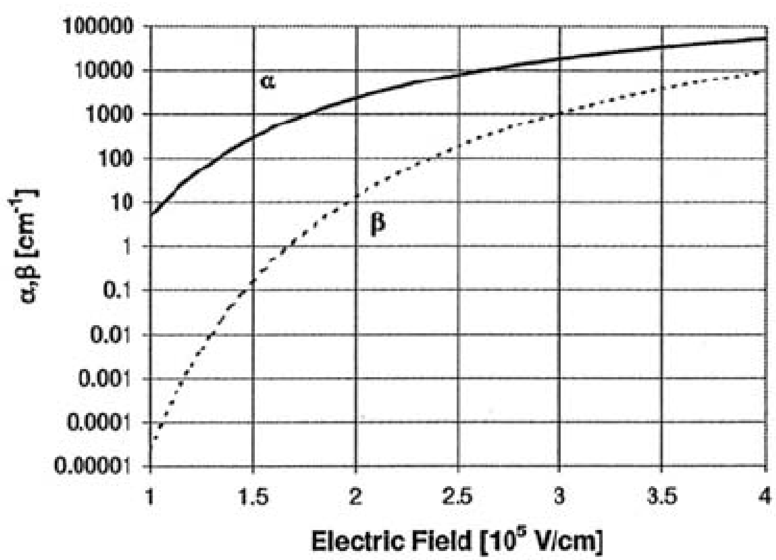


Ionization coefficients for electrons (α) and holes (β) in silicon

# Photon Detection Efficiency (PDE)

Photons with short wavelengths will be absorbed in the very first layer of Si and create an electron-hole pair.

In a structure with a n-type substrate (right) the electrons drift towards the high field of the p-n junction and trigger with high probability a breakdown.

A G-APD made on a n-type substrate will be preferential sensitive for blue light.

A G-APD made on a p-type substrate (left) needs long wavelengths for the creation of electrons in the p-layer behind the junction and will have the peak sensitivity in the green/red.

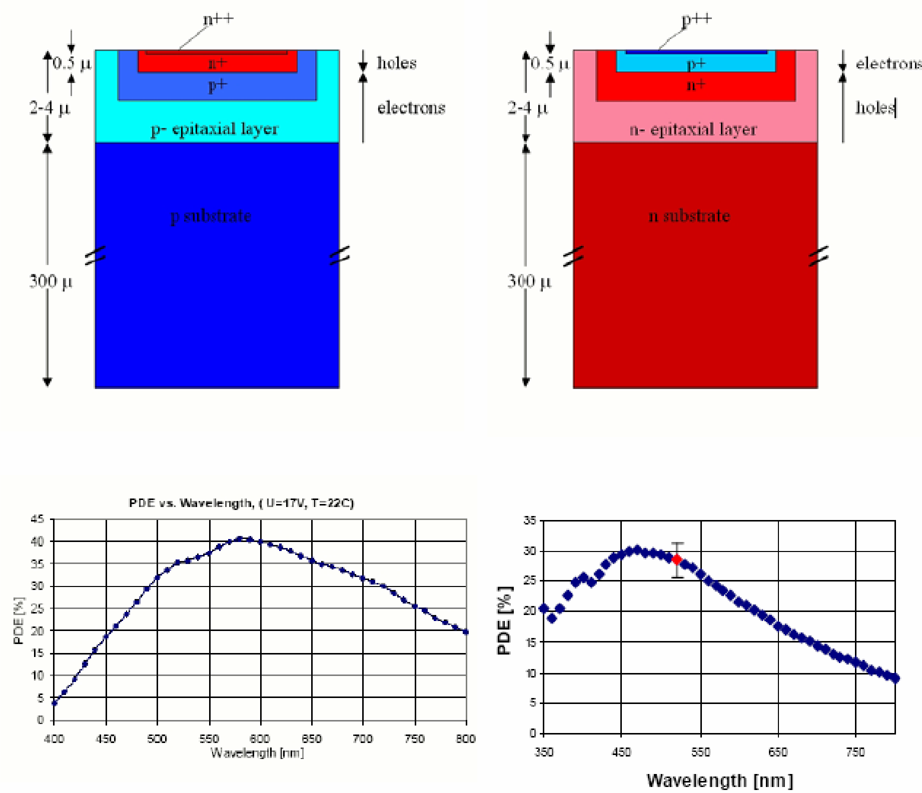


Photonique/CPTA (SSPM_0710G9MM)

Hamamatsu (PSI-33-050C)

# Consequences of the basic properties

We want the highest possible PDE and the best time resolution.

➔ operate G-APDs at high overvoltage (high gain)

Consequences are:

- Large number of dark counts
- High crosstalk probability
- High afterpulse probability
- Large currents and possible self-heating in a high rate environment

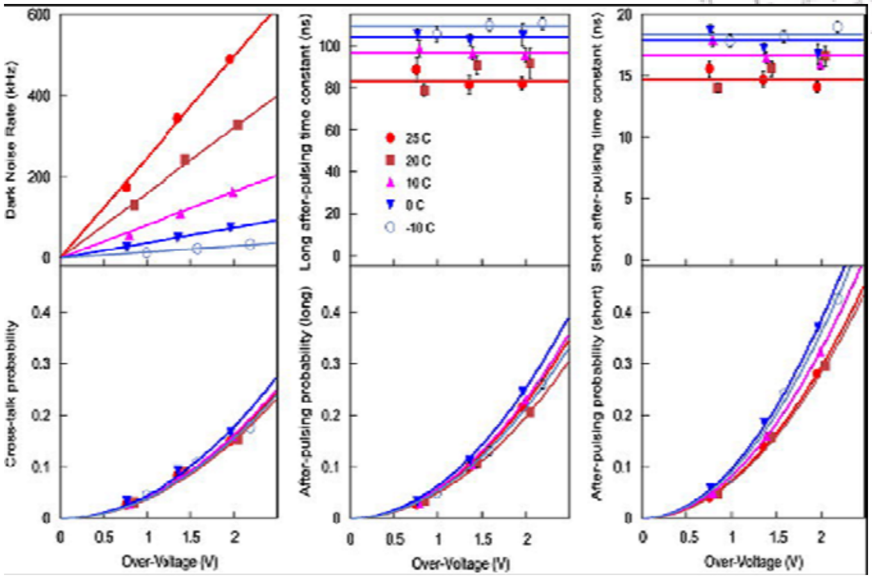


The operation is different compared to that of a PMT where the gain can be chosen in a wide range with no or little consequences on the PDE.

G-APDs need a re-engineering (e.g. reduction of C) when the gain has to be modified.

# SiPM voltage dependence

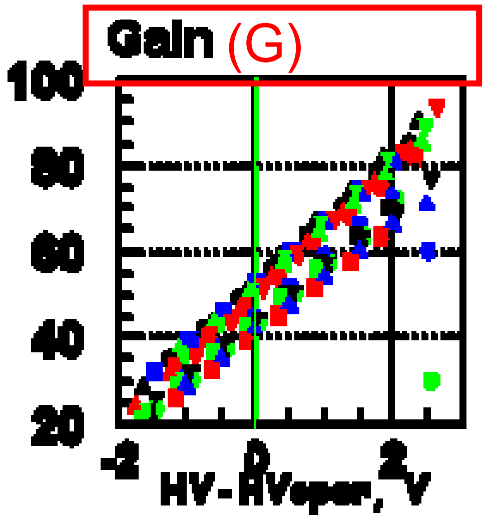


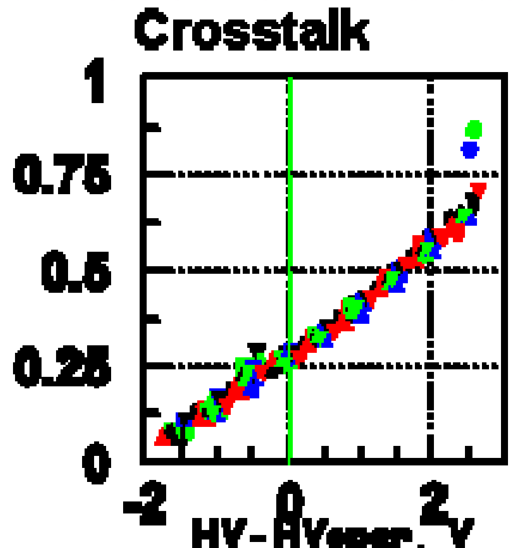


Gain (G)

$$\frac{dG}{dV} \sim 2.5 \frac{\%}{0.1V}$$

Total Charge (Q) = G*PDE

$$\frac{dQ}{dV} \sim 7.0 \frac{\%}{0.1V}$$

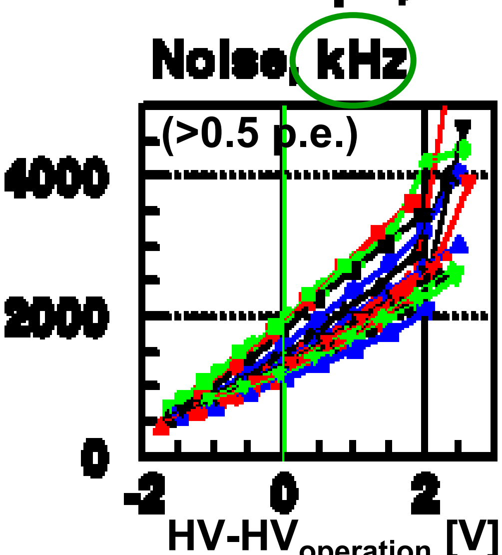


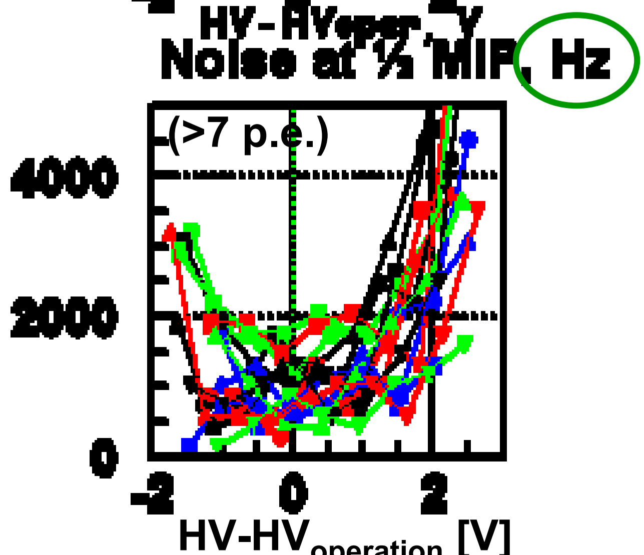


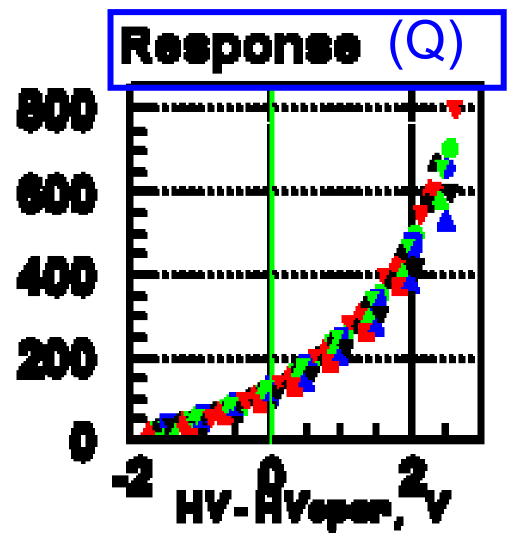


characterization of 4000 SiPM MEPHI/Pulsar, from E. Tarkovski, ITEP

# SiPM temperature dependence

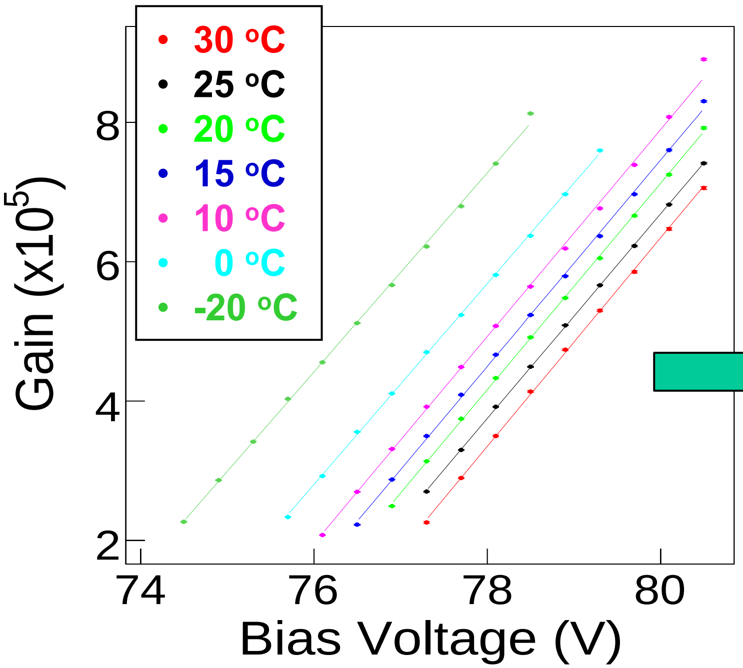


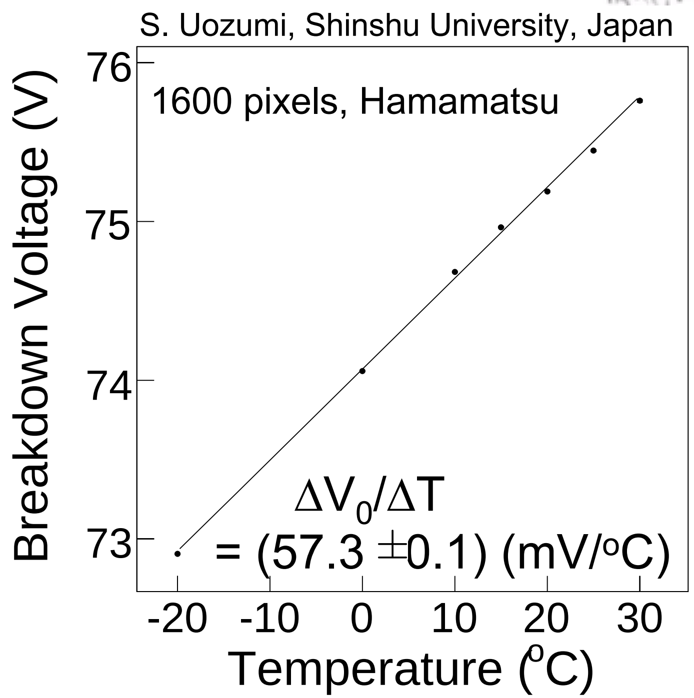


Gain = C ($V_{bias}$-$V_0$) / e

C : Pixel capacity

$V_0$ : Breakdown voltage

$V_0$ is linear to temperature.

➔temperature changes affect the over-voltage = $V_{bias}$-$V_0$(T)

→ therefore all SiPM properties

**Gain (G)**

$$\frac{dG}{dT} \sim -1.7 \frac{\%}{K}$$

**Total Charge (Q) = G*PDE**

$$\frac{dQ}{dT} \sim -4.5 \frac{\%}{K}$$

🡐 1200 pixels, MEPHI/Pulsar

# Summary of SiPM features

High gain (~$10^6$) ➔ simplest r/o electronics
Low electronics noise
Low bias voltage (~50 V)
Low power consumption (≤50 μW/mm$^2$)
Insensitivity to magnetic field ➔ next generation of HEP detectors
Compact and light ➔ direct couple to active material / space mission
Excellent photon counting capability ➔ astro-particle physics
Very low charge particle sensitivity (negligible nuclear counting effect)
Very good timing (≤100 ps) ➔ medical applications
Small recovery time
Good temperature and voltage stability
Room temperature operation
Relatively low cost ➔ high r

**Drawbacks and limitations:**

- Small size (established up to 3x3mm²)
- Not enough PDE (~20-40%)
- High dark rate
- Limited dynamic range

- Optical crosstalk being reduced (<10%)
- Sensitivity to blue established, what about UV?

➔ Fast developing technology
Solutions to the remaining open issues are coming

# The measurement of showers

or “from energy to signal”

Step 1: Convert energy to light

Step 2: Convert light to electrical signal

Step 3: Reading an electrical signal

# Signal Acquisition

## Determine energy deposited and event time in detector

- Detector signal generally a short current pulse:

| | |
|---|---|
| – thin silicon detector (10 –300 µm): | 100 ps–30 ns |
| – thick (~cm) Si or Ge detector: | 1 –10 µs |
| – proportional chamber: | 10 ns –10 µs |
| – Microstrip Gas Chamber: | 10 –50 ns |
| – Scintillator+ PMT/APD: | 100 ps–10 µs |

$$E \propto Q_s = \int i_s(t)\,dt$$

- Necessary to integrate detector signal current:
  - – integrate charge on input capacitance
  - – use integrating (“charge sensitive”) preamplifier
  - – amplify current pulse and use integrating ADC

# Relevant aspects of electronics for calorimetry

Dynamic range: maximum signal/minimum signal (or noise)

typically: $10^3$–$10^5$

often specified in dB (=20log $V_{max}/V_{min}$) = 60 –100 dB

also in bits: $2^n = V_{max}/V_{min}$ = 10 –18 bits

The large dynamic range is a key parameter for calorimeter electronics

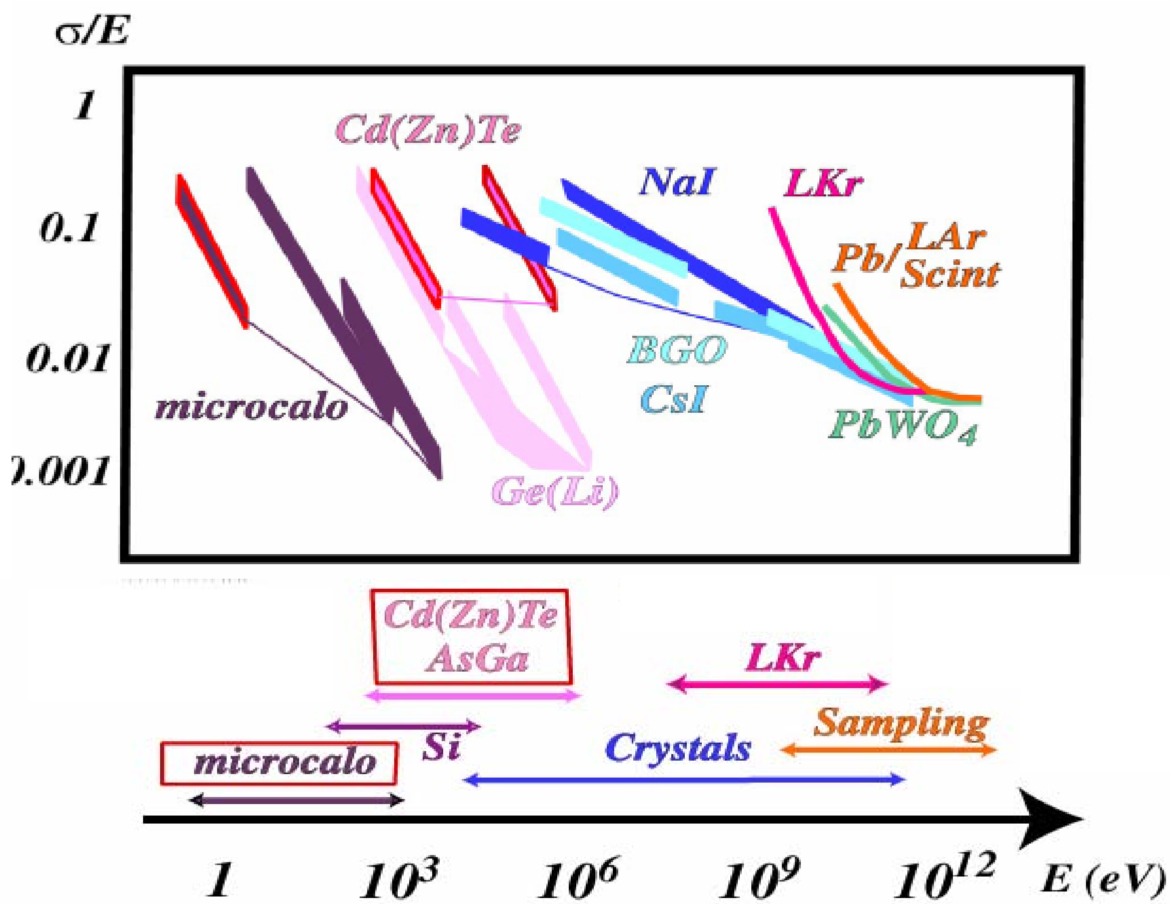

# Readout electronics requirements

Low noise

Low power

High speed


High reliability

Large dynamic range

Radiation hardness

Low cost !

(and even less)

Low material

# Overview of readout electronics

Most front-ends follow a similar architecture

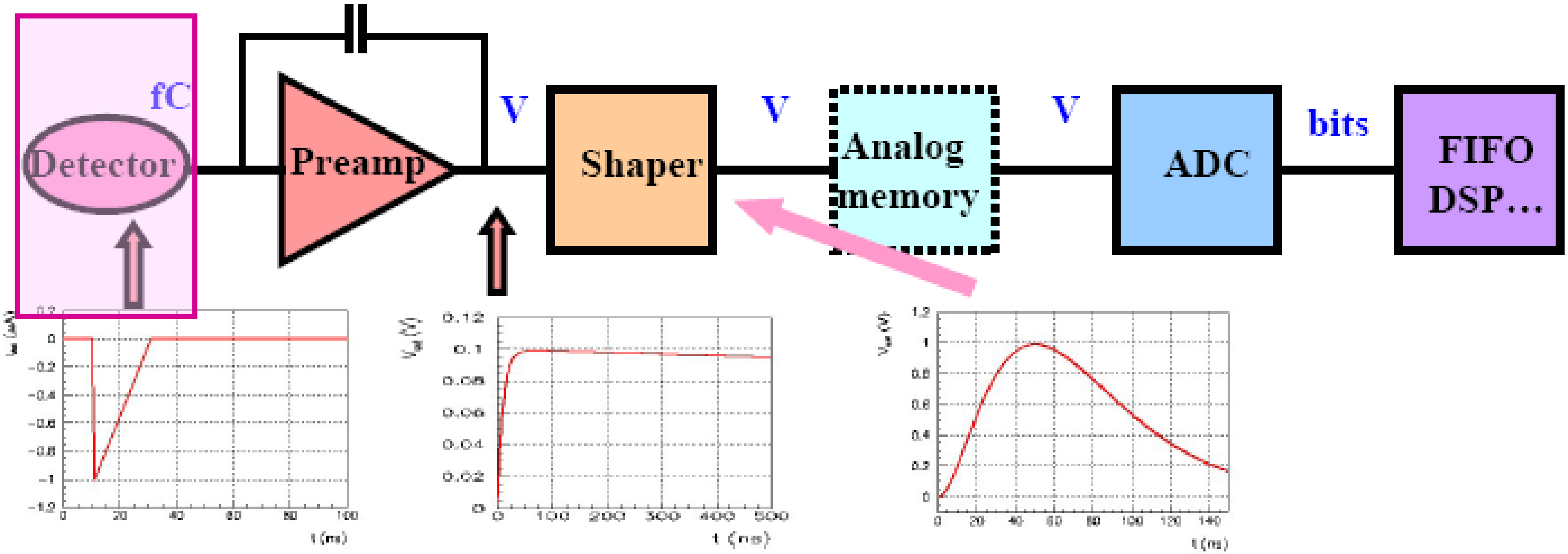


- Very small signals (fC) -> need amplification
- Measurement of amplitude and/or time (ADCs, discriminator, TDCs)
- Thousands to millions of channels

# Detector(s)

A large variety of detectors

But similar modeling

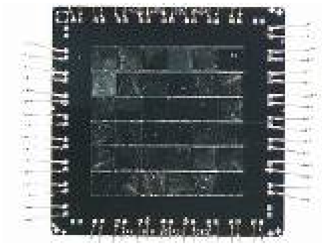

6x6 pixels,4x4 $mm^2$
HgTe absorbers, 65 mK
12 eV @ 6 keV

PMT in ANTARES

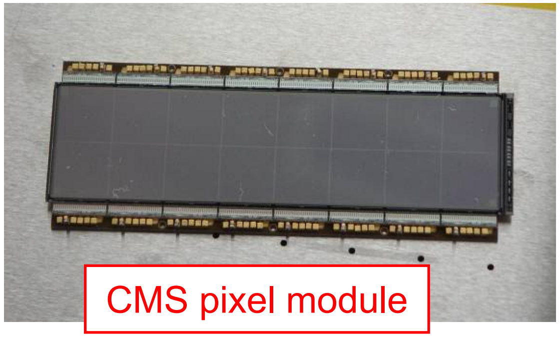

CMS pixel module

ATLAS LAr calorimeter

# Detector modeling

Detector = capacitance Cd

- Pixels : 0.1-10 pF
- PMs : 3-30 pF
- Ionization chambers: 10-1000 pF
- Sometimes effect of transmission line

Signal : current source

- Pixels : ~100 $e^-/\mu m$
- PMs : 1 photoelectron -> $10^5$-$10^7$ $e^-$
- Modeled as an impulse (Dirac) : $i(t)=Q_0\delta(t)$

Missing :

- High Voltage, bias
- Connections, grounding
- Neighbors
- Calibration…

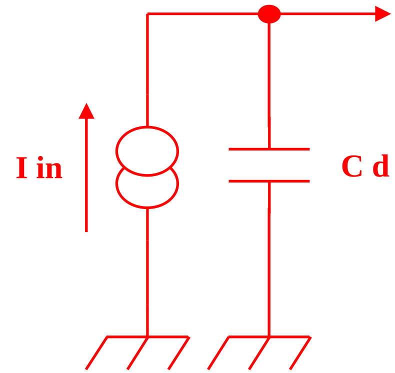


Detector model

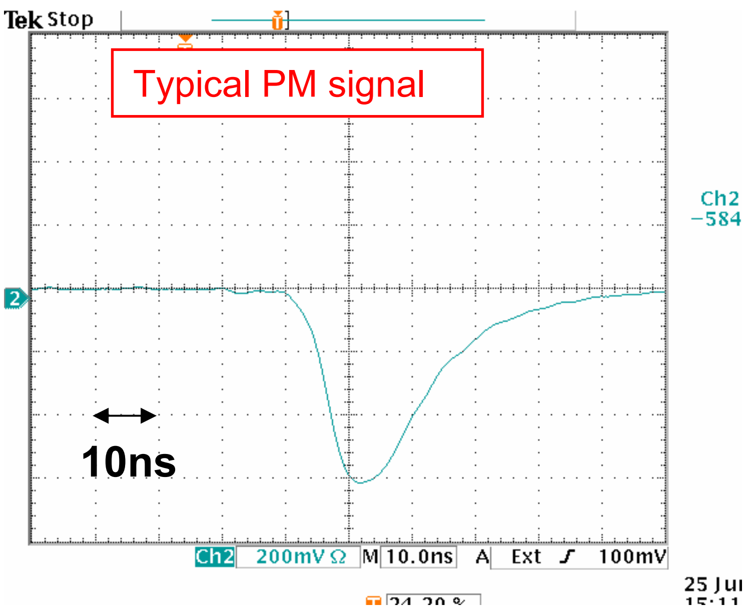

# Overview of readout electronics

Most front-ends follow a similar architecture

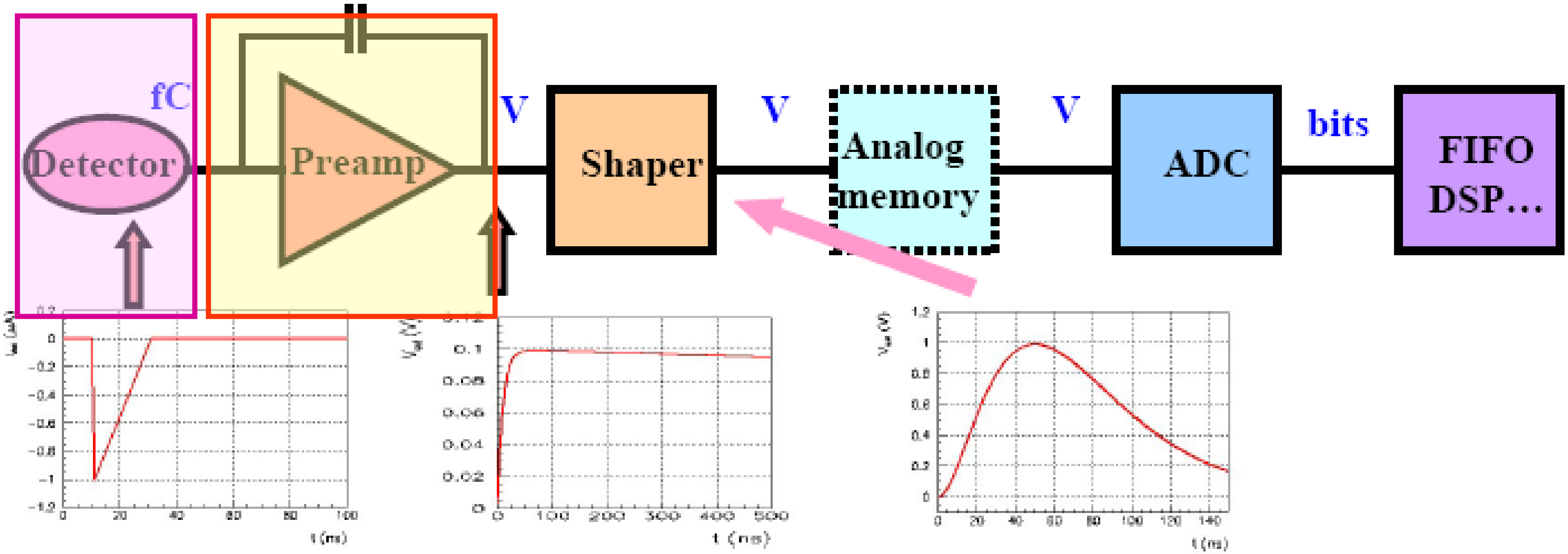


- Very small signals (fC) -> need amplification
- Measurement of amplitude and/or time (ADCs, discriminator, TDCs)
- Thousands to millions of channels

# Reading the signal

## Signal

- Signal = current source
- Detector = capacitance $C_d$
- Quantity to measure
  - Charge ➔ integrator needed
  - Time ➔ discriminator + TDC

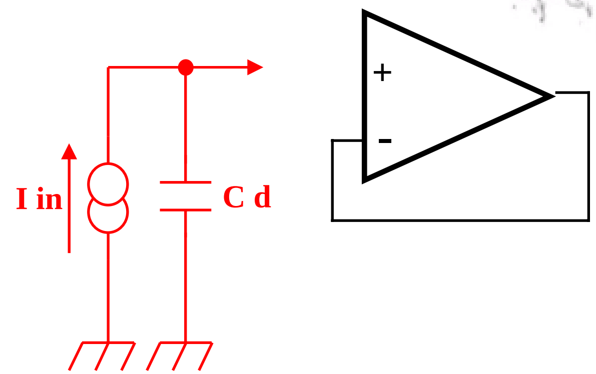


Voltage readout

## Integrating on $C_d$

- Simple : $V = Q/C_d$
- « Gain » : $1/C_d$ : 1 pF ➔ 1 mV/fC
- Need a follower to buffer the voltage ➔ parasitic capacitance
- Gain loss, possible non-linearity
- crosstalk
- Need to empty Cd…

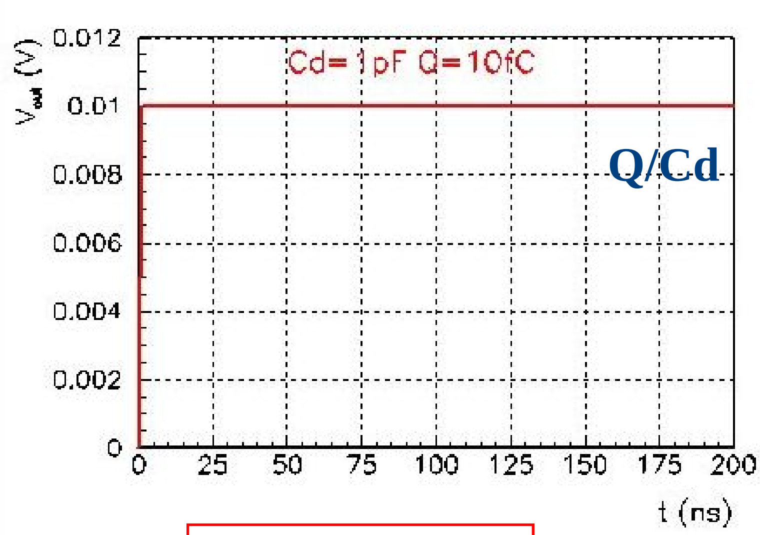


Impulse response

# Reading the signal (II)

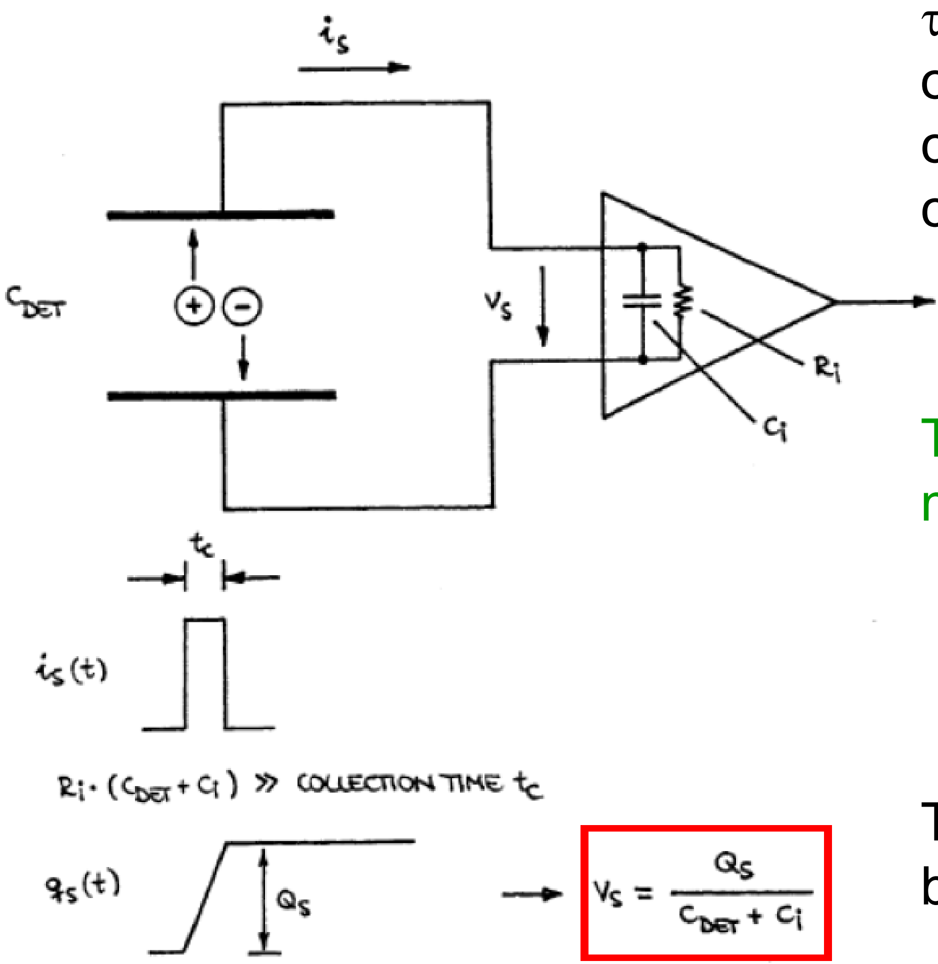


If the input time constant of the amplifier, $\tau = C_i R_i$ is large compared to the duration of the current pulse of the detector, $t_c$ the current pulse will be integrated on the capacitance $C_i$.

The resulting voltage at $C_i$ and $R_i$ is

$$v_i = v_s = Q_s / (C_{det} + C_i)$$

The fraction of the signal charge measured is:

$$\frac{Q_i}{Q_s} = \frac{C_i v_i}{v_i (C_i + C_{det})} = \boxed{\frac{1}{1 + C_{det}/C_i}}$$

The dynamic input capacitance $C_i$ should be >> $C_{det}$ to get a good ratio close to 1

Depends on the detector capacitance

# Charge sensitive amplifier

Add feedback capacitor $C_f$:

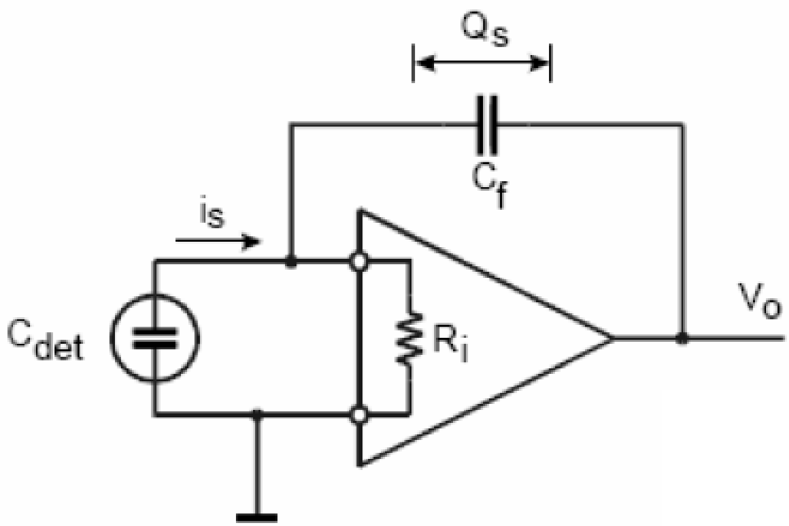


Voltage gain $dV_o/dV_i$=-A ➔ $v_o=-Av_i$
Input impedance = ∞ (no signal current flows into amplifier input)

Voltage diff. across $C_f$: $v_f=(A+1)v_i$
➔Charge deposited on $C_f$: $Q_f=C_f v_f$
$Q_i = Q_f$ (since $Z_i = \infty$)
➔Effective input capacitance

$$C_i = Q_i/v_i = C_f(A+1)$$

*"dynamic input capacitance"*

Amplifier gain:

$$A_Q = \frac{dV_o}{dQ_i} = \frac{A \cdot v_i}{C_i \cdot v_i} = \frac{A}{C_i} = \frac{A}{A+1}\frac{1}{C_f} \approx \frac{1}{C_f} \qquad (A >> 1)$$

# Charge sensitive amplifier (II)

So finally the fraction of charge signal measured by the amplifier is:

$$\frac{Q_i}{Q_s} = \frac{C_i v_i}{v_i(C_i + C_{\det})} = \frac{1}{1 + C_{\det} / C_i} \qquad C_f \approx \frac{A}{C_i} \quad (A >> 1)$$

Example: $A = 10^3$

$C_f = 1pF$ ➔ $C_i = 1nF$

$C_{det} = 10pF$ ➔ $Q_i/Q_s = 0.99$ $(C_i >> C_{det})$

$C_{det} = 500pF$ ➔ $Q_i/Q_s = 0.67$ $(C_i \sim C_{det})$

↑

Si det: 50um thick, 500mm$^2$ area

# Charge sensitive (pre)-amplifier

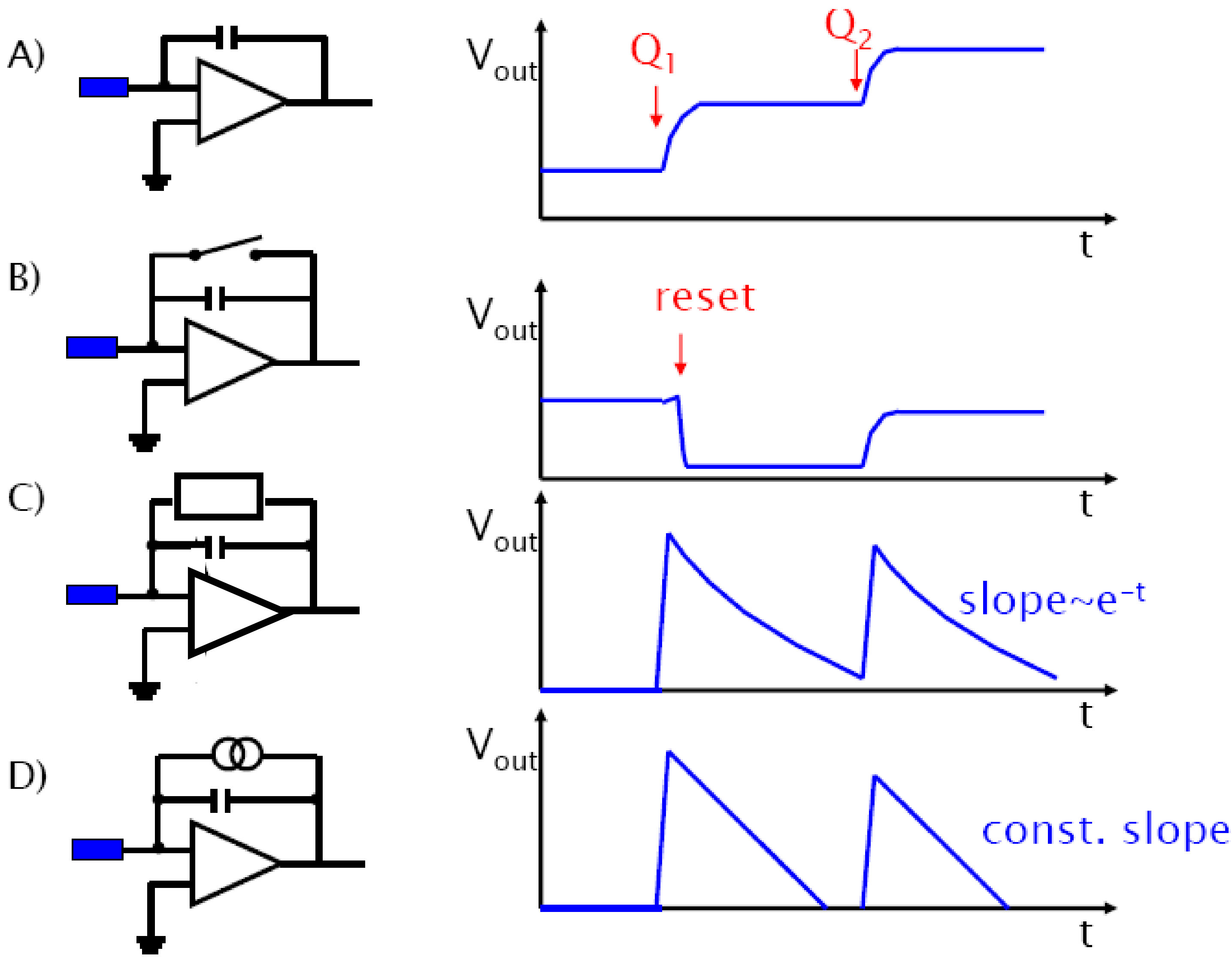

# Current preamplifiers :

Transimpedance configuration

- $V_{out}(\omega)/i_{in}(\omega) = - R_f / (1+Z_f/GZ_d)$
- Gain = $R_f$
- High counting rate
- Typically optical link receivers

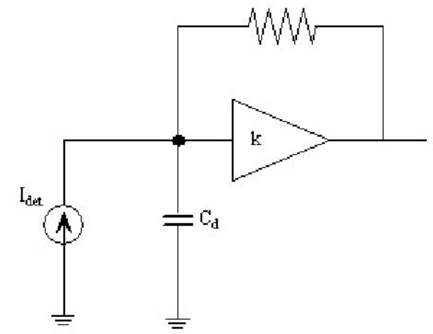


Easily oscillatory

- Unstable with capacitive detector
- Inductive input impedance

  $L_{eq} = R_f / \omega_C$
- Resonance at : $f_{res} = 1/2\pi \sqrt{L_{eq}C_d}$
- Quality factor : $Q = R / \sqrt{L_{eq}/C_d}$
  - $Q > 1/2$ -> ringing
- Damping with capacitance $C_f$
  - $C_f=2 \sqrt{(C_d/R_f\, G_0\omega_0)}$
  - Easier with fast amplifiers

Current sensitive preamp

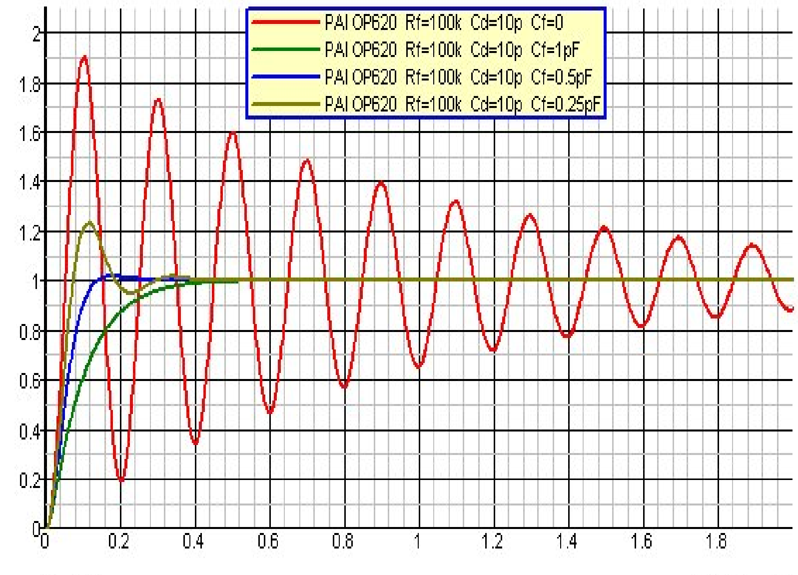


Step response of current sensitive preamp

# Charge vs Current preamps

Charge preamps

- Best noise performance
- Best with short signals
- Best with small capacitance

Current preamps

- Best for long signals
- Best for high counting rate
- Significant parallel noise

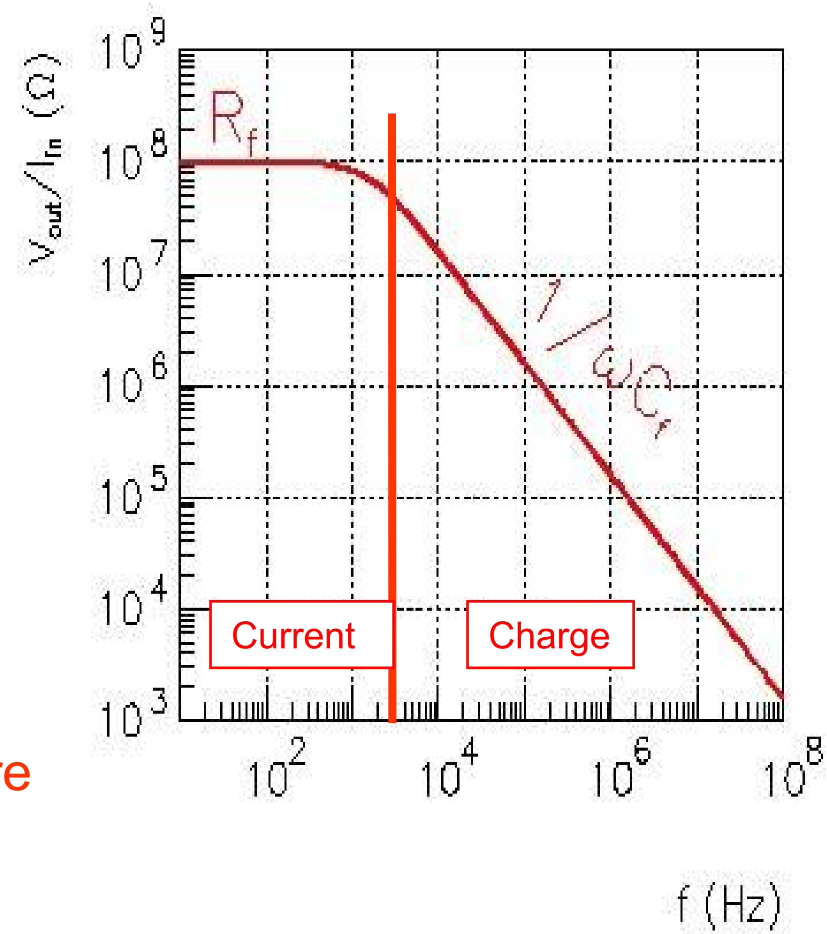


Charge preamps are not slow, they are long

Current preamps are not faster, they are shorter (but easily unstable)

# Overview of readout electronics

Most front-ends follow a similar architecture

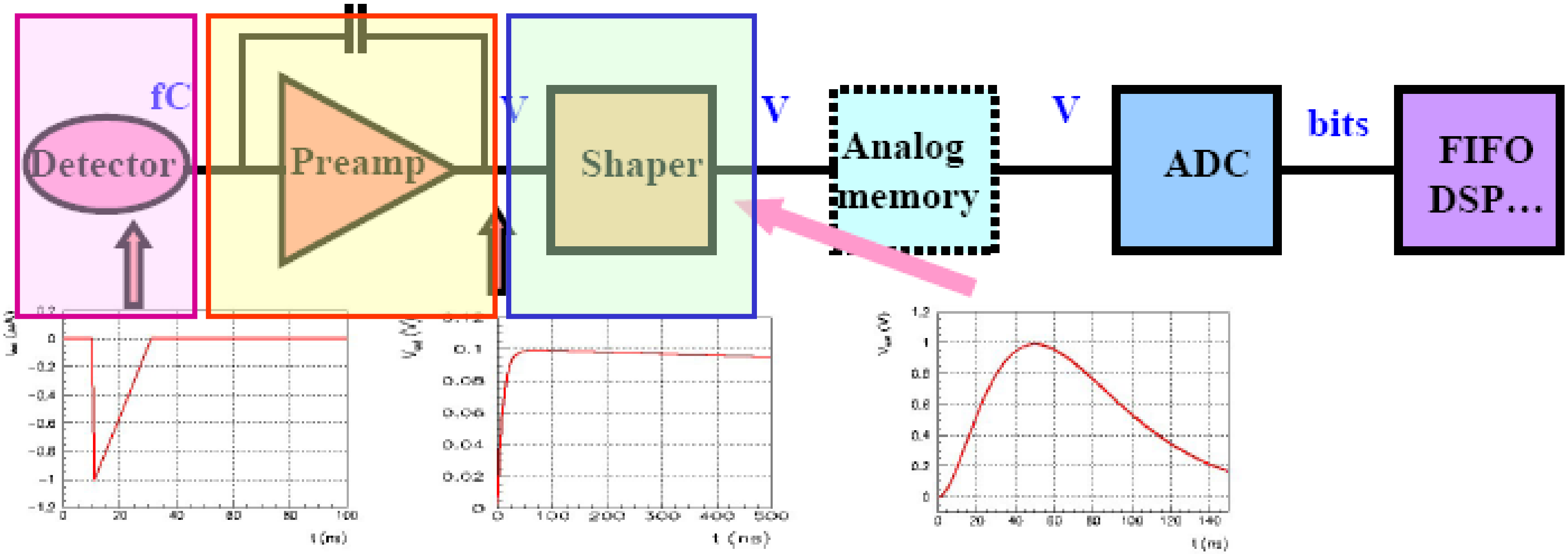


- Very small signals (fC) -> need amplification
- Measurement of amplitude and/or time (ADCs, discriminator, TDCs)
- Thousands to millions of channels

# Pulse shaping

Two conflicting objectives:

1) Limit the bandwidth to match the measurement time.
   ➔ too large bandwidth increases the noise

2) Contain the pulse width so that successive signal pulses can be measured without overlap (pile-up)

➔ Short pulse duration increases the allowed signal rate but also noise

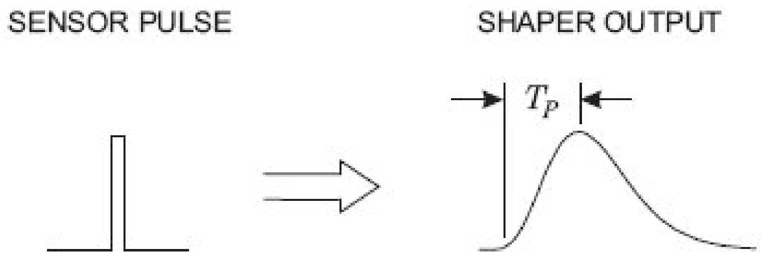


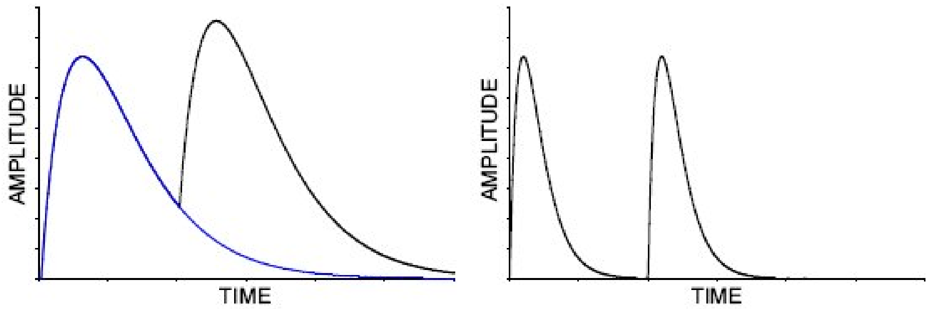

# CR-RC shaper

Example of a simple shaper: CR-RC

- the high-pass filter sets the duration of the pulse to have a decay time $\tau_d$
- the low-pass filter increases the rise time to limit the noise bandwidth

key design parameter: peaking time ➔ it dominates the noise bandwidth

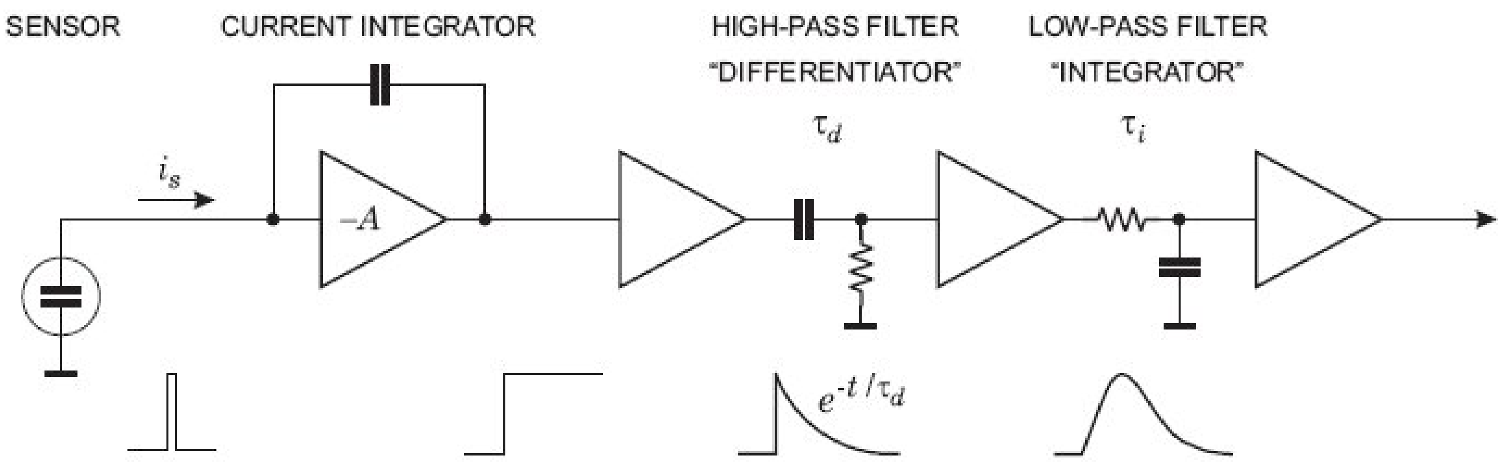

# CR-RC shaper (II)

Effect of a CR-RC shaper with
fix integrator time constant = 10ns
and variable differentiator time constant

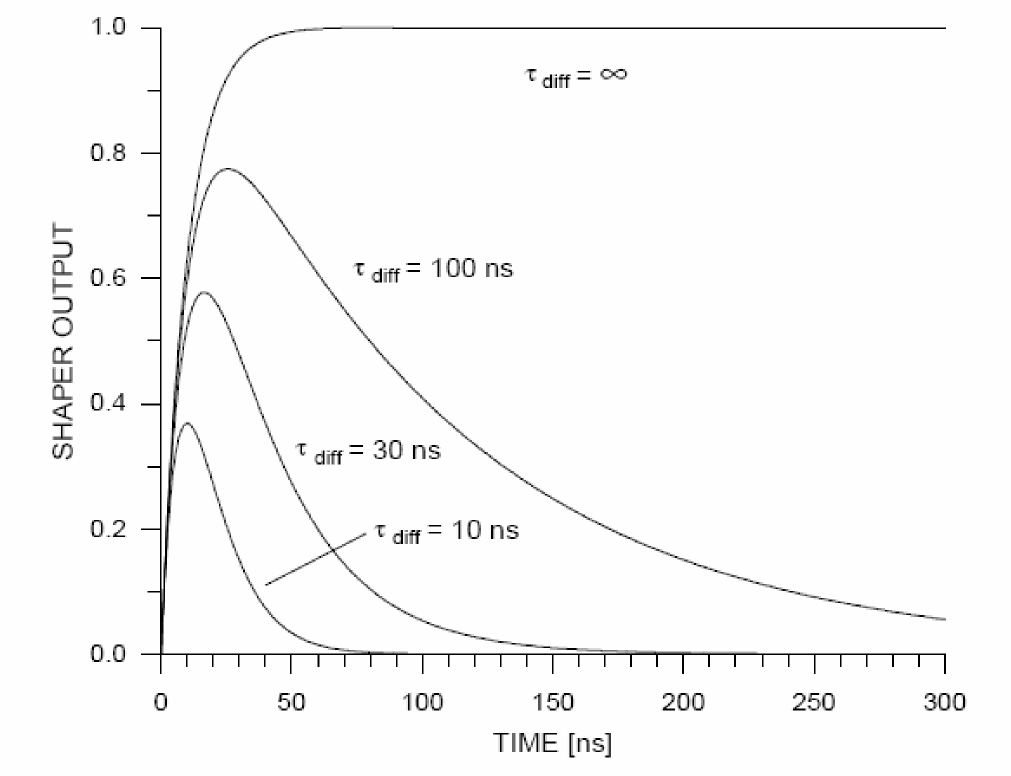

# Time measurements

Time measurements are characterized by their slope-to-noise ratio

Two main effects contribute to the deterioration of a time measurement i.e. time of threshold crossing fluctuates due to:

jitter

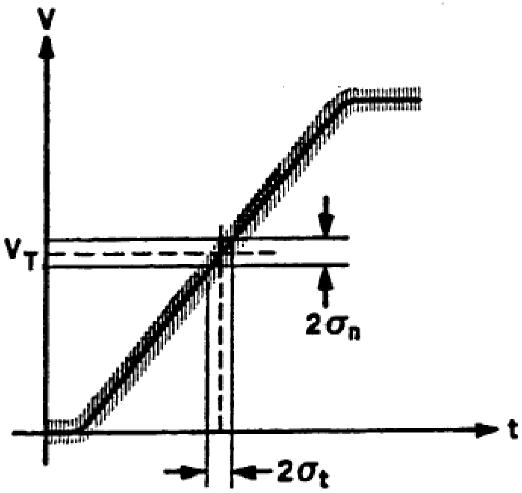


time walk

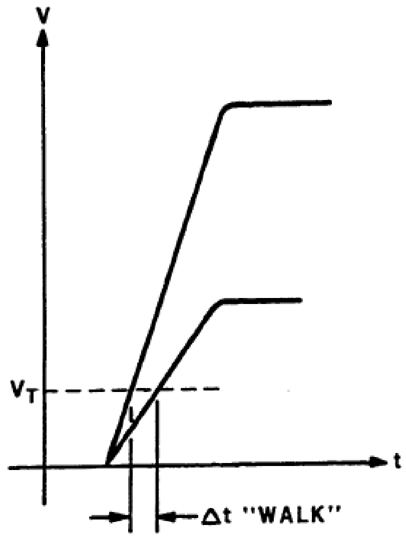


Often driven by the time constant of the shaper which determines rise time & amplifier bandwidth

# Readout overview

| Experiment | Shaping | tp | Technology | Dyn. Rge | Gains | ADC |
|---|---|---|---|---|---|---|
| ATLAS em | $CRRC^2$ | 50 ns | BiCMOS 1.2μ | 16 bits | 1-10-100 | 12 bits 5 MHz |
| ATLAS had | Bessel 9 | 50 ns | Passive hybrid | 16 bits | 1-64 | |
| BABAR | $CRRC^2$ | 400 ns | BiCMOS 1.2μ | 18 bits | 1-4-32-256 | 10 bits 4 MHz |
| CMS em | $RC^2$ | 50 ns | CMOS 0.25μ | 16 bits | 1-6-12 | 12 bits 40 MHz |
| CMS had | Gated int | 25 ns | | | | |
| DØ | CR | 350 ns | Bipolar hyb | 15 bits | 1-8 | 12 bits |
| FLC | CRRC | 150 ns | BiCMOS | 16 bits | 1-8-64 | |
| KLOE | Bessel 3 | 200 ns | Bipolar hyb. | 12 bits | 1 | |
| LHCb em | DLC | 50 ns | BiCMOS 0.8μ | 12 bits | 1 | 12 bits 40 MHz |
| NA48 | Bessel 8 | 70 ns | BiCMOS 1.2μ | 14 bits | 1-2.5-6-18 | 10 bits 40 MHz |
| Opera TT | $CRRC^2$ | 150 ns | BiCMOS 0.8μ | | 1 | |
| | | | | | | |

# Why bother about resolution and noise?

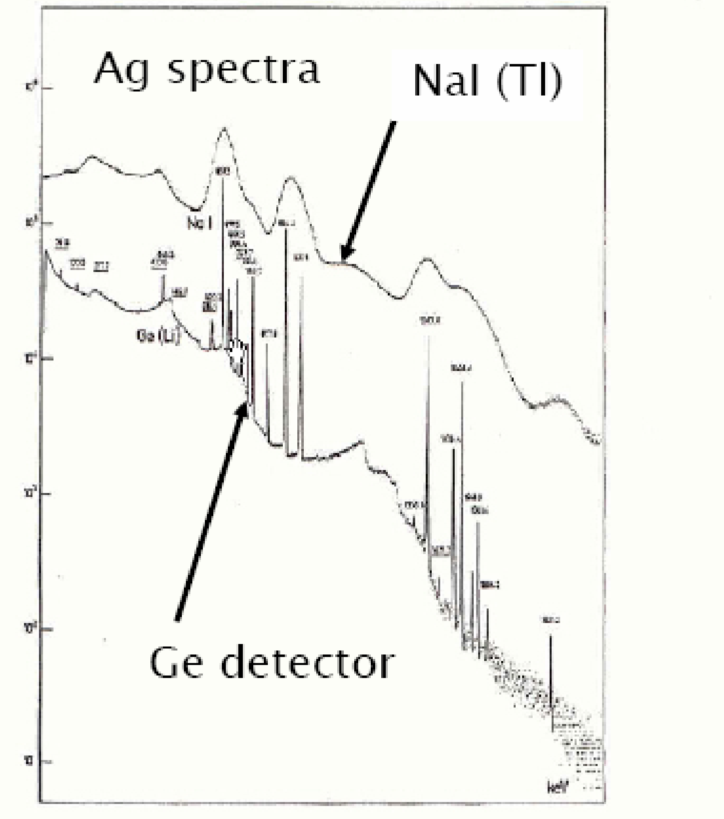


(J.Cl. Philippot, IEEE Trans. Nucl. Sci. NS-17/3 (1970) 446)

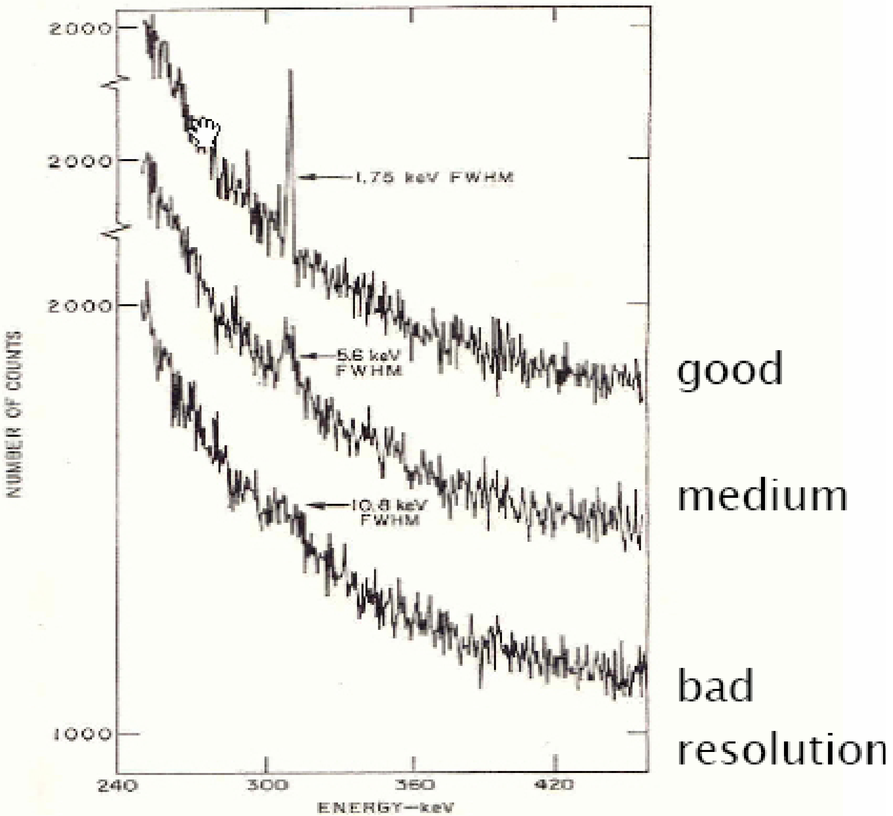


G.A. Armantrout *et al.*, IEEE Trans. Nucl. Sci. NS-19/1 (1972) 107

low noise improves the resolution and the ability to distinguish (signal) structures

low noise improves the signal to back-ground ratio (signal counts are in fewer bins and thus compete with fewer background counts)

# Electronics noise

Definition of Noise

- Random fluctuation superimposed to interesting signal
- Statistical treatment

Three types of noise

- Fundamental noise (Thermal noise, shot noise)
- Excess noise (1/f …)
- Parasitic → EMC/EMI (pickup noise, ground loops…)

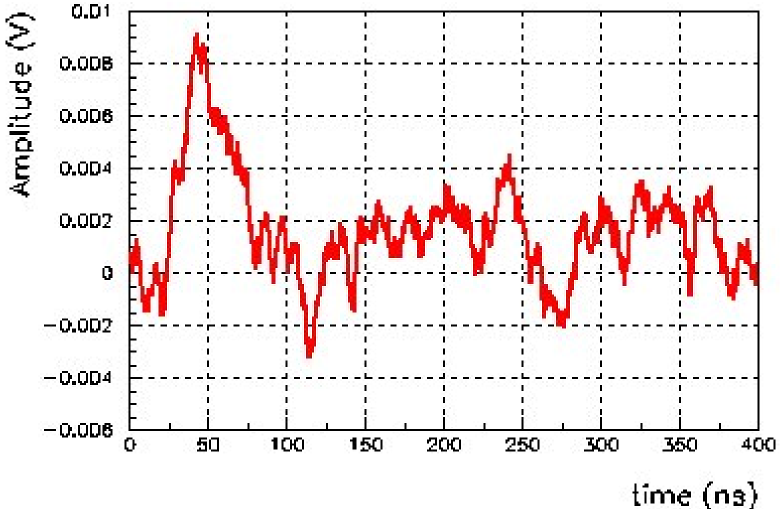


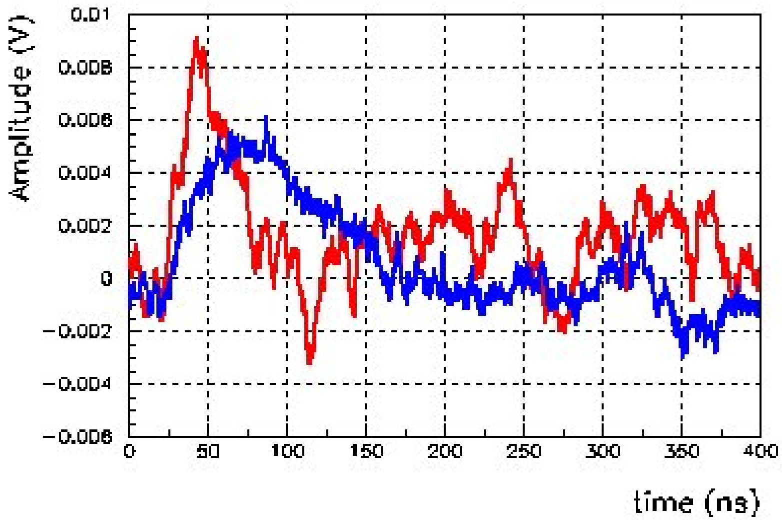

# Calculating electronics noise

Fundamental noise

- Thermal noise (resistors) : $S_v(f) = 4kTR$
- Shot noise (junctions) : $S_i(f) = 2qI$

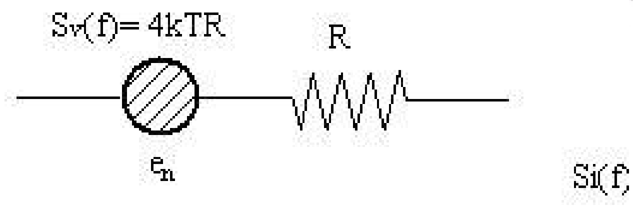


Noise referred to the input

- All noise generators can be referred to the input as 2 noise generators :
- A voltage one $e_n$ in series : series noise
- A current one $i_n$ in parallel : parallel noise
- Two generators : no more, no less…

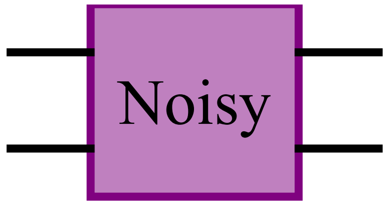


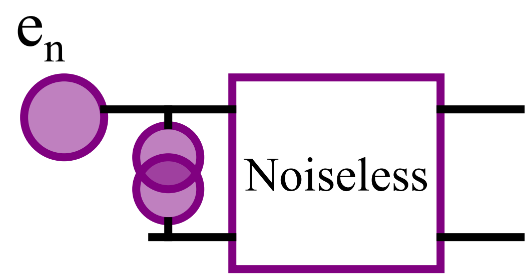


- To take into account the Source impedance

Noise generators referred to the input

- **Golden rule**
  - **Always calculate the signal before the noise what counts is the signal to noise ratio**

# Noise in charge pre-amplifiers

2 noise generators at the input

- Parallel noise : ( $i_n^2$) (leakage currents)
- Series noise : ($e_n^2$)  (preamp)

Output noise spectral density :

- $S_v(\omega) = ( i_n^2 + e_n^2/|Z_d|^2 ) / \omega^2 C_f^2$
  $= i_n^2 /\omega^2 C_f^2 + e_n^2 C_d^2/C_f^2$
- Parallel noise in $1/\omega^2$
- Series noise is flat, with a « noise gain » of $C_d/C_f$

*rms* noise $V_n$

- $V_n^2 = \int Sv(\omega)\, d\omega/2\pi \to \infty$ (!)
- Benefit of shaping…

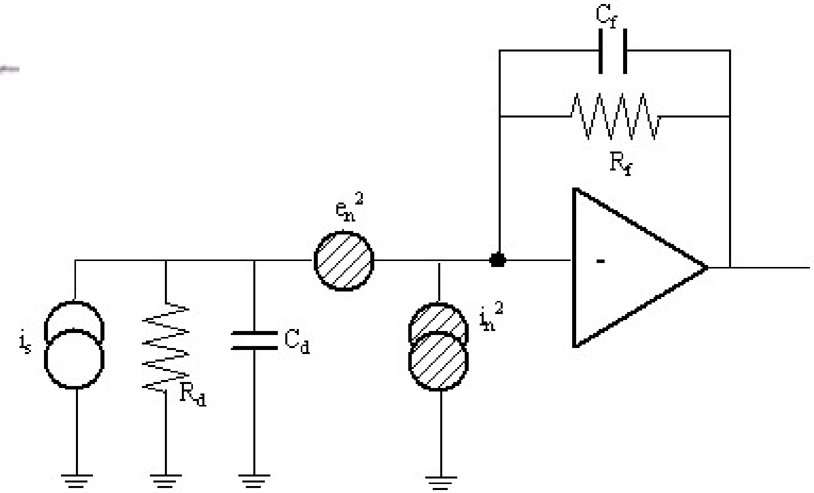


Noise generators in charge preamp

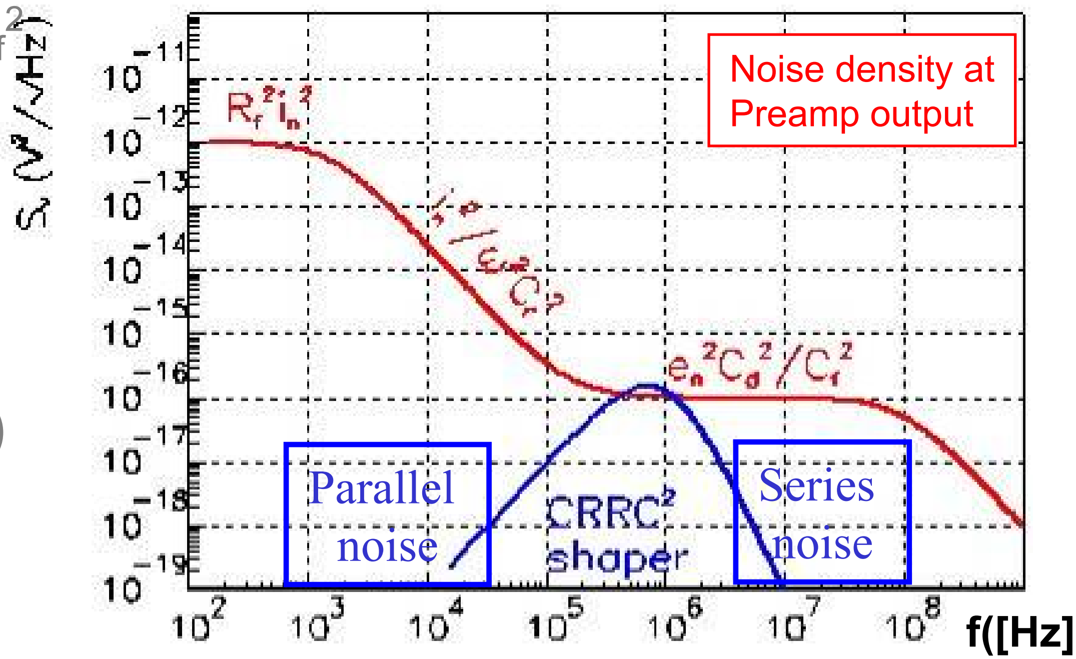

# Equivalent Noise Charge (ENC)

Two basic noise mechanisms: input noise current $i_n$ [pA/√Hz]
input noise voltage $e_n$ [nV/√Hz]

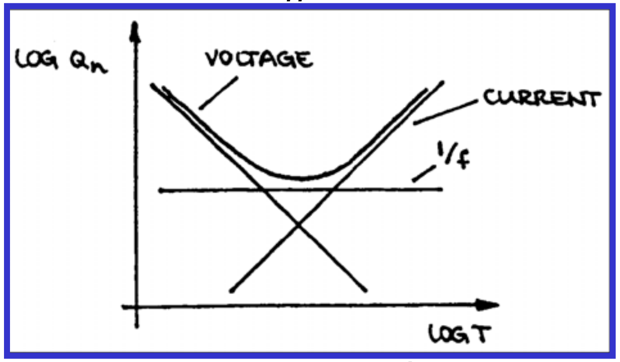


Equivalent Noise Charge:

$$Q_n^2 = i_n^2 \, T_s \, F_i + C_i^2 \, v_n^2 \, \frac{F_v}{T_s}$$

**from Front End**
**from Shaper**

where $T_s$ = characteristic shaping time (*e.g.* peaking time)
$F_i$, $F_e$ "Form Factors" that are determined by the shape of the pulse (calculated in the frequency or time domain)
$C_i$ = total capacitance at the input node (detector capacitance + input capacitance of preamplifier + stray capacitance + … )

➔ Current noise contribution increases with *T*
➔ Voltage noise contribution decreases with increasing *T*
only for "white" voltage & current noise sources + capacitive load
"1/*f* " voltage noise contribution constant in *T*

# Preamps overview

| Experiment | Detector | Q/I | Technology | | Power | Noise : $e_n$ |
|---|---|---|---|---|---|---|
| ATLAS em | LAr | I | Bipolar | Hybrid | 50 mW | 0.4 nV/√Hz |
| ATLAS had | Tiles + PMT | Q | None | | | |
| ATLAS HEC | LAr | I | GaAs | ASIC | 108mW | 0.8 nV/√Hz |
| BABAR | CsI + PD | Q | JFET | Hybrid | 50 mW | 0.6 nV/√Hz |
| CMS em | PbWO4+APD | Q | CMOS | ASIC | 50 mW | 0.9 nV/√Hz |
| CMS had | Tiles + HPD | Q | BiCMOS | ASIC | | |
| DØ | LAr | Q/I | JFET | Hybrid | 270 mW | 0.5 nV/√Hz |
| FLC | W/Si | Q | BiCMOS | | 3 mW | 1 nV/√Hz |
| KLOE | CsI + PD | Q | Bipolar | Hybrid | 60 mW | |
| LHCb em | PMT | Q | None | | | |
| NA48 | LKr | I | JFET | Hybrid | 80 mW | 0.4 nV/√Hz |
| Opera TT | PMTMA | Q | BiCMOS | ASIC | 5 mW | |
| | | | | | | |

# Coherent noise in a multi-channel system

Coherent noise problem :

- Noise adds linearly instead of quadritically
- Particularly sensitive in calorimetry as sums are performed to reconstruct jets or $E_t^{miss}$

$\Sigma\ a_i^2 = n\,\sigma^2_{incoh} + n^2\,\sigma^2_{coh}$ (i=channels)

Coherent noise estimation

- Perform Direct and Alternate sums to extract coherent noise
- $SD^2 = \Sigma\ a_i^2$
- $SA^2 = \Sigma\ (-1)^i\ a_i^2$
- $SA^2 = n\,\sigma^2_{incoh}$
- Incoherent & coherent noise :
  - $\sigma^2_{incoh} = SA^2/n$
  - $\sigma^2_{coh} = (SD^2 - SA^2)/n^2$

Usually $\sigma_{coh} / \sigma_{incoh}$ <~ 20 %

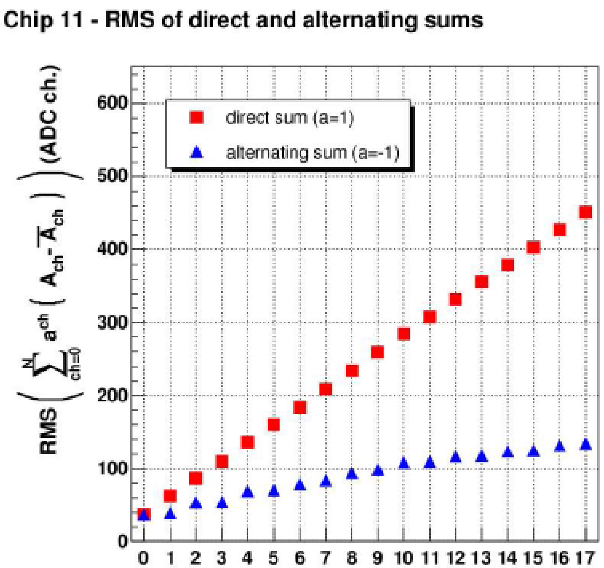


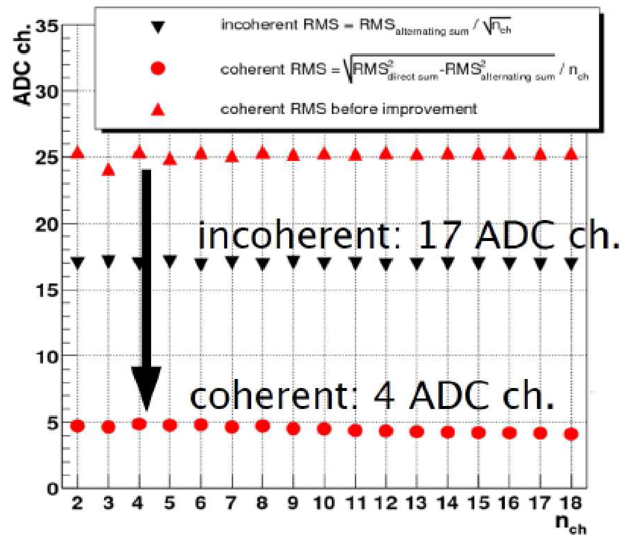

# Overview of readout electronics

Most front-ends follow a similar architecture

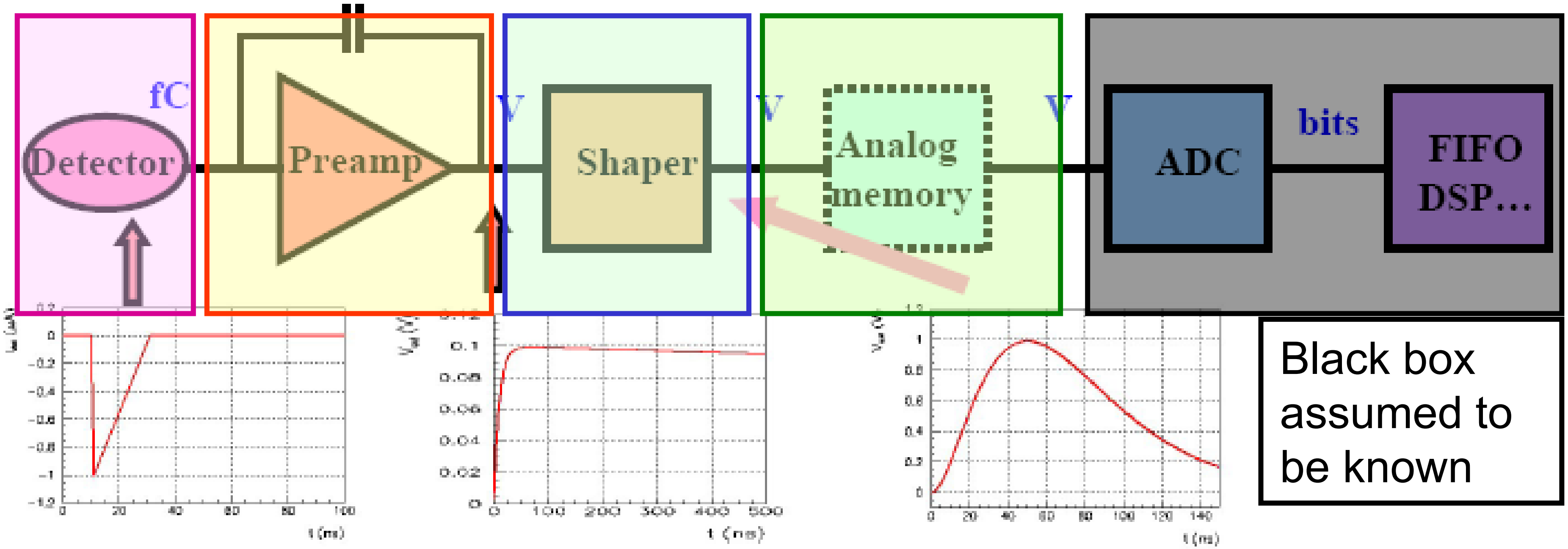


- Very small signals (fC) -> need amplification
- Measurement of amplitude and/or time (ADCs, discriminator, TDCs)
- Thousands to millions of channels

# Analog memories

Switched Capacitor Arrays (SCAs)

- Store signal on capacitors (~pF)
- Fast write (~ GHz)
- Slower read (~10MHz)
- Dynamic range : 10-13 bits
- depth : 100-2000 caps
- Insensitive to absolute value of capa (voltage write, voltage read)
- Low power
- Possible loss in signal integrity (droop, leakage current)

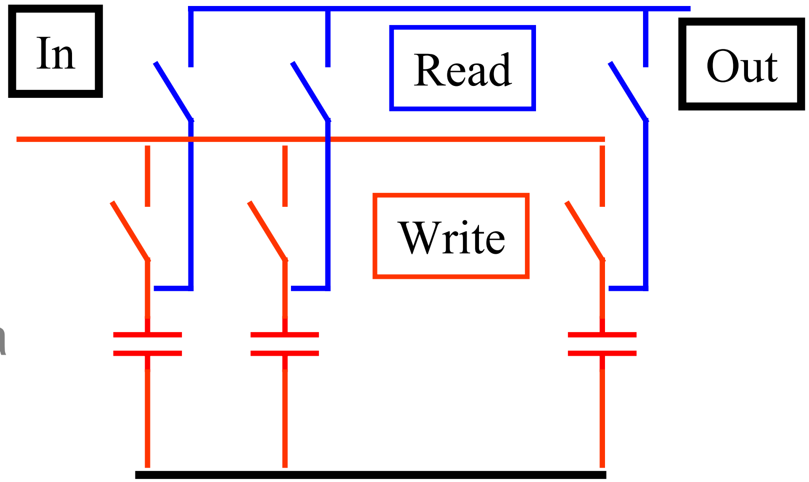


Principle of a « voltage-write, voltage-read » analog memory

The base of 90% of digital oscilloscopes !

# Ionization calorimeters

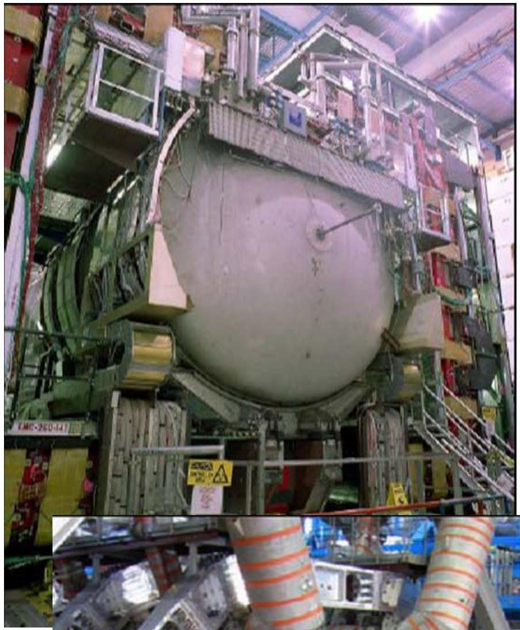

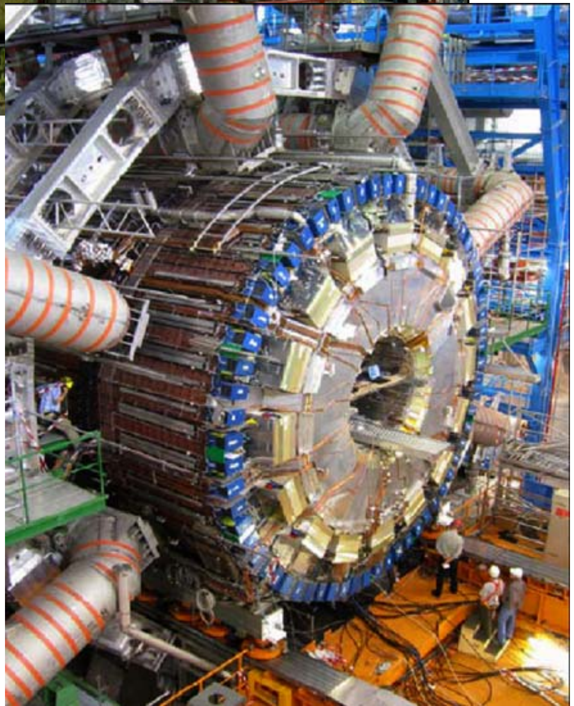

Examples:
DØ(LAr)
NA48 (LKr)
ATLAS (LAr)
H1

Stable, Linear
Easy to calibrate (!)
Moderate resolution

# ATLAS LAr: Front End boards

**Amplify, shape, store and digitize Lar signals**

128 warm preamps
128 tri-gain shapers
128 quad pipelines
32 ADCs (12bits 5 MHz)
1 optical output (Glink)

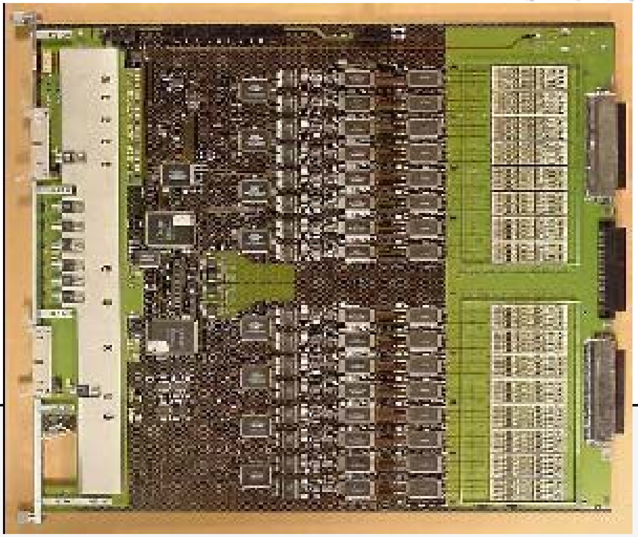

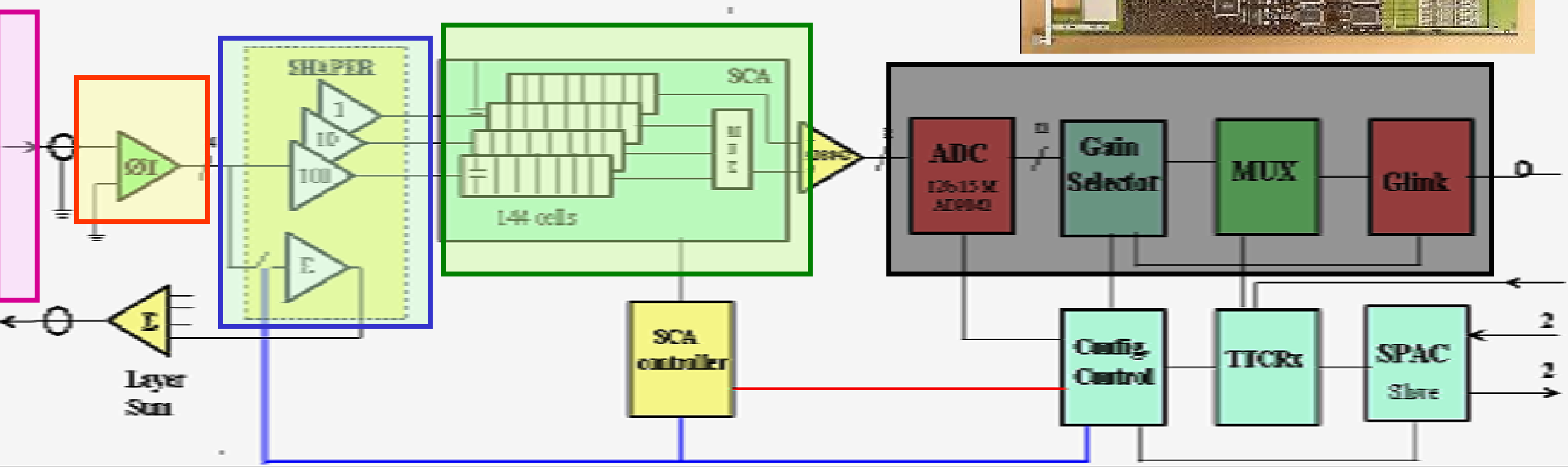

# ATLAS : LAr shaper

**Goal : optimize signal to noise ratio between electronics noise and pileup noise**

Ionization signal ~500ns=20 LHC bunch Xings

Reduced to 5 bunch Xings with fast shaper ➔ worse S/N due to loss of charge

Choice of peak time varies with luminosity ➔ 45ns at L=$10^{34}cm^{-2}s^{-1}$

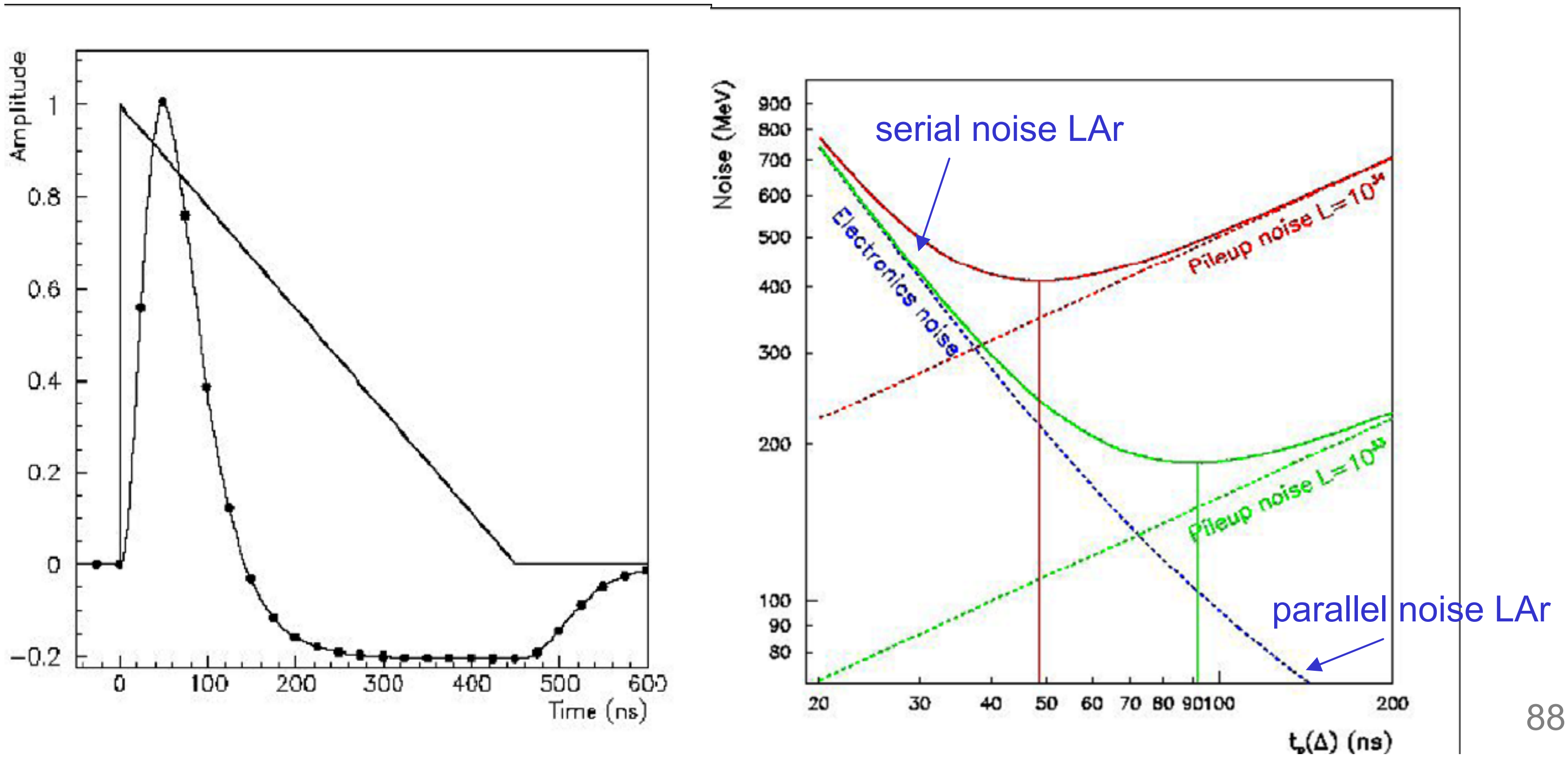

# Crystal calorimeters

Babar(CsI)
Kloe(CsI)
CMS ($PbWO_4$)
L3, CLEO, Belle, ALICE

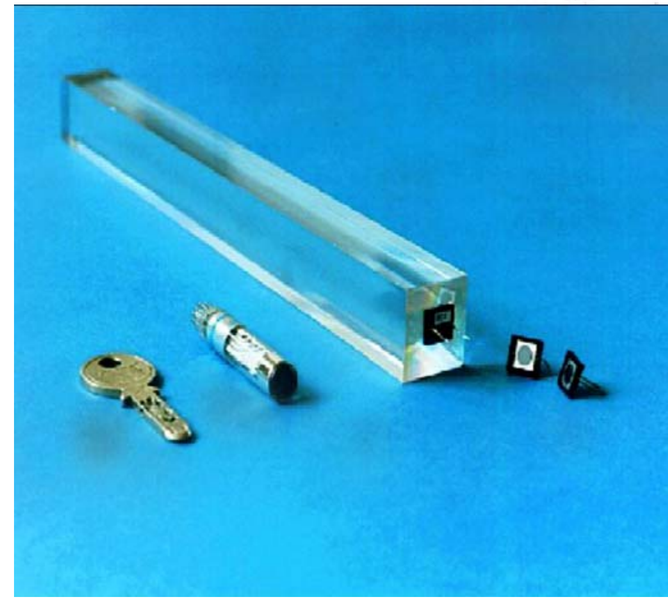

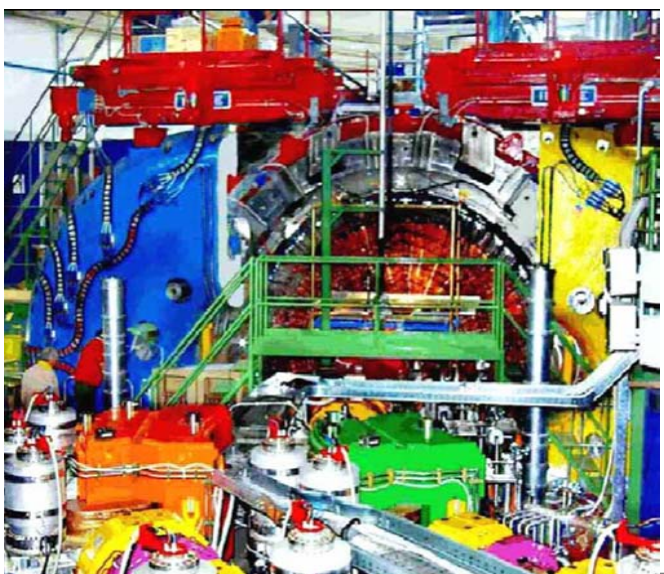

Fast
Best resolution
Difficult to calibrate
expensive

# CMS: ECAL Electronics

building block :

Trigger Tower (25 channels)

-1 mother board

-1 LV regulator board

-5 VFE boards (5 channels each)

-1 FE board

2 fibres per TT sending

-trigger primitives (every beam crossing)

-data (on level 1 trigger request)

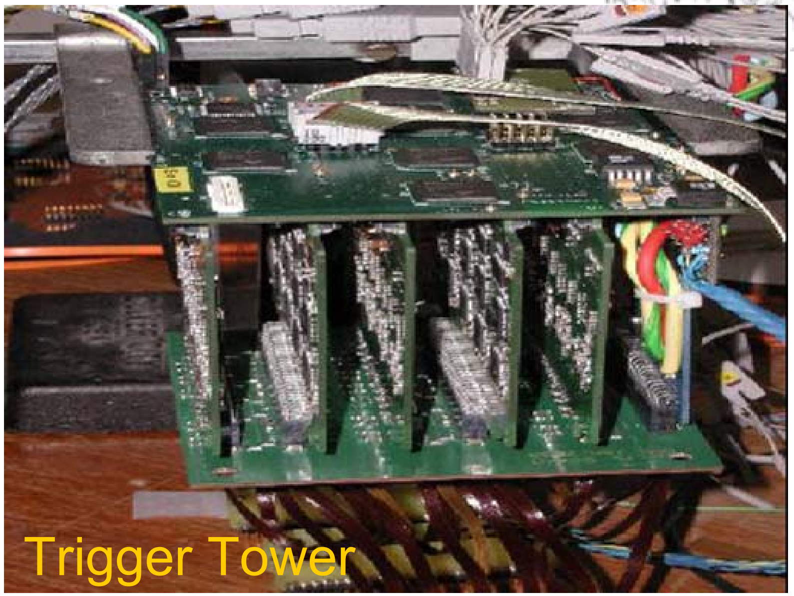


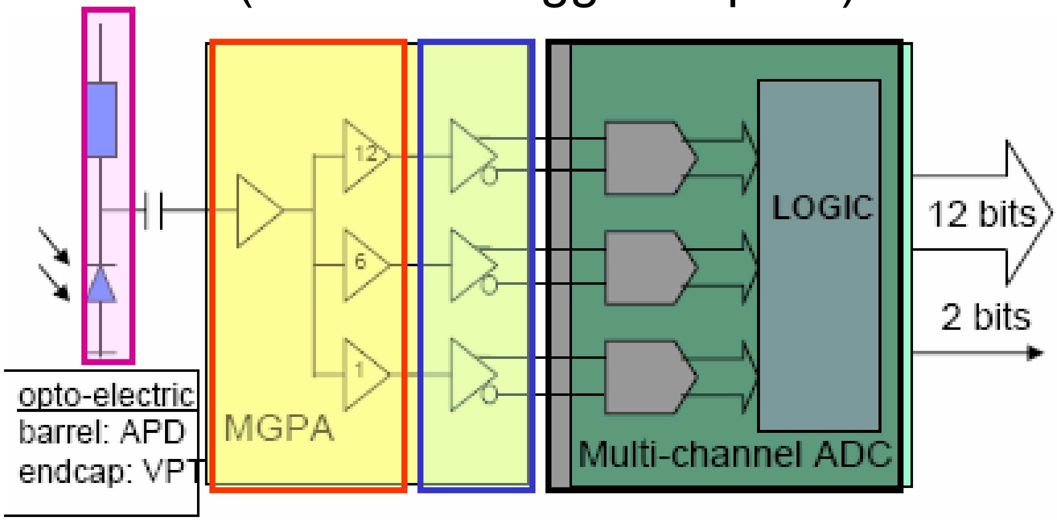


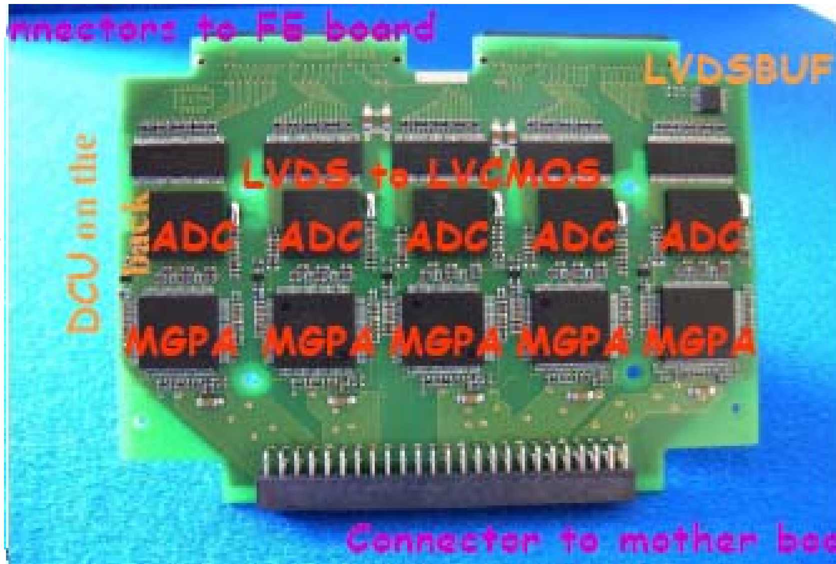

# Scintillating calorimeters

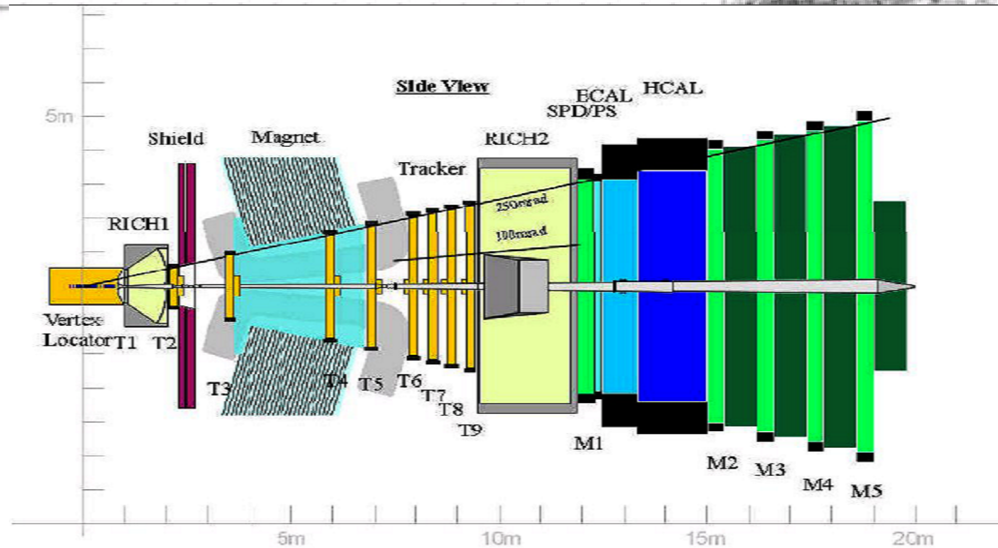


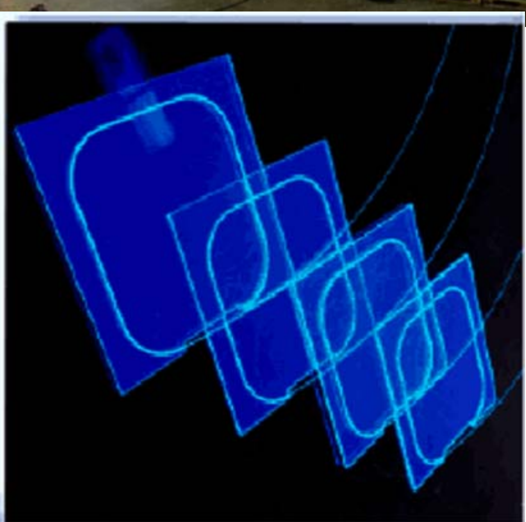

CMS hadronic
LHCb
OPERA
ILC hadronic
ILC em
ATLAS hadronic

Fast
Cheap
Moderate resolution
Difficult to calibrate

# ILC: hadronic calorimeter (CALICE)

Iron/plastic(tiles) sandwich

Single tile readout with WLS fiber + SiPM:
pixel device operated in Geiger mode

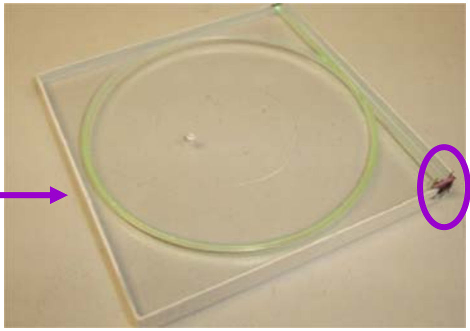

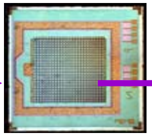

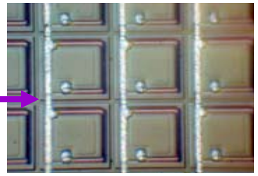

Read out 216 tiles/module
38 sampling layers
~8000 channels

VFE: control board for 12 ASICs / layer
connect to SiPMs

ASIC: amplification + shaping + multiplexing (18 ch.)

# ILC: HCAL readout chip

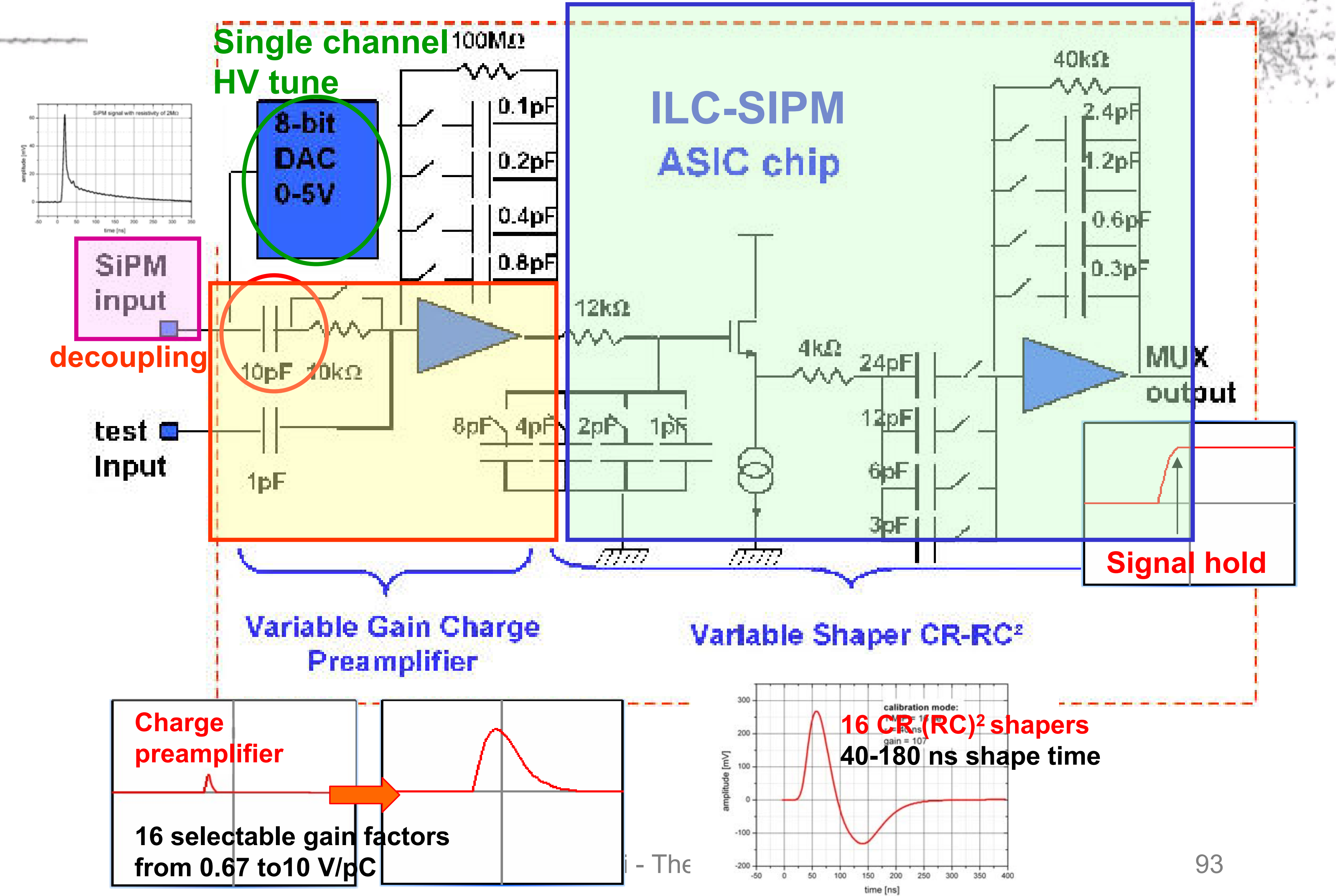

# Semiconductors calorimeters

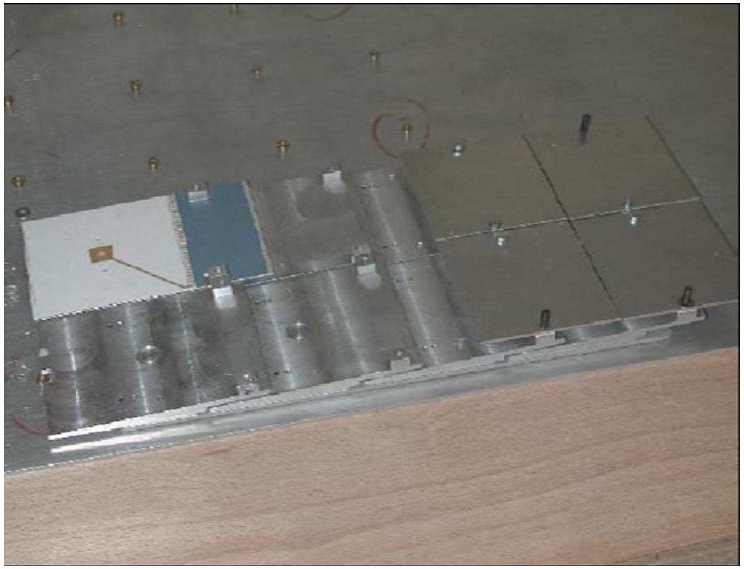

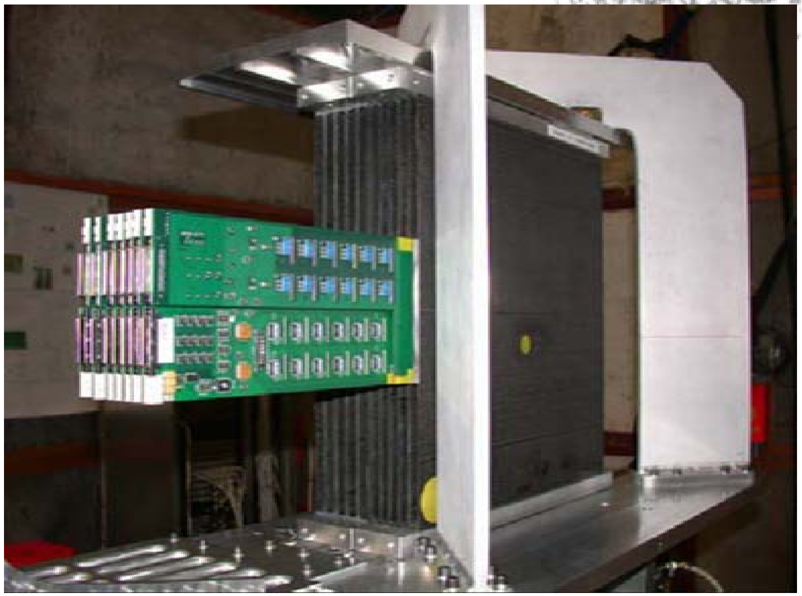

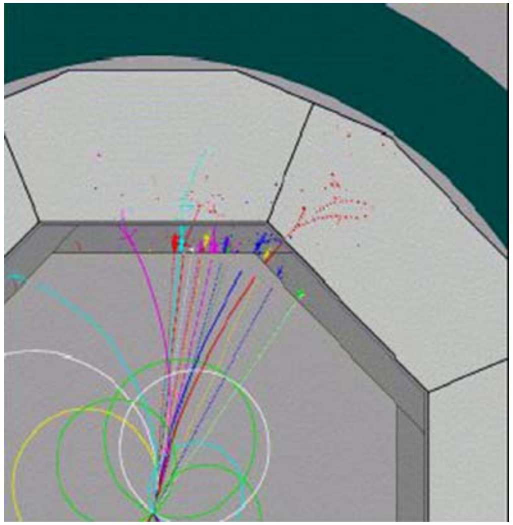

CMS pre-shower
ILC CALICE ECAL

Highly granular
Good resolution
Expensive

# CMS PreShower : readout chip PACE2

- **Aluminium**
- **Silicon sensor:**

  1 $cm^2$

  $V_{depl}$= (60 +/- 5) V

  $I_{leak}$= 100 nA

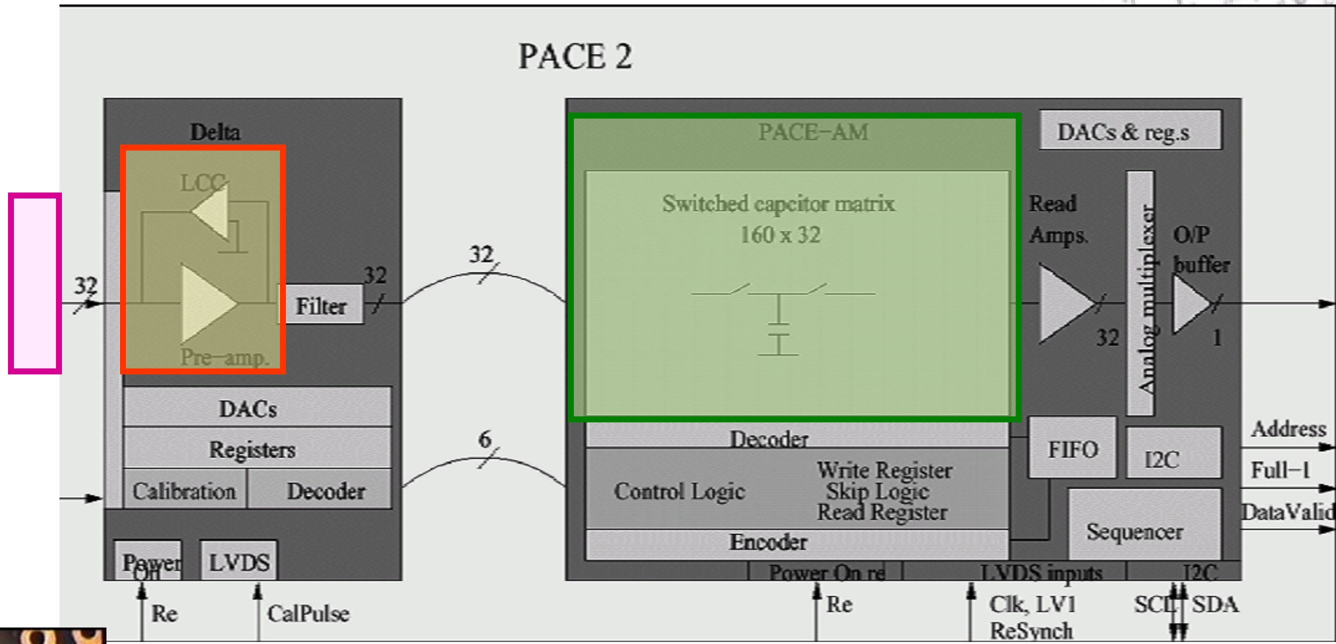


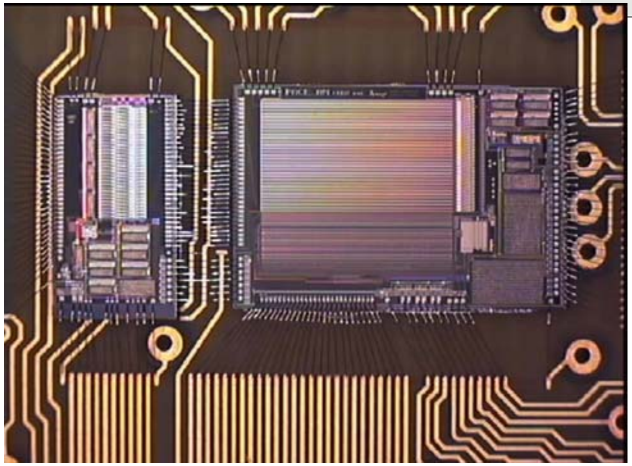

**MCM**

Delta preamp

PACE analogue memory

**Requirements**

10 bit dynamic range

Low gain and high gain

Leakage current comp

# ILC: W-Si em calorimeter (CALICE)

**"Imaging calorimeter"**
30 layers W-Si
1 cm$^2$ SiPADs
~10000 channels

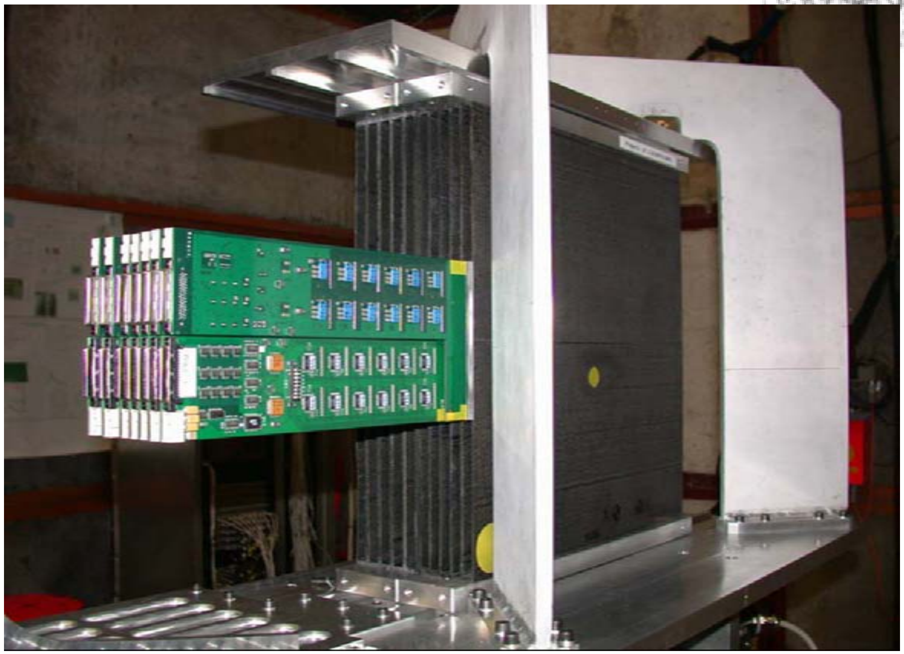

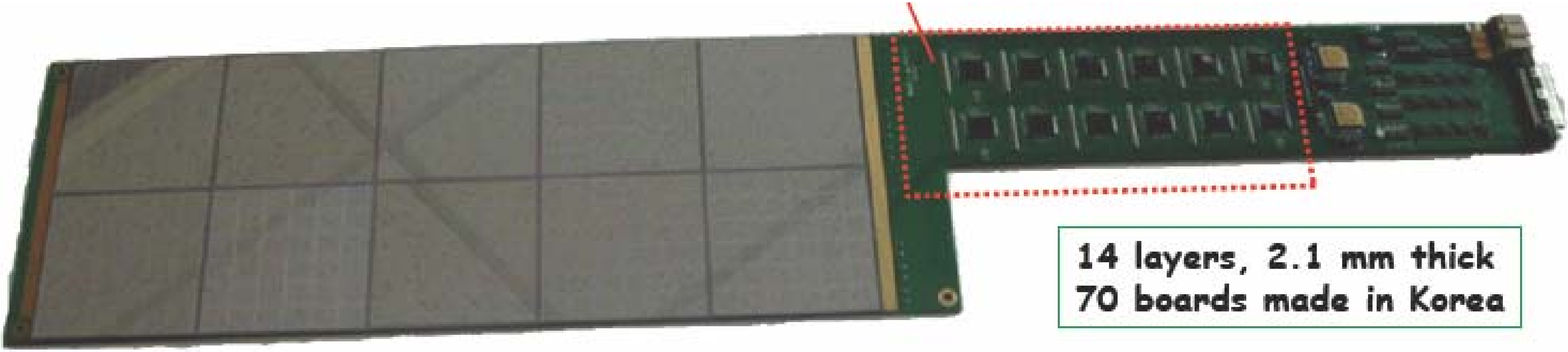

# Trends & Future

- More channels / more functionality in the chip (analog+digital)
  ➔ more integration
- Detector imbedded electronics
  ➔ reduce cable volume = dead volume
  ➔ ultra-low power consumption

ILC : **100µW/ch**

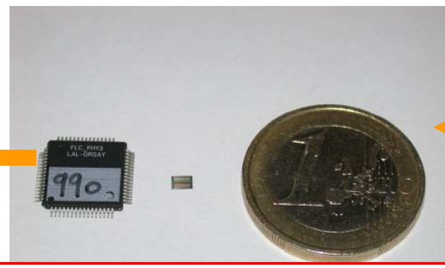

FLC_PHY3 18ch 10*10mm **5mW/ch**

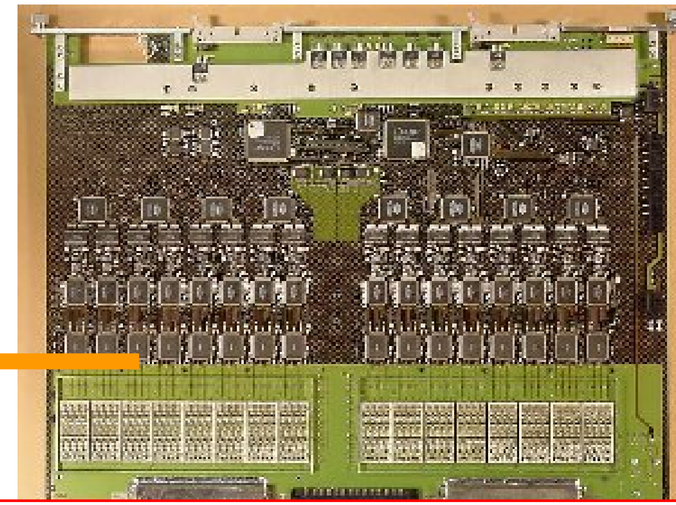

ATLAS LAr FEB 128ch 400*500mm **1 W/ch**

**Readout chip integrated in active layer (Si-W ECAL for ILC)**

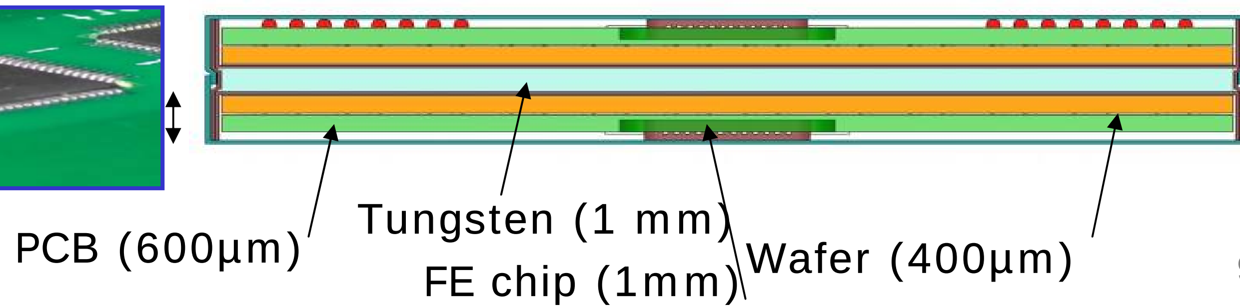

# Imbedded electronics (ILC ECAL)

Front-end ASICs embedded in detector

- Very high level of integration
- Ultra-low power with pulsed mode
- Target 0.35 μm SiGe technology

All communications via edge

- 4,000 ch/slab, minimal room, access, power
- small data volume (~ few 100 kbyte/s/slab)

Elementary motherboard ‘stitchable’
24*24 cm ~500 ch. ~8 FE ASICS

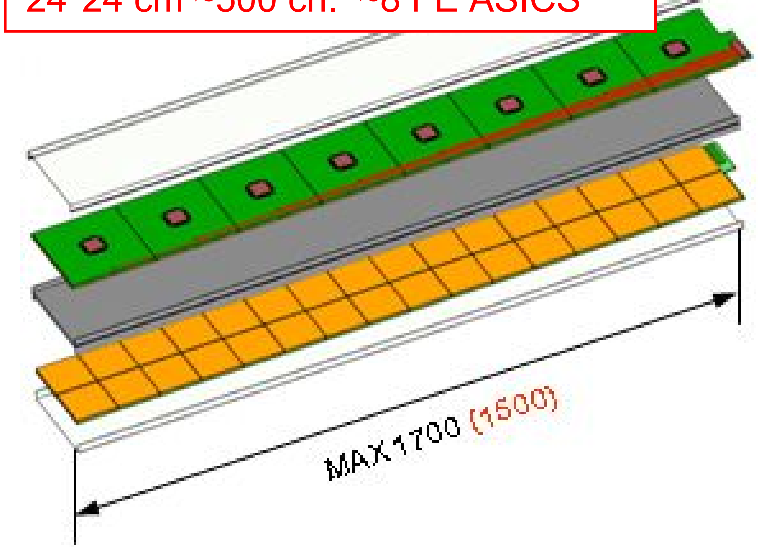


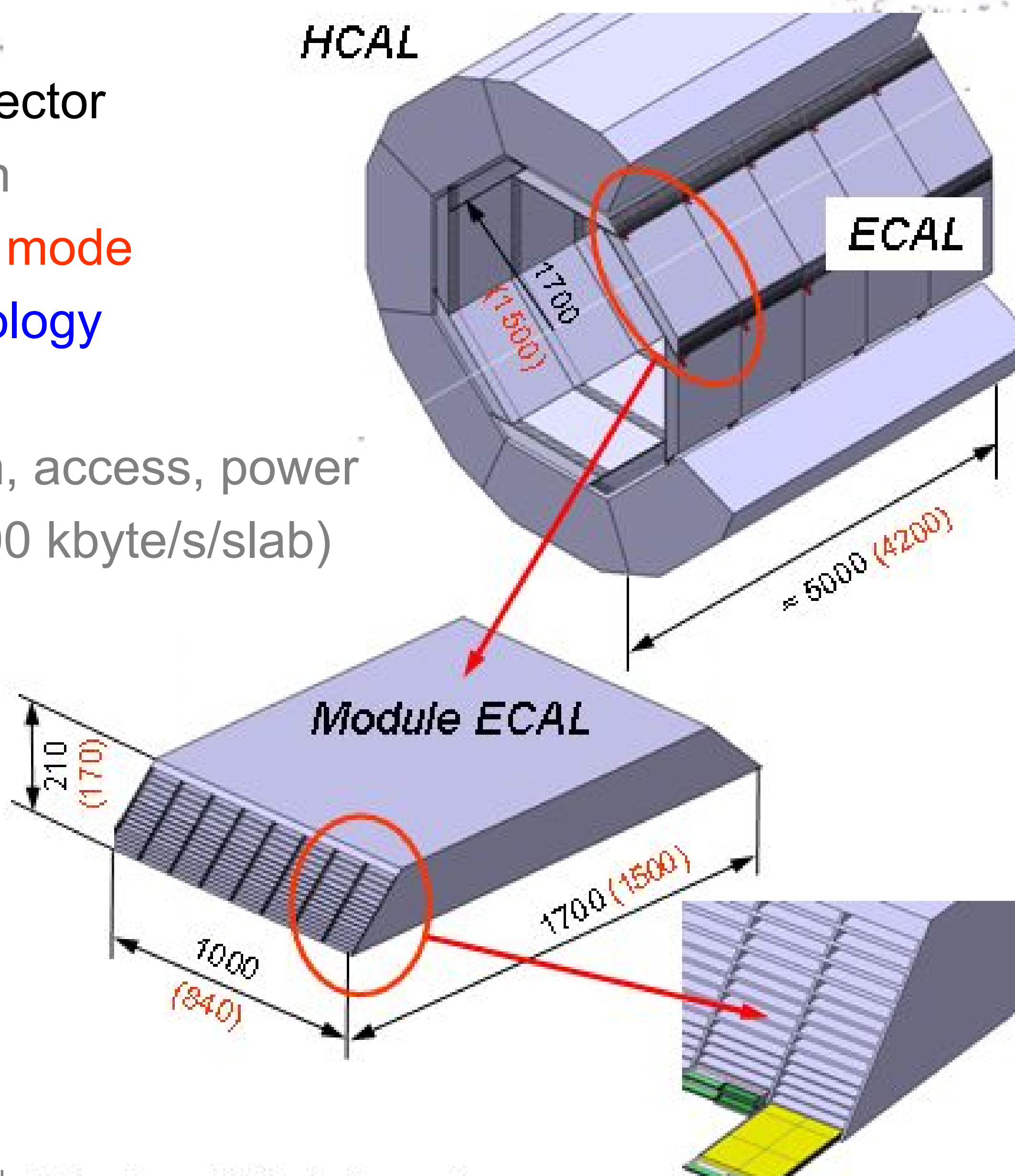

# Imbedded electronics (ILC HCAL)

*Front end ASICs embedded*
*Interfaces accessible*

AHCAL Slab
*6 HBUs in a row*

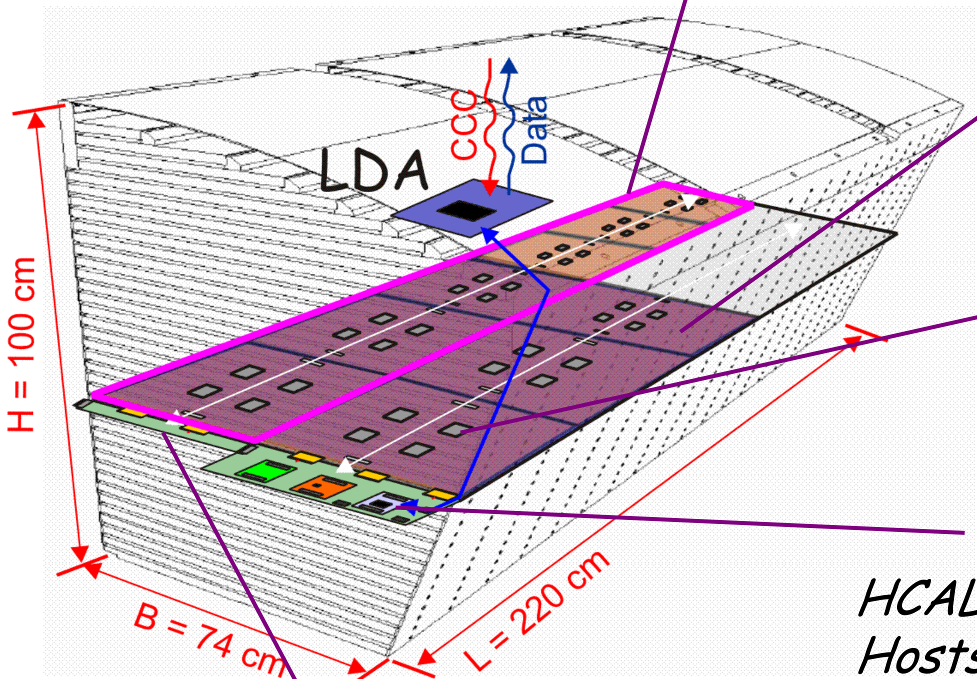


**HBU**
*HCAL Base Unit*
12 x 12 tiles

**SPIROC**
4 on a HBU

**HEB**
*HCAL Endcap Board*
*Hosts mezzanine modules:*
DIF, CALIB and POWER

**HLD**
*HCAL Layer Distributor*

***Power:***
*40 μW / channel*

***Heat:***
*T grad. 0.3K/2m*
*Time constant: 6 d*

# More pixels / more functionality

SPIROC layout (CALICE chip for Analog HCAL readout)

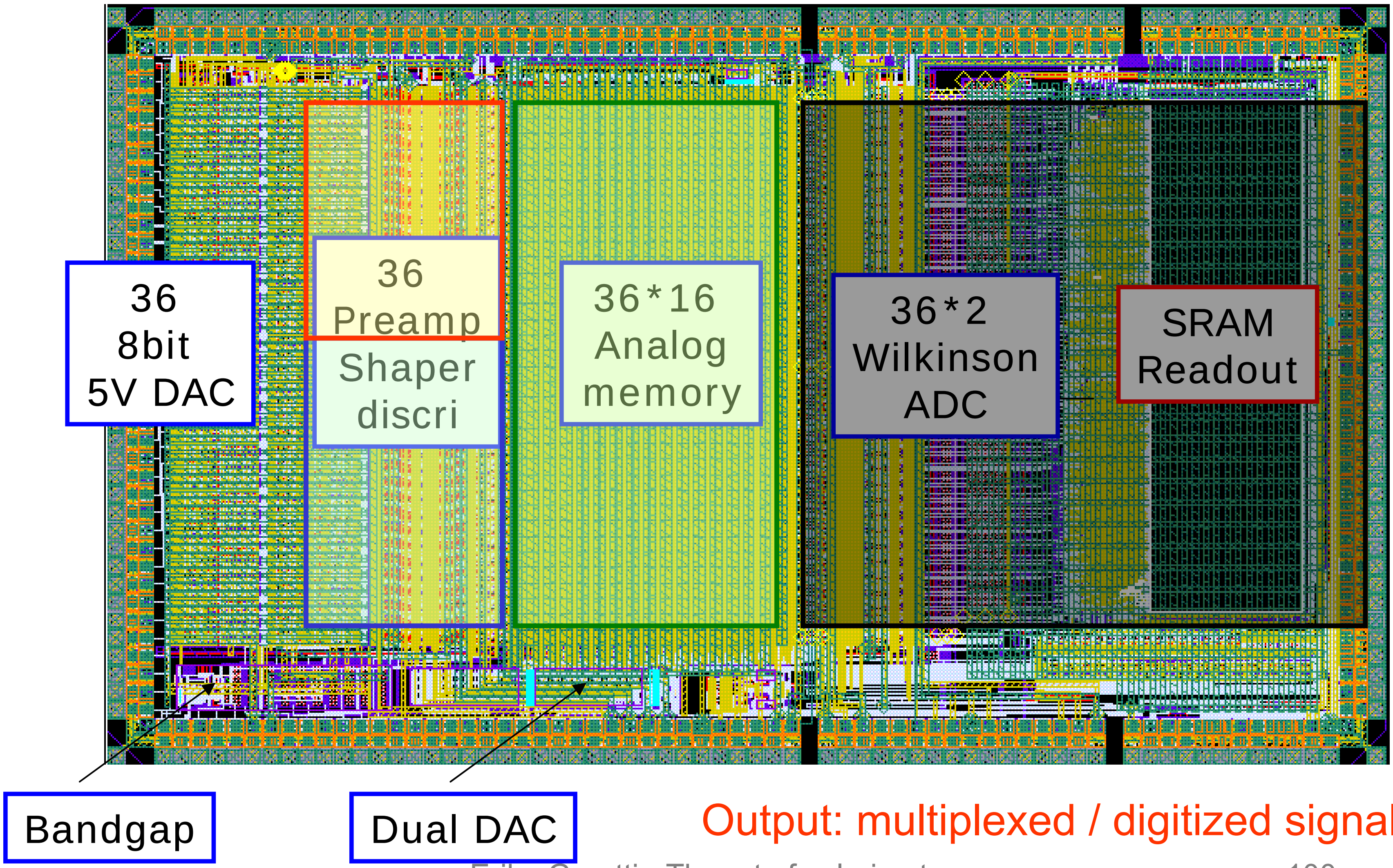


Output: multiplexed / digitized signals

# SPIROC : One channel schematic

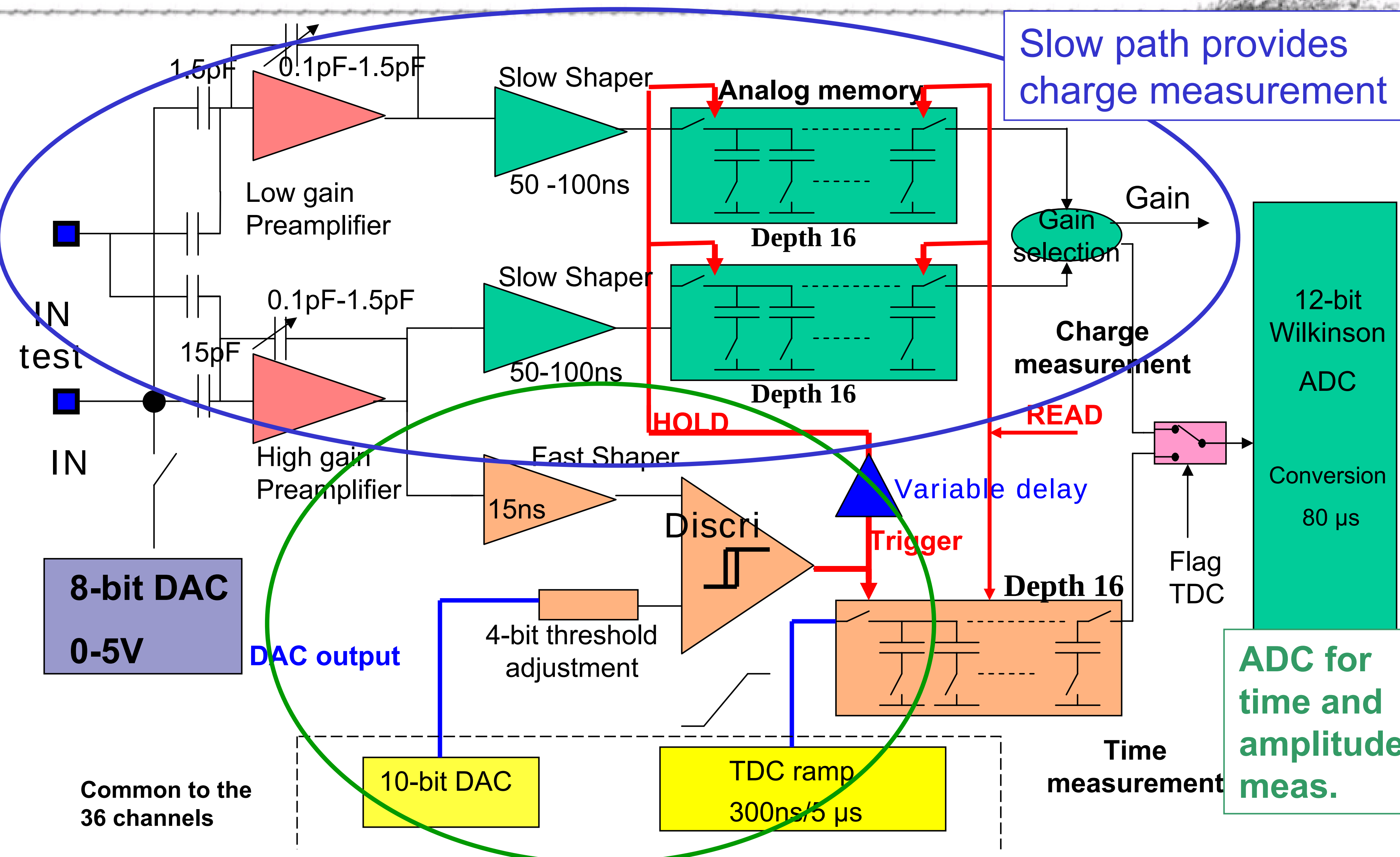


Fast path provides auto-trigger and time measurement

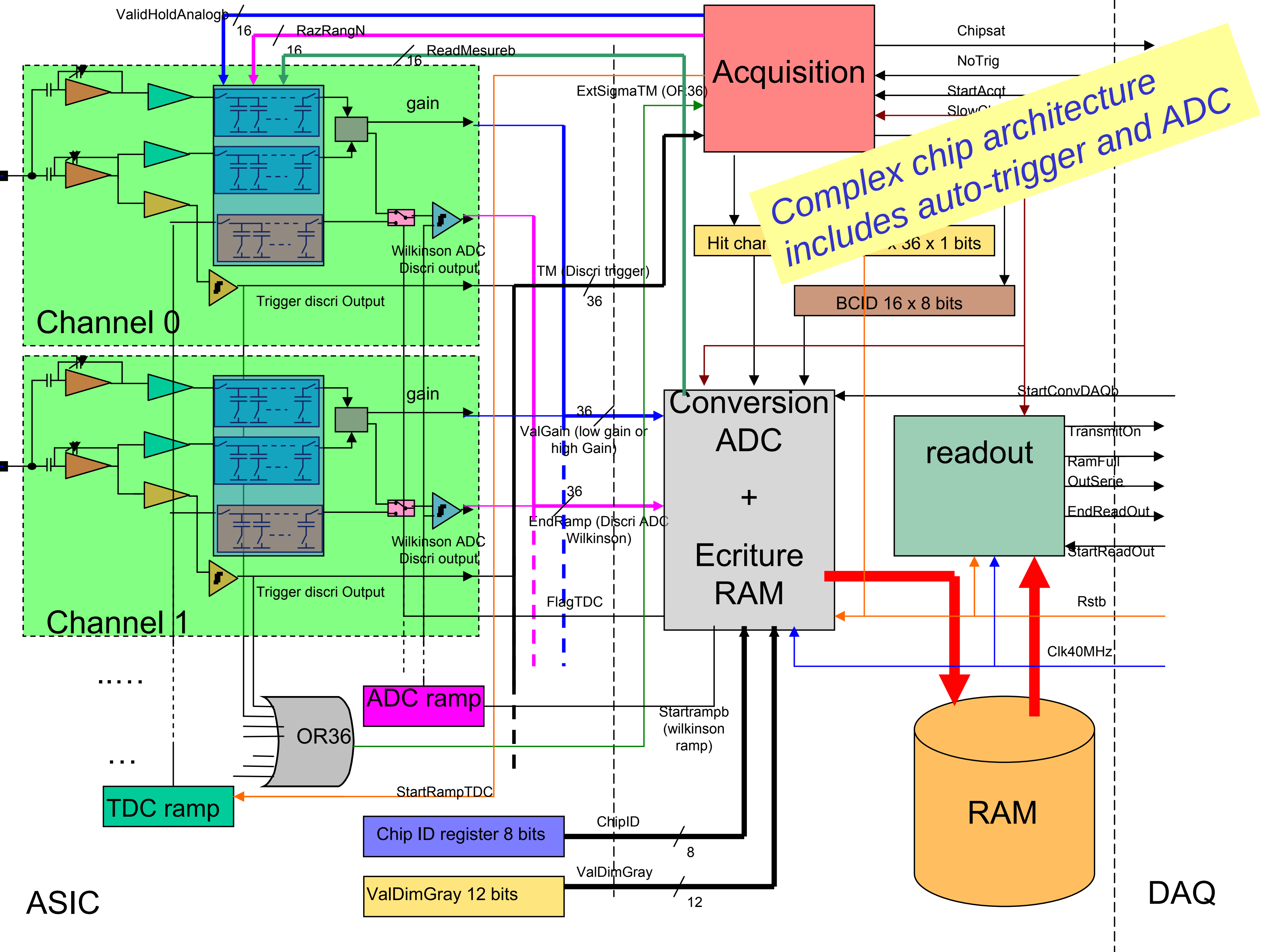

ValidHoldAnalogb
16
RazRangN
16
ReadMesureb
16
Acquisition
Chipsat
NoTrig
StartAcqt
ExtSigmaTM (OR36)
gain
Wilkinson ADC
Discri output
TM (Discri trigger)
36
Trigger discri Output
Channel 0
Hit char
x 36 x 1 bits
BCID 16 x 8 bits
Complex chip architecture
includes auto-trigger and ADC
StartConvDAQb
Conversion
ADC
+
Ecriture
RAM
36
ValGain (low gain or high Gain)
readout
TransmitOn
RamFull
OutSerie
EndReadOut
StartReadOut
36
EndRamp (Discri ADC Wilkinson)
Channel 1
FlagTDC
Rstb
Clk40MHz
ADC ramp
OR36
Startrampb (wilkinson ramp)
RAM
TDC ramp
StartRampTDC
Chip ID register 8 bits
ChipID
8
ValDimGray 12 bits
ValDimGray
12
ASIC
DAQ

# Acknowledgments

For these slides I have to give credit to the work of

C. D'Ambrosio, Dieter Renker, H. Spieler, C. de La Taille

from whom I have taken many plots and figures